2006

Control of lysogeny in marine bacteria: Studies with phiHSIC and natural populations

Amy K. Long
University of South Florida

Control of Lysogeny in Marine Bacteria: Studies with ϕHSIC and Natural Populations

by

Amy K. Long

A thesis submitted in partial fulfillment
of the requirements for the degree of
Master of Science
College of Marine Science
University of South Florida

Major Professor: John H. Paul, Ph.D.
Valerie Harwood, Ph.D.
Kathleen Scott, Ph.D.

Date of Approval:
August 11, 2006

Keywords: Gene Expression Analysis, Salinity Stress, Pseudolysogeny, Viral Production, Prophage Induction

Acknowledgements

I would like to acknowledge my major advisor, Dr. John H. Paul, for his guidance and support during my time in his lab. I am also grateful for the assistance of my other committee members, Dr. Valerie Harwood and Dr. Kathleen Scott. The financial support given to me by the National Science Foundation and the Wachovia Endowed Fellowship made this research possible. I am thankful to Erica Casper, Lauren McDaniel, Stacey Patterson, and David John for their help, encouragement, and humor. Special thanks to Jennifer Mobberley and Kathryn Bailey for never letting me go it alone, no matter how much I tried to ignore them. Finally, I'd like to thank my parents, my brother, and all my friends for their support and encouragement over the years.

Table of Contents

List of Tables

List of Figures

Control of Lysogeny in Marine Bacteria: Studies with ϕHSIC and Natural Populations

Amy K. Long

ABSTRACT

Viruses have an estimated global population size of 10^{31}, with a significant proportion found in the marine environment. Viral lysis of bacteria affects the flow of carbon in the marine microbial food web, but the effects of lysogeny on marine microbial ecology are largely unknown. In this thesis, factors that influence the control of lysogeny were studied in both the ϕHSIC/*Listonella pelagia* phage-host system and in bacterioplankton populations in the Gulf of Mexico. Using macroarrays dotted with ϕHSIC amplicons, viral gene expression over the course of a synchronous infection experiment was measured. Early, middle, late, and continually expressed genes were identified, and included open reading frames 45, 28, 18 and 17, respectively. Viral gene expression in cultures of the HSIC-1a pseudolysogen grown in low and normal salinity media was also analyzed. Overall, levels of viral gene expression were higher in the 39 ppt treatment as compared to the 11 ppt treatment for most ORFs. In the 11 ppt treatment, free phage concentrations were one to two orders of magnitude lower than the 39 ppt treatment while intracellular phage concentrations were one-fold lower. Therefore, at low salinities, expression of ϕHSIC genes is repressed resulting in a lysogenic-like state, while at 39 ppt, lytic interactions dominated. Few viral genes were highly expressed at low salinity, suggesting that repression of viral genes was controlled by host genes. Samples from the

eutrophic Mississippi River Plume and the oligotrophic Gulf of Mexico were analyzed for lytic phage production and occurrence of lysogeny. Significant lytic viral production was only observed three stations, none of which were located within the MRP. This signifies that system productivity is not an accurate predictor of viral productivity. The lysogenic fraction was also inversely correlated to bacterial activity, which decreased with depth. These findings support the hypothesis that lysogeny is a survival mechanism for phages when host cell density is low or when conditions do not favor growth. A unifying theme from these experiments was that lytic processes dominated when bacterial growth conditions were optimal, while lysogeny was observed at unfavorable growth conditions or environmental stress (low salinity).

Chapter 1

Introduction

1.1 Viruses in the Marine Environment

Seventeen years ago, scientists made the surprising discovery that there were nearly 2 x 10^8 virus-like particles per mL of seawater (6, 83). Until then, marine scientists had believed that any viruses that were present in seawater had little to no effect on the marine environment. Bergh's breakthrough revolutionized the field of marine microbiology, and led to the realization that viruses play a significant role in many different marine processes (6).

Viruses are the most abundant organisms on the planet with an estimated population size of 10^{31}, the majority of which are found in the world's oceans (6, 10, 29, 33, 78, 121). In a mL of seawater, viral concentrations can be as high as 10^8 particles per mL while a cubic centimeter of marine sediment has greater than 10^9 particles (10, 81, 82). Many of these viruses are bacteriophages, viruses that infect bacteria (81).

Bacteriophages were first discovered by Felix d'Herelle in 1917 and viruses were first isolated from seawater in 1946 (34, 126). Phages are essentially obligate intracellular parasites (16). They can infect the host cell and lyse it (lytic state), or they can infect the cell, enter a dormant state, and the viral genome is replicated every time the host genome is replicated (lysogenic state). In both cases, phages use the host to survive and propagate with a negative effect on the host.

Over the years, a great deal of research has been done on marine bacteriophages and while much has been learned, there are still many questions. The extent of the role that phages play in global biogeochemical and nutrient cycles is still not fully understood, nor are the factors that affect phage distribution and infection.

1.1.1 Viral Distribution in the Marine Environment

With the realization that viruses, specifically bacteriophages, were the most abundant organism in the ocean, numerous studies were carried out to determine the distribution of marine phages and factors that affect that distribution. Based on microscope counts, it appears that viral abundance typically increases with system productivity as viral abundance is typically greater in coastal waters than in the deep ocean. Freshwater systems have more viruses than marine systems possibly due to the increased organic material input into lake systems as well higher numbers of cyanobacteria, both of which would cause an increase in bacterial productivity and viral abundance (59). Anoxic environments have higher viral counts than oxic but this trend has not been observed in all oxic/anoxic basins. However, in all anoxic basins, the viral abundance is greatest at the oxic/anoxic interface (reviewed in 107).

Temporal variance has also been observed in virus abundance. Typically, viral abundance is greatest in the late fall, after the occurrence of the fall phytoplankton bloom, but is also high immediately after the spring phytoplankton bloom and summer months as well (reviewed in 121). To better understand the temporal scale of viral abundance, simulated environmental studies in meso- and microcosms were carried out. Viral abundance tends to change rapidly over a short period of time but these studies showed

that changes in abundance were typically preceded by an increase in bacterial counts and chlorophyll *a* concentrations (reviewed in 106, 121).

Other environmental conditions that can influence viral distribution in the marine environment include temperature, hydrostatic pressure, radiation, pH, oxygen levels, and organic material (107). While marine phages have been found in every niche examined, including sea ice and hot springs, they appear to be more sensitive to changes in temperature than bacteria and other non-marine phages. Studies have shown that phages isolated from deep-water sediment were unable to produce plaques at temperatures above 23° C even though the host was able to grow at that temperature (reviewed in 106). Another observed effect of temperature is that cyanophage decay rate increases as the temperature increases (106).

Depth is an additional parameter that has been shown to influence viral distribution. Studies have shown that viral abundance in the open ocean is greatest in surface waters and declines until the subsurface chlorophyll maxima where it peaks as does bacterial abundance, both then steadily decline with depth (121).

1.1.2 Viral Effects on Nutrient Cycling

In the same way that studies have been done to understand viral distribution in the marine environment, similar efforts have been made to understand the role of phages on the nutrient cycles in the ocean. The discovery of viruses led to the realization that the accepted model for the marine microbial food web first described by Azam et al. (1983) was incomplete. The marine microbial food web includes heterotrophic and autotrophic prokaryotes as well as their predators. Azam postulated that energy and nutrients were

transferred from microbes to higher trophic levels which influenced carbon and other nutrients cycles in the oceans such as nitrogen, phosphorus, and iron (2).

The largest sink of carbon in the ocean is the dissolved organic matter (DOM) pool (reviewed in 81). While microbes are not typically limited by the DOM pool, they can be limited by other nutrients such as phosphorus, nitrogen, and iron, and some heterotrophic bacteria can be limited by carbon availability (reviewed in 29, 31, 111). Marine microbes are also regulated by top-down controls, i.e. predation and viral-induced mortality. When a microbe is grazed upon, the carbon from the microbe has a chance of being transferred up the food chain. When a microbe is lysed by a virus, the cellular carbon enters the DOM pool. As the DOM pool is only used by heterotrophic bacteria, the carbon will be recycled and cycled through the marine microbial food web, never leaving it. The biomass is being permanently sequestered in the smallest members of the marine food web.

Heterotrophic bacteria alone represent 40-70% of living carbon in surface waters and marine bacterial production of carbon in the photic zone is ~26-70 Gt yr^{-1} (reviewed in 111). Photosynthetic bacteria are also an important part of living organic carbon pool. Of the total number of bacteria in the upper 200 meters of the ocean, cyanobacteria comprise 8%, and fix between 20 and 80% of the carbon in the aquatic environment (111). The percent of bacterial carbon released via viral lysis is estimated to be between 8 and 42% in offshore environments and 6 to 25% in nearshore environments (111). For those reasons, understanding the effects of viral lysis on the carbon pool in the ocean has become the focus of much research.

One of the first studies that quantitatively analyzed the effects of viral lysis was done by Gobler et al. (1997) using *A. anophagefferens*, a chrysophyte responsible for brown tides. Using radiotracer technology, changes in the concentrations of carbon, nitrogen, phosphorus, iron, and selenium in an infected and uninfected culture were quantitatively assessed. Gobler found that while dissolved C and Se concentrations increased in the infected culture, P and Fe concentrations increased and then decreased until they were roughly the same level as in the control sample. Finally, there was actually an increase in the organic nitrogen concentrations in the particulate phase with no loss of nitrogen to the dissolved phase during viral lysis .

The most labile forms of DOM were the ones most quickly utilized by the bacterial and phytoplankton cells. Carbon was lost from the system either by being unused or as refractory DOM, but most of it did remain in the particulate phase (31). This proved that viral lysis can and does impact community structure and production. More importantly, the loss of carbon indicated that there was a leak in the microbial loop where carbon is being lost which lead to the restructuring of the microbial loop to include viral lysis. In addition, lysis of phytoplankton blooms are able to provide an organic carbon source for heterotrophic bacteria (31, 111).

Numerous models studying the fate of carbon in the ocean were developed as a result of the study by Gobler and coauthors. One model, subsequently proven correct by experimental results, states that when 50% of bacteria in a population are lysed from viruses, there is a 27% increase in bacterial respiration and a 37% decrease in grazing which leads to a 7% reduction in macrozooplankton production as compared to a population that has no viral lysis (reviewed in 29). Even when the model is corrected to

account for viral lysis of phytoplankton and grazing of the virus production, the overall effects are the same. Viruses in the marine environment are a sink in the microbial loop as they play a large role in the cycling and partitioning of carbon and other nutrients that would typically be transferred to higher trophic levels, and viral production may impact global CO_2 levels as shown in Figure 1.

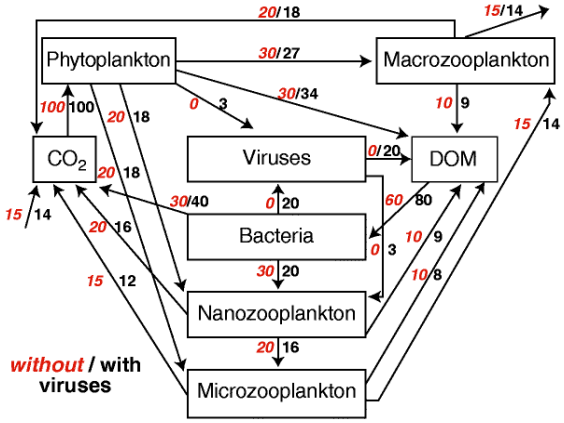

Figure 1. Reprinted by permission from Macmillan Publishers Ltd: Nature 399: 541-548, copyright 1999. Flow of carbon in the marine food web. The red numbers are the units of carbon transferred between trophic levels in a system without viruses and the black numbers are units of carbon transferred between trophic levels in a system that has viruses.

Middleboe and Lyck (2002) proved Fuhrman's model to be accurate when they studied effects of viral lysis on bacterial carbon turnover. Using infected and uninfected batch cultures, bacterial production was measured by ^{3}H-thymidine incorporation, and bacterial and viral abundance were measured by epifluorescence microscopy.

^{3}H-thymidine uptake was greater in the virus-free samples than in the control treatment. When the samples were size-fractionated, it was shown that thymidine uptake

in the infected samples was concentrated in the DOM pool as opposed to the virus-free samples which had the greatest thymidine uptake occur in the bacterial biomass. Bacterial efficiency dropped from 77% in the virus-free samples to the 44% in the control treatments (64). From this, Middleboe and Lyck concluded that the release of dissolved organic matter by lysis increased the organic matter recycling leading to reduced net bacterial production even though total respiration was the same between the two treatments.

The effects of marine phages on the oceanic nitrogen cycle has been studied but to a lesser extent. *Trichodesmium* is a marine cyanobacterium fixes nitrogen to NH_4^+ under aerobic conditions (36, 73). NH_4^+ can then be used by microbes in nitrogen-limited ecosystems. *Trichodesmium* has a very large biomass and is capable of fixing ~80 Tg N y^{-1}, making it an extremely important primary producer in the open ocean (36).

Blooms of *Trichodesmium* have been observed to disappear rather quickly in nature which is unusual because it is not grazed upon by predators due to its ability to produce toxins. The only other top-down factor that could be controlling the blooms is viral lysis. Initial studies found the presence of bacteriophages in the induced laboratory cultures but the presence of phages in field samples of induced *Trichodesmium* could not be confirmed (73).

Using indirect methods of measuring virus mortality, Hewson et al. (2004) were able to quantitatively study the mortality rate of *Trichodesmium* as caused by viral lysis. Virus production was greatest the first six hours after sample collection but there was no significant difference between untreated samples and samples treated with mitomycin C which indicates that prophage induction may have been a result of the methods used to

collect and contain the samples (36). Microscopy showed a large number of viral-like particles associated with *Trichodesmium* cells that could not be solely attributed to the heterotrophic bacteria coupled to *Trichodesmium*. Viral decay rates in both culture and natural samples agreed with the rates found in other studies of virioplankton in the open ocean. Cyanophage abundance was measured to be, on average, 3.96×10^3 viruses ml^{-1} by the most probable number (MPN) assay (36). Viral lysis is an important source of mortality for *Trichodesmium*.

By extrapolating from the growth rate of *Trichodesmium* and the mortality rates derived from this study, it was hypothesized that viral lysis of cells could result in the release of 3 to 65% of fixed N d^{-1} (36). Considering that *Trichodesmium* typically fixes 100 to 300 μmol N m^{-2} d^{-1} in Pacific, it is not unreasonable to conjecture that lysis of *Trichodesmium* cells from viruses would lead to the release of 3 to 195 μmol N m^{-2} d^{-1} which would have a large impact on the marine microbial activity (13, 36).

1.1.3 Gene Transfer and Other Viral-Mediated Processes

There are four ways that bacteria can get new genetic material: conjugation; gene transfer agents; transformation; and transduction (12, 47, 81). A gene transfer agent (GTA) was first identified in *Rhodopseudomonas capsulata* as a filterable agent that was able to mediate genetic recombination (60). However, the agent could not be induced by Mitomycin C, there was no lysis of a culture, and no complete phage particles were observed under TEM. It is now believed that a GTA is a small phage whose sole purpose is gene transfer by way of transduction (7, 47, 61). Genomic analysis of VSH-1, a putative GTA, revealed the presence of viral genes in the host chromosome, *Brachyspira*

hyodysenteriae, including head, tail, and lysis modules. However, VSH-1 virions contained only fragments of the bacterial chromosome thereby supporting the hypothesis that gene transfer agents are defective phages that act to facilitate transduction (61).

Other types of transduction that can be done by infectious bacteriophages are generalized and specialized. Transduction is believed to be an important process in both the marine and terrestrial environment (40). Generalized transduction occurs when fragments of bacterial DNA are accidentally packed in a new phage particle instead of viral DNA. The bacterial DNA is injected into the new host and, if it is not degraded by host enzymes, it can be integrated into the bacterial genome (12). Previous research by Jiang and Paul (1998) in the Tampa Bay estuary showed that generalized transduction events can occur at rates up to 1.3×10^{14} per year.

The second type of transduction, specialized transduction, has been well documented in both the laboratory and the environment. Prophages are temperate bacteriophages whose genome has integrated into the host genome. When prophages receive the signal to excise themselves from the genome and enter the lytic cycle, they can sometimes take the host DNA that flanks their DNA with them. The host DNA is then replicated and packaged in a new viral particle with the virus DNA. When the virus infects a new host, the bacterial DNA is injected as well. The viral DNA will then integrate both its genome and the bacterial DNA into the genome of the host. Many times, these bacterial genes can encode virulence factors that the new host will use. One such example of specialized transduction is that of *V. cholerae*. Uninfected *V. cholerae* is harmless to humans and does not cause cholera. However, *V. cholerae* that has been infected with CTXphi and has the toxin-coregulated pili will cause cholera (104).

Recent research has shown that bacteria are capable of transferring genetic material to phages. Mann et al (2003) discovered, upon sequencing the genome of the *Synechococcus* virus S-PM2, that two genes necessary for photosynthesis were present. The two genes encode the D1 and D2 proteins which are located at the core of the photosystem II reaction center and bind the necessary pigments and co-factors for PSII to function. DI is turned over rapidly during the course of photosynthesis due to light damage but when the rate of damage exceeds the rate of replacement, PSII can no longer operate at its maximum efficiency (58). The presence of *psbA* and *psbD* genes in the viral genome would ensure that host machinery is still operating and energy is being produced even as the virus is using the host to replicate. While it appears that the two genes were acquired through separate mechanisms, they are functional (58).

It turned out that S-PM2 was not alone in possessing these genes. When the genomes of three viruses isolated from both high-light and low-light strains of *Prochlorococcus* were analyzed, photosynthesis genes were found (49). P-SSP7, P-SSM2, and P-SSM4 all had the *psbA* gene and the *hli* gene, whose product protects PSII from excess excitation energy during photosynthesis. In addition, P-SSM4 had a full copy of *psbD*.

Phage genes undergo a high rate of mutation. The fact that the viral photosynthesis genes are similar to the host genes indicates that phages are under a selective pressure to protect them from mutation and deletion events. Reverse transcription-PCR, a technique that is able to detect mRNA levels in cells, has shown that transcripts of regions from the particular genes are present and phage D1 protein levels increase as the infection cycle occurs (48, 49). Furthermore, bioinformatic analysis of these genes indicates that host

species, *Prochlorococcus* or *Synechococcus*, will determine the genes that are transferred to the viruses (49).

A final benefit that phages can confer upon bacteria is homoimmunity. When a bacterial host is homoimmune, that means that it has acquired immunity against phages that are similar to the one that initially infected and the similar phages are unable to infect the cell thereby preventing super infection (1, 81, 94, 116). Homoimmuity is thought to be controlled by a protein, CI in λ and Rep in the halophilic bacteriophage ϕH, that binds to the early lytic gene region but the exact mechanism is still unknown (1, 94).

1.2 Virus Lifecycles

When a bacteriophage infects a cell, depending on the phage, one of three things can happen: lysis; lysogeny when the phage is temperate; or pseudolysogeny. Lytic phages lyse the host generally within a half-hour to an hour after infection and new phages are released into the environment while temperate phages can enter either the lytic cycle or the lysogenic cycle after infecting the host. Temperate phage DNA can exist as a plasmid in the cytoplasm of the cell, or the viral genome can integrate into the host genome. Theoretically, when a prophage is in the latent stage, every time the host genome replicates, the viral genome will be replicated as well.

1.2.1 Lysis

In the first step of the infection cycle, the tail fibers of the phage attach to receptors on the outer cell wall of the host cell and viral DNA is injected into the host cell. The viral DNA circularizes, allowing for the start of early gene-transcription, and, if the virus is

temperate and capable of entering the lysogenic cycle, a molecular decision must be made as to whether the lysogenic or lytic cycle will be entered. This decision is likely based on the host cell physiology and environmental cues but the exact mechanism is not well understood in most phage-host systems. It is known that when there is a high of multiplicity of infection, phages are more likely to enter lysogenic interaction with the host (reviewed in 106).

The best understood model of lysogeny is that of the coliphage λ. In this system, three promoters are necessary for the transcription of lysis genes; they are P_L, P_R, and P_R'. A host sigma factor, σ^{70}, a subunit of the RNA polymerase that binds it to the DNA and initiates transcription, binds to P_L and one of the first proteins made is N which alters the RNA polymerase such that it does not recognize termination points in the genome. The next essential protein for lytic growth is Q, found on the P_R transcript. Normally, the P_R' transcript is terminated at T_R' but when Q is present, the transcript is extended and late genes such as those necessary for packaging the new viral DNA are expressed (50). Q cannot be expressed if N is not present and as such, if P_L and P_R are repressed, then no lytic gene expression occurs and the lysogeny pathway begins.

1.2.2 Lysogeny

In λ, the phage genome integrates into the bacterial genome at the *attB/attP* site and is then known as a prophage. Research with lambda has shown that maintenance of lysogeny is a delicate balance of the CII, CIII, and the repressor proteins.

CI, the product of the *cI* gene, blocks P_L and P_R expression. When the decision to enter the lysogenic pathway is made, P_{RE} (promoter for repressor establishment) is

expressed and CI is made. P_{RE} is dependent on another gene product, CII, which is affected by the status of the cell. High levels of CII allow for P_{RE} expression which allows for CI production.

CII, also responsible for the transcription of the promoter that produces the integrase protein, must be stable if lysogeny is to occur (20, 21). CII is degraded by HflB, a host protease that binds to the C-terminal tail of CII in order to degrade it and induce the lytic cycle (20, 21). HflB, also known as FtsH, can be regulated by CIII, a competitive inhibitor of HflB that is expressed from the P_L promoter. The higher the levels of CIII, the more stable CII is.

Once the lysogenic state had been firmly established, P_{RM} (promoter for repressor maintenance) takes over CI expression. P_{RM} is a somewhat weak promoter and its effectiveness is increased by the presence of CI and in this way, CI is able to negatively regulate transcription levels of *cI* (50, 84).

Figure 2. Reprinted with permission from PNAS 2005; 102(12): 4465–4469. The lysogenic module in λ. Note the main promoters and genes necessary for either lytic or lysogenic infection.

CI acts in the O_R regulatory region of the lambda genome which is also where P_{RM} is located (Figure 2). Cro, the product of the *cro* gene, acts in an opposing manner to CI. Lysis occurs when Cro is present but the presence of CI signals that lysogeny is taking place. This has to do with five different and equally important sites in the O_R region.

There are the two promoters, P_R and P_{RM}, and three binding sites, O_R3, O_R2, and O_R1. When Cro binds to O_R3, P_{RM} is repressed, CI is not made, and lysis occurs. As Cro levels in the cell rise, the O_R3 binding site fills up and Cro binds to O_R2 and then O_R1. When O_R1 is bound, P_R is repressed and production of Cro ceases. In that way, Cro is able to negatively autoregulate itself.

CI, on the other hands, binds to O_R1, an action that increases CI's affinity for O_R2. When it binds to O_R2, PR is repressed while expression of P_{RM} is enhanced. In this case, CI is acting as a positive autoregulator and stimulating its own expression. When CI binds to O_R3, however, it partially represses P_{RM} and CI production begins to decrease.

For a long time, it was thought that O_R operated by itself with no other part of the viral genome playing a role. However, it was recently discovered that O_L, located 2.4 kB left of O_R, plays an integral role in repressing CI expression (22, 23, 50). CI binds to OL at O_L1, O_L2, and O_L3 and can also bind to CI molecules bound to O_R, forming a loop structure (Figure 3). There is a tetramer-tetramer interaction between O_L1 and O_L2 and O_R1 and O_R2 (23, 50). The consequences of this are that lytic promoters are more effectively repressed and CI levels are better regulated in the lysogens due to the negative autoregulation of *cI*. It is also thought that that the long-range interaction may play an important role when the prophage is induced and lytic promoters must be expressed.

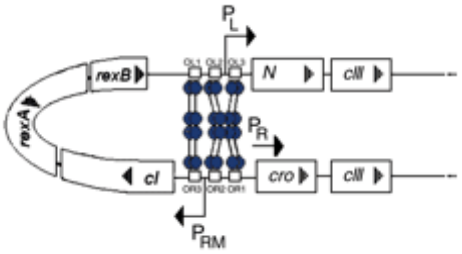

Figure 3. Reprinted with permission from PNAS USA: 2005; 102(12): 4465–4469. Illustration of the loop that forms from the octamerization of the CI dimers (blue molecules) bound at O_R and O_L.

Induction, when the prophage excises itself from the host genome and enters the lytic pathway, happens spontaneously at an observed frequency of about 10^{-2} to 10^{-5} (1). Induction can also be triggered by physical, biological or chemical agents. The most common inducing agents are mitomycin C and ultraviolet light but other agents such as polyaromatic hydrocarbons, hydrogen peroxide, pesticides, and temperature have been observed to act as inducing agents (reviewed in 19, 41, 50, 84, 106).

Induction works by damaging the host cell DNA which sends out the signal to initiate the SOS response. The SOS response turns on a series of genes that act to help the bacterial cell recover from whatever damage it has just undergone. RecA is a protein produced during the SOS response that mediates the cleavage of CI causing it to fall off the viral promoters P_R and P_L, at which point the lysis genes are expressed (50, 84).

1.2.3 Pseudolysogeny

Pseudolysogeny was first described by Twort in 1915, but the implications of this state were not fully recognized until the 1960s (86, 98). There are currently at least three different definitions of pseudolysogeny. Ripp and Miller (1997) defined pseudolysogeny

as a function of the nutrients in the environment in which the host bacterium is found. The marine environment is typically low in nutrients and, as such, bacteria exist under starvation conditions. When the phage infects a host that has limited energy, its genome does not integrate into the host as it would if it was lysogenic but it does not enter the lytic life cycle either. Rather, the phage genome is inactive because the host cell does not have enough energy to allow phage replication.

Ripp and Miller hypothesized that once nutrients increased in the environment, there would be enough energy for the cell to grow. Cell growth would signal to the phage genes to begin expression and enter either the lytic or lysogenic cycle. In this respect, pseudolysogeny would be one way of maintaining abundant phage populations in the marine environment (85).

To prove their hypothesis, Ripp and Miller studied phage-host dynamics in a nutrient-limited and a nutrient-spiked mesocosm. Increases in virion production were typically observed 12 hours after nutrient addition but control treatments had no change in virion production during the same time period (85). Additionally, pseudolysogenic clones from a colony grown in a chemostat were probed with phage DNA to determine if the phage genome was present in the cells. Very few colonies had phage DNA supporting the hypothesis that phage DNA had entered an inactive state in the parent cell and could not be transferred to the daughter cells because of energy limitations (85). However, no further molecular work was done to prove this definitively.

Recently, a new definition of pseudolysogeny was proposed based on a phage in the *Siphoviridae* family, VHS1, that infects *V. harveyi*, a bacterium that causes disease in marine animals (45). When challenging the cells with VHS1, using subclones of one

strain of the isolated bacterium, Khemayan et al. (2005) discovered that 74% of the clones were spontaneously cured and that only one of the twenty subclones examined was lysogenic. Southern analysis of restriction digests of the VHS1 DNA showed that the phage was not integrating into the host genome but existing as an unstable episome. Finally, when dot plaque assays were performed, researchers discovered three distinct colony phenotypes that seemed to indicate the presence of both lysogens and pseudolysogens.

Based on their experimental data, Khemayan et al. (2005) hypothesized that pseudolysogeny occurs when a lysogen has lost the prophage DNA but has retained phenotypic traits such as varying colony morphologies. While it is possible that the subclones lost the virus, in order to exhibit the phenotypic traits observed in the experiments, i.e. the production of turbid plaques when plated, some phage DNA would need to have retained so that the host cell was lysed. Therefore, the subclones have not truly lost the prophage DNA as Khemayan and coauthors claim and do not fit their definition of pseudolysogeny.

The final and most often cited definition of pseudolysogeny was developed by Ackermann and DuBow (1987). Pseudolysogeny is a persistent infection where both phage and host cells exist in high abundance simultaneously in culture. In this case, the phage DNA has not integrated into the host genome and only some of the host cells are infected. As such, a phage-free strain of the host can be obtained. Another hallmark of pseudolysogenic cultures is that they cannot be induced with typical inducing agents such as mitomycin C (1, 116).

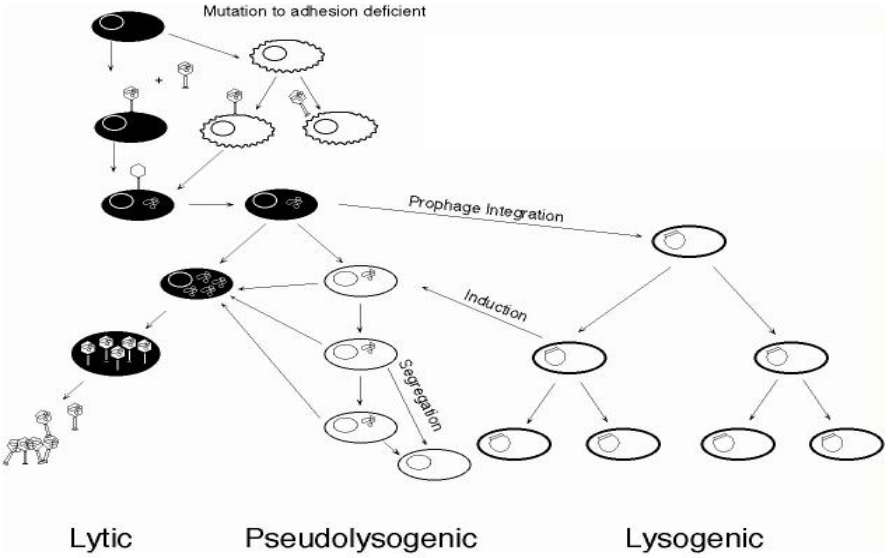

When a virus infects a cell, the infection can result in cell lysis (black ovals). However, temperate phages can have their Genomes integrated and exist as a "lysogenic" silent viral infection (right side of figure).

Figure 4. The three different pathways available to a phage upon infection of a bacterium.

Most likely, pseudolysogeny is caused by a mixture of sensitive and resistant host cells in the culture. The resistant cells may lack the outer membrane receptors that phages use when adsorbing to a host cell (Figure 4). An experimental result from Moebus (1997) studying pseudolysogeny in H24, a marine bacterium, appears to support this theory. The wild-type strain of H24 had a turbid culture but the bacterial lawns were lysed, a result that agrees with the Ackermann and DuBow definition of pseudolysogeny. Moebus also found that nutrient starvation did not affect pseudolysogenic cultures disproving Ripp and Miller's theory of pseudolysogeny. Moebus hypothesizes that one of the factors that may promote pseudolysogeny is the production of an extracellular polysaccharide that binds to the outside of host cells and prevents phage adsorption, however this has yet to be proven.

1.2.4 ϕHSIC

ϕHSIC was first isolated from Mamala Bay in Oahu, Hawaii in 1994 from turbid plaques on HSIC, a marine bacterium. It was isolated as part of a study to characterize temperate phage-host systems in the marine environment (43). The host bacterium has been identified as *Listonella pelagia*, a gram-negative bacterium that was previously known as *Vibrio pelagius* (57). Strains of *L. pelagia* have been show to produce tetrodotoxin, a powerful neurotoxin typically found in animals in marine habitats (90). Other members of this taxon have been shown to produce an extracellular protease that is detrimental to fish and have been implicated in mass mortalities of juvenile turbot (26, 103). Clearly, *L. pelagia* is an important marine bacterium that requires further study to determine its pathogenicity mechanisms as well as means of neutralizing it.

When ϕHSIC was first isolated, it was characterized and its infection cycle studied. Electron microscopy showed that ϕHSIC had a long, flexible, noncontractile tail that was typically 146 ± 3.7 nm and a head size of 47 ± 3.7 nm leading to grouping ϕHSIC in the *Siphoviridae* family (43).

Initial studies showed that ϕHSIC DNA was in the host cell but a probe made with ϕHSIC DNA did not hybridize to *L. pelagia* chromosomal DNA indicating that the phage had not integrated (43). Based on these and other results, ϕHSIC was characterized as a temperate phage. When ϕHSIC was further studied, it was discovered that it was in an unstable relationship with *L. pelagia*, and the host lost the virus. The host was re-infected with the virus using the plate survival method which allowed for the isolation of both an infected strain, HSIC, and an uninfected strain, *L. pelagia* (116). In this phage-host

system, HSIC was found to have integrated into the host genome (116). Differences in colony morphology between the infected and uninfected strains were noticed. Uninfected *L. pelagia* has a smooth round colony while the infected strain gives rise to colonies that are flat and crinkly.

Due to the isolation of both ϕHSIC and *L. pelagia*, the relationship between the phage and the host in the re-infected system was characterized as well. Growth curves of the infected host showed a sigmoidal growth curve, a characteristic of pseudolysogenic cultures (67, 116). Constant phage production was observed in the culture, as well, another hallmark of a pseudolysogenic infection (67).

Homoimmunity was observed in the cultures and Southern blot analysis indicated that ϕHSIC integrated into the host genome, both traits of a lysogenic infection. However, induction studies with ϕHSIC showed that the prophage could not be induced with either mitomycin C or naphthalene, a polyaromatic hydrocarbon that is capable of inducing many prophages (116). All of this plus the fact that ϕHSIC has such a low adsorption coefficient, 1.05×10^{-6} mL^{-1} min^{-1}, led to the conclusion that ϕHSIC is a pseudolysogenic phage.

1.2.5 Lysogeny in the Marine Environment

Lysogeny in the marine environment and its effect on the marine microbial population has been a subject of debate for years. Due to the unique role of temperate phages in the marine environment, in that they replicate every time the host cell replicates, it is important to determine the extent of the role that lysogenic phages play in marine microbial communities. The main reason that this has been problematic is that many

marine bacteria are non-culturable and there is no definitive way to accurately estimate the role of lysogeny in the marine environment. Additionally, several studies have yielded dissimilar results which has led to conflicting opinions about the role of lysogeny in the marine environment (75, 95, 108, 121).

Initial studies focused on determining the percent of the bacteria that had inducible prophages. Samples were collected from different marine environments and subjected to different induction treatments, typically mitomycin C or UV radiation. One of the first comprehensive studies looking at this in nearshore and offshore environments found that 0.07 to 3.0% of the bacteria examined were lysogenic and that there was no difference in induction between the two different environments even though one was oligotrophic and the other eutrophic (108). The viral populations only increased when the bacterial population went above 10^6 cells mL^{-1} (108). It was concluded that lysogenic infections were not a significant source of mortality for marine microbes, and that cycling and flow of matter were more affected by lytic infections.

However, Jiang and Paul (1994) found that 43% of the bacterial isolates obtained from the Gulf of Mexico contained inducible prophage. Additionally, Ackermann and DuBow (1987) looked at 1200 different bacterial isolates to determine how many contained an inducible prophage. They discovered that almost 50% of the isolates had prophages. In an attempt to elucidate the effects of lysogeny on marine microbes, Jiang and Paul (1998) looked at isolates from the Atlantic and Pacific Oceans. One hundred and sixteen bacterial isolates were treated with mitomycin C and UV exposure, in separate experiments, they discovered that over 40% of the isolates had phage-like particles when

examined under electron microscopy, and the greatest percent of the isolates with inducible prophages were from an oligotrophic environment (41).

Using viral decay rates and abundance measurements, the lysogenic contribution to viral production in Tampa Bay was estimated to be 1.8×10^{-6} to .018% (42). In an oligotrophic environment, they estimated that 2×10^{-5} to 0.02 % of viral production was from lysogens. As that is less than what the lytic fraction contributes, the lysogenic cycle is not as important as the lytic cycle in the production of phage particles.

Methods have changed and new protocols have been developed in the hopes of accurately estimating the proportion of the marine bacterial community that is lysogenic. In 2002, it was discovered that natural populations of autotrophic picoplankton such as *Synechococcus* are lysogenic (62). A *Synechococcus* bloom in 2002 allowed for the unprecedented study that looked at the lytic viral production and prophage induction in both autotrophic and heterotrophic bacteria. Viral lysis removed 27% of heterotrophic productivity and 1% of autotrophic productivity (75). Astonishingly, 80% of the heterotrophic bacteria were inducible with mitomycin C while 0.6% of the cyanophages specific for a specific host, WH7803, were inducible (75).

These results were much higher than those previously obtained and were somewhat unexpected. However, the samples were exposed to both sunlight and had a high growth rate, both of which can cause induction, as well as mitomycin C which may explain why the rates were so high (75). Under natural conditions in the marine environment, it is possible that there is not nearly as much induction. The most important result of this study, however, was the conclusion that perhaps it is the composition of the microbial

community and not the trophic state that affects lysogeny. Similar results were obtained in a study measuring rates of viral production in the Gulf of Trieste (95).

Marine bacteria are typically in a state of starvation and host cell density is low. Under nutrient limitation conditions, it makes sense that lysogenic phages would refrain from entering the lytic cycle as a survival strategy. Environmental cues that favor lysogeny in the marine environment have been studied as has inorganic nutrient flux, salinity, and temperature (81, 119).

Bratbak et al. (1993) found that, in a mesocosm deprived of phosphate, viruses that infect *Emiliania huxleyi*, a marine coccolithophore, had reduced development while viruses in mesocosms lacking nitrate showed no effects of inorganic nutrient starvation. Changes in cyanophage production, titer, and adsorption kinetics were also seen when a culture of *Synechococcus* WH7803 went from phosphate replete conditions to phosphate limited conditions (119). In phosphate depleted conditions, 9.3% of WH7803 cells grown in phosphate depleted conditions released viruses while 100% of the WH7803 cells grown in replete conditions released phages. However, the adsorption kinetics had similar contact and adsorption rates in the treatment compared to the control. Taken together, the one-step growth and adsorption kinetic experiments showed that while 90% of the phage absorbed to the host cell under all conditions, not all produced cyanophage progeny. It is possible that the viruses that produce progeny entered a lysogenic state instead, a theory that is supported by the results of the plaque assays using cells grown in depleted conditions (119). The most likely explanation for these findings is that since viruses have a high nucleic acid to protein ratio (~50% DNA by weight), a phosphate limitation would affect them severely when viral DNA replication is occurring (81, 119).

Numerous studies have been done on viral production but there are conflicting results. For example, in one seasonal study conducted in the Tampa Bay estuary, lysogeny was seen from November through February while induction events were more likely to occur after February, when the water temperature had risen above 19° C (18). Conversely, a later seasonal study in Tampa Bay found that 73% of the induction events in the heterotrophic samples occurred during the time that bacterial production was the lowest, i.e. the winter (117). The same seasonal trend in lysogeny was also observed in autotrophic samples studied at the same time (62). A possible explanation for the trend observed in the later seasonal study is that during the summer months, virus production may be more likely to undergo the lytic pathway because host cell density is high as are nutrient levels. In addition, increased UV radiation and water temperatures could act as inducing agents.

1.3 Genomics

The genome sequencing era began in the 1970s when the genomes of phi-X174, a bacteriophage that infects *E. coli*, and MS2, an RNA virus, were completed (88). In the ensuing years, the cost of sequencing has decreased while technology and data processing abilities have increased. Genome sequencing is common, and technologies have been developed to measure gene expression and factors that affect it.

1.3.1 Marine Viral Genomics

As of May 2006, there were 362 bacteriophage genomes catalogued in GenBank. Many of the marine phage genomes in GenBank have genes that have no hits in GenBank

and are classified as unknown or hypothetical. There is a need not only for additional marine phage genome sequencing so that scientists can better understand factors that affect marine phages but also for dedicated studies on the cryptic genes to elucidate their function.

Some notable examples of marine viruses whose genomes have led to a greater understanding of marine phages include the cyanophage P60, EhV-86 which infects *E. huxleyi*, ϕJL001 isolated from a sponge-associated bacterium, and ϕHSIC (15, 52, 82, 120). P60 and EhV-86 are both lytic viruses whereas ϕJL001 is a temperate phage with some pseudotemperate characteristics and ϕHSIC is pseudotemperate with temperate characteristics.

When the genome of ϕJL001 was compared to other phages, the genome was discovered to be highly mosaic with hits to other viruses, bacteria, and eukaryotes. The mosaic trend has been observed in both temperate and virulent phages (11, 33, 34, 52, 82). Finding this trend in marine phages such as ϕJL001 and ϕHSIC lends support to the theories of modular phage evolution and indicates that marine phages may have shared the same global gene pool as other phages such as those that infect *Streptococcus thermophilus*, a dairy bacterium (11).

P60 is a lytic podovirus that infects *Synechococcus*, and is organizationally similar to T7, a terrestrial podovirus. However, P60 is also similar to another marine lytic podovirus, roseophage SIO1. DNA replication genes in P60 were similar to the replication genes found in terrestrial phages like T7 and YeO3-12 (15). EhV-86 is a lytic virus that infects eukaryotic algae but it has genes more commonly seen in higher-level

animals and plants. Neither genome exhibits mosaic behavior but they do appear to have evolved from terrestrial phages.

While the genomes of P60, EhV-86, ϕJL001, and ϕHSIC have shed some light on marine phages, more marine phage genomes are necessary to truly understand marine phages. This is difficult because almost 99% of the total marine bacterial population are viable but not culturable (87). If the bacterial hosts cannot be isolated, then marine phages cannot be isolated and maintained. One way to circumvent this problem is to concentrate water samples, and then sequence the genetic material in the sample producing what is known as a metagenome or metavirome, depending on the final goal. The two most notable examples of this were done off the coast of California, and in the Sargasso Sea (9, 99).

Environmental sequencing of the Sargasso Sea was done to establish the bacterioplankton composition of the environment and understand the abundance of organisms as well as distribution. As bacteriophages were not emphasized, no special methods were used and only double-stranded DNA bacteriophages were picked up during the study. Almost one-third of the greater than 10kb scaffolds were similar to genes of already sequenced phages that infect *Burkholderia* and *Shewanella* species, which were the predominant members of the sequenced bacterioplankton fraction. In addition, most of the phage sequences were matches to either lytic phages, most commonly the KVP40 phage which infects *Vibrio*, or an archaeal phage that infects *Sulfolobus islandicus* (99).

In 2002, samples from two different locations off the coast of California were concentrated and viral DNA recovered from each by a cesium chloride gradient to produce a "metavirome" or uncultured viral community genomes. Viral DNA was

sheared and ligated before being amplified and electroporated into MC12 cells to make linker-amplified shotgun sequence libraries. The clones were sequenced and the metaviromes from the two different locations compared to one another (9). In this way, sequence fragments were generated so that while no complete phage genome could be generated, at the very least, when these sequences were compared to GenBank, it could be determined what kind of phages were present and their abundance.

Unfortunately, most of the generated sequences had no significant hits to any of the phages genomes archived in GenBank. Sequences that did have significant hits were most significant to Roseophage or previously sequenced Podoviruses (9). In general, the community composition between the two sample sites was noticeably different with Podoviruses being the dominant member at one site and Podoviruses and Siphoviruses being equally dominant at the other site. Using mathematical models, the authors were able to predict that there were anywhere from 423 to 3,318 viral genotypes at the site that had less tidal flushing and algae. At the site that experienced daily tidal exchanges and had a greater population of algae, it was predicted that there were 374 to 7,114 viral genotypes (9). These experiments provided the first estimates of viral diversity in the marine environment and that viral community structure does indeed change from niche to niche as had been suspected (75, 112).

1.3.2 The Genome of ϕHSIC

In 2004, the complete genome of ϕHSIC was sequenced and annotated. ϕHSIC has 37,966 nucleotides with 47 putative open reading frames, and the G+C content is 44% (82). Pulsed-field gel electrophoresis and restriction analysis proved that it is a circularly

permuted genome. As there is no easily recognized point of termination in the genome, but there are putative terminases, it is believed that ϕHSIC uses the headful packaging mechanism similar to that of Sf6, a phage that infects *S. flexneri* (82).

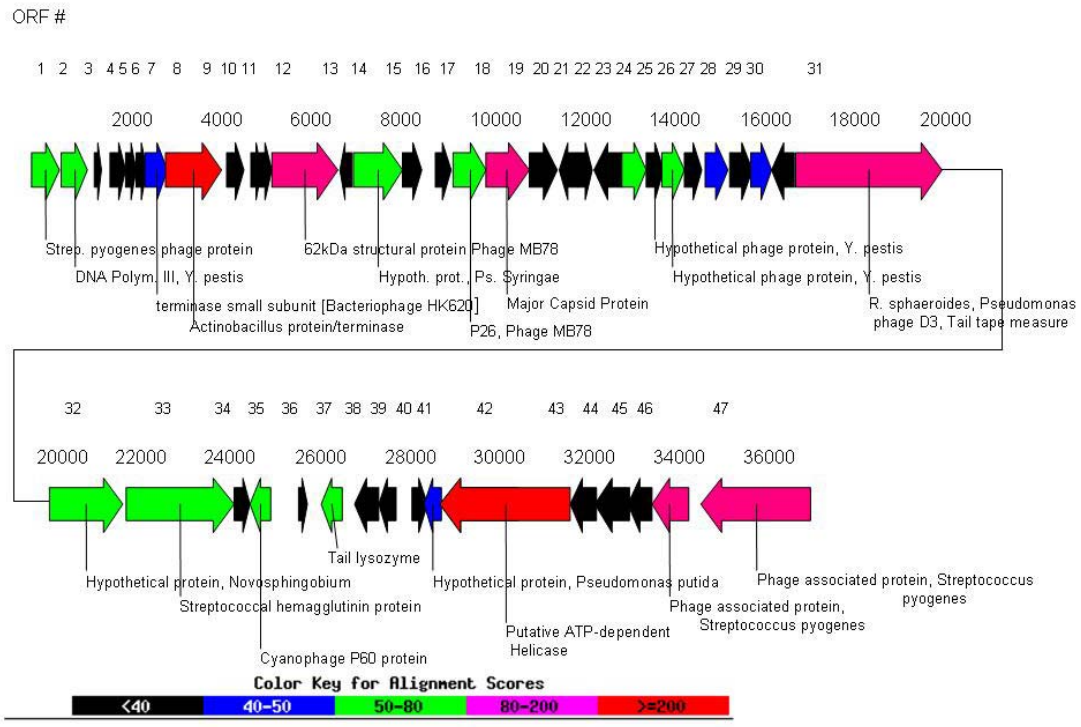

Figure 5. Color map of the ϕHSIC genome. Coloring of ORFs represents the BLASTP score used by the National Center for Biotechnology Information (www.ncbi.nlm.nih.gov/blast) (red, >200; magenta, 80-200; green, 50-80; blue, 40-50; black, 0-40). Numbers above the figure are the ORF numbers, the second row of values indicates base pair location.

There are left-oriented and right-oriented blocks of genes, as observed for other temperate phages (Figure 5) (55). Of the 47 ORFs, 17 have e values less than 0.001 (Table 1). Putative ORFs include a fragment of a DNA Polymerase III (ORF 2), the small and large subunits of the terminase protein (ORFS 7 and 8) which packages concatameric

DNA into phage heads using ATP, and the major capsid protein (ORF 18), a function later confirmed by MALDI TOF-TOF protein analysis (82). There are also ORFs that encode for a putative tail tape measure protein (ORF 31) used for assembling a tail of correct length, a tail lysozyme (ORF 37), and a helicase (ORF 42) which can unwind and transport DNA. Many of the ORFs have hits to unidentified genes from other phage sequencing projects including *Y. pestis* phages. However, they were all distant relationships and no conclusions could be drawn about the function of the genes.

In fact, many of the genes could not be assigned functions because of the lack of biochemical characterization of existing phage genomes. This is not unexpected as other marine phage genomes have few genes that can be assigned function based solely on BLAST searches (15, 52, 120). Re-BLASTing the genes has been performed periodically with little to no change in gene annotation. However, 60% of the ORFs that had significant similarities to those in GenBank were related to temperate phages and four of the 20 ORFs with hits were related to lytic genes (82). Phages that infect *S. pyogenes*, *S. aureus*, and *B. pertussis* as well as cyanophage P60 were just a few of those hits indicating that ϕHSIC has engaged in horizontal transfer like other temperate phages, marine and terrestrial leading to its mosaic genome (Table 1).

To better understand marine phages in the natural environment and study the factors that affect them, more phages must be isolated. However, just having the genome is an important step and studies of gene expression under varying environmental conditions will lead to a more complete understanding of these processes.

Table 1. Open Reading Frames of the ϕHSIC genome and best BLASTP hits

ORF	Nucleotide Position	Best BLASTP Hits, (expect values)
1/+	2-625	Hypothetical protein, *Streptococcus pyogenes*, (3e-04); ORF188, *Lactobacillus* phage ϕAdh (0.001)
2/+	679-1254	DNA Polymerase III, Beta Subunit (7e-6)
3/+	1393-1542	Unknown
4/+	1757-2101	Unknown
5/+	2095-2328	Unknown
6/+	2374-2568	Unknown
7/+	2586-3029	Terminase small subunit [Bacteriophage HK620], (0.009)
8/+	3010-4236	Phage terminase [*Actinobacillus pleuropneumoniae* serovar 1 str. 4074], (e-100); large terminase [*Staphylococcus aureus* phage phi 11], (8e-30)
9/+	4354-4719	Unknown
10/+	4874-5107	Unknown
11/+	5104-5325	Unknown
12/+	5372-6799	Structural protein, *Salmonella* phage KS7, (8e-27); 60kDa Structural Protein, *Salmonella typhimurium* phage MB78, (2e-20)
13/-	6829-7110	Unknown
14/+	7182-8252	Hypothetical protein, *Salmonella* phage KS7, (6e-23); Head morphogenesis protein, *Pseudomonas syringae*, (1e-16)
15/+	8258-8662	Unknown
16/+	8984-9313	Unknown
17/+	9382-10,086	Hypothetical protein, *Salmonella* phage KS7, (9e-6); P26, *S. typhimurium* phage MB78, (1e-5)
18/+	10098-11045	Hypothetical protein, *Pseudomonas fluorescens*, (5e-113); putative phage protein, *Y. pestis* minor capsid, (e-103)
19/+	11173-11669	Unknown
20/-	11702-12130	Unknown

Table 1 Cont.

ORF	Nucleotide Position	Best BLASTP Hits, (expect values)
21/+	12164-12445	Unknown
22/-	12474-13058	Unknown
23/+	13153-13650	Hypothetical protein, *Salmonella* phage KS7, (9e-10); Hypothetical phage protein, *Y. pestis*, (5e-9)
24/+	13654-14052	Hypothetical phage protein, *Y. pestis*, (0.073)
25/+	14027-14485	Hypothetical phage protein, *Y. pestis*, (4e-7)
26+	14485-14868	Unknown
27/+	14985-15461	Unknown
28/+	15530-16012	Unknown
29/+	16024-16428	Unknown
30/-	16452-16928	Unknown
31/+	17022-20231	Probable tail tape measure, lambda family, *R. sphaeroides*, (1e-21); Putative phage tail tape measure protein, *Acinetobacter* Sp ADP1, (1e-16); ORF19 *Pseudomonas* phage D3, (5e-16); phage tail tape measure protein, lambda family, (3e-15)
32/+	20231-21817	Hypothetical protein, *Silicibacter*, (3e-17); Hypothetical protein, *Novosphingobium* (6e-13)
33/+	21870-24275	Streptococcal hemagglutinin protein, *Staphylococcus epidermidis* (2e-6)
34/+	24308-24643	Unknown
35/-	24648-25079	Conserved hypothetical protein *Candidatus Pelagibacter ubique* (Sar 11), (1e-9); Cyanophage P60 protein, (7e-7)
36/+	25708-25905	Unknown
37/-	26214-26672	gp5 Baseplate hub subunit and tail lysozyme , *Aeromonas* phage 31, (2e-11); gp5 Baseplate hub subunit and tail lysozyme, phage 44RR2.8t, (2e-11); lysozyme murein hydrolase, Bacteriophage 44RR2.8t, (1e-8)
38/-	26940-27488	Unknown
39/-	27485-27829	Unknown

Table 1 Cont.

ORF	Nucleotide Position	Best BLASTP Hits, (expect values)
40/+	28235-28564	Unknown
41/-	28476-28859	Hyp. Protein Bacteriophage JK06 (Siphoviridae), (7e-6); Putative phage morphogenetic protein of enterobacteriophage P1, (0.001)
42/-	28856-31717	Putative Helicase, *Erwinia carotovora,* (4e-81) Putative ATP-dependent Helicase, *E. coli,* (4e-80); Helicase precursor, *Deinococcus radiodurans* (3e-20)
43/-	31723-32265	Unknown
44/-	32262-33017	Unknown
45/-	33017-33550	Unknown
46/-	33557-34315	Cons. Hyp. Protein, phage associated, *Magnetococcus*, (5e-22); *Bacillus clarkii* bacteriophage BEJA1c, (3e-18); Phage associated protein, *Streptococcus pyogenes*, (3e-16)
47/-	34641-37088	Hyp. Protein, *Pelobacter propionicus*, (4e-17); Plasmid/phage primase, *Clostridium thermocellum* (3e-13); Integrase, Vibriophage VP2, (3e-10); Primase, *Bordatella* phage BP-1, (3e-08); phage protein, *S. pyogenes* (3e-08)

1.3.3 Gene Expression Analysis

Genome sequences can show how the genes are organized but they cannot explain the function of particular genes or how they work in tandem with other genes. Gene expression analysis has developed alongside genome sequencing and, as a result, there are several methods to analyze gene expression. They include northern blots, RT-PCR, cDNA fingerprinting, and clone hybridization (51). None of these techniques allow for easy analysis of an entire genome at once, and array technology was developed to combat this shortcoming. Subtractive hybridization arrays use single-color labeled DNA or RNA whereas competitive hybridization arrays, typically microarrays, utilize a two-color

process. The labeled cDNA is hybridized to a comprehensive non-redundant DNA sequences or oligonucleotides immobilized on a solid support (51). The probe can either be labeled with a radioactive isotope such as ^{32}P or ^{35}S, or nonradioactive labels such as Biotin-16-dUTP, which allow for chemiluminscent detection. The level of fluorescence measured at each spot represents the relative level of the transcript in the cDNA probe that corresponds to the dot (51). The membrane is then imaged to determine levels of hybridization (Figure 6).

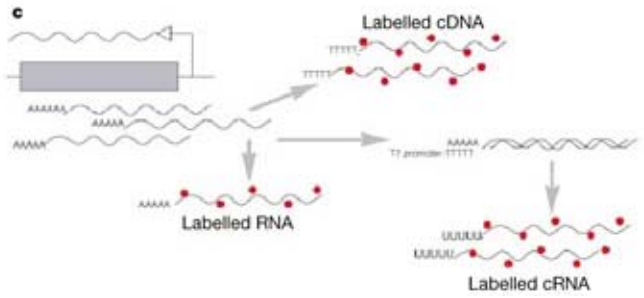

Figure 6. Reprinted by permission from Macmillan Publishers Ltd: Nature 405: 827-836, copyright 2000. Illustration of probe production for array hybridization. Biotin-16-dUTP ($C_{32}H_{48}N_7O_{18}P_3SLi_4$) can be used to replace dTTP as the cDNA is synthesized from RNA by reverse transcription. To detect biotin labeled cDNA that has hybridized to a blot, streptavidin-alkaline phosphatase conjugate and CDP-Star, a chemiluminscent substrate, are used to detect.

While there have been no expression analyses done on marine bacteriophages, array studies with other phages have had interesting results. Not only have array studies led to the classification of phage genes into temporal classes such as early, middle, and late but they have also helped determine if predicted genes that have no matches in GenBank are actually being expressed over the course of an infection (25, 54, 120). Comparisons of

two phages that infect the same host showed that genes that code for DNA replication and transcriptional regulation were expressed at different times in the infection cycle (25). In addition, studies examining host gene expression and viral gene expression throughout the same experiment have shown that unexpected host genes such as those responsible for responding to acid stress can be upregulated or downregulated as a result of the phage infection (16, 28, 44).

Arrays are a powerful tool for measuring gene expression in both bacteria and viruses. Combined with genome sequencing and studying phage genes in a marine community, they will allow for a more complete understanding of marine phage genomics and environmental conditions that influence gene expression.

Chapter Two

Macroarray Analysis of Gene Expression in a Marine Pseudotemperate Bacteriophage

Abstract

The isolation of ϕHSIC-1a and its host, *Listonella pelagia*, from Mamala Bay, Oahu, Hawaii has allowed for the characterization and sequencing of the first marine pseudotemperate bacteriophage. The genome of ϕHSIC-1a is circularly permuted and is 37, 966 nt in length. There are 47 putative open reading frames (ORFs). Biochemical substrate utilization was studied using Biolog testing. Differences between uninfected *L. pelagia* and the HSIC-1a strain indicated that certain pathways are up-regulated upon infection of the host cell by ϕHSIC, while others are repressed. Primers were designed to amplify approximately 300bp from each ϕHSIC open reading frame by PCR. To evaluate the gene expression patterns of this phage, ϕHSIC-1a macroarrays were generated by dotting each amplicon onto a filter membrane. Viral gene expression over the course of an infection cycle was examined as was gene expression in the HSIC-1a pseudolysogen grown at normal (39 ppt) and low (11 ppt) salinity. Gene expression was significantly higher in the 39 ppt treatment than in the 11 ppt treatment in two experiments. Free phage and intracellular phage concentrations were significantly lower in the low salinity treatment. The results of these experiments indicate that changes in environmental conditions, such as lowered salinity, lead to lysogeny in the HSIC-1a pseudolysogen.

These experiments have provided a window into the expression of the ϕHSIC phage genes in response to environmental changes, and may be a model for how phages and their hosts respond to changing conditions in the oceans.

2.1 Introduction

Genomic sequencing can provide valuable information on genome organization, putative gene content, evolutionary relationships between organisms, and metabolic pathways. However, information on regulation and expression cannot be gleamed from sequence information alone. Techniques such as Northern blotting and RT-PCR have been used to detect and measure levels of phage gene expression (28, 96, 100). These techniques are limited to the study of a few genes at any one time. As such, array technology has been developed to study whole genome expression in an organism.

Analysis of viral gene expression by use of array technology has led to the mapping of the entire infection process over the course of a lytic infection (25, 54, 89). In addition, many viral genes have no counterparts in genetic databases and no conclusions can be drawn about their function. Data from expression analysis of a viral genome can allow for preliminary classification of unknown genes by comparing the initial time of expression and changes in expression for unknown genes to the known genes around it (54). Finally, viral genome expression analysis may lead to the use of antisense RNA to develop anti-phage treatments that can prevent phage infection, thereby reducing the negative effect that phage can have on bacteria (25).

ϕHSIC, a temperate phage with pseudotemperate characteristics, was one of the first marine phages to be sequenced (43, 82, 116). ϕHSIC infects the bacterium *Listonella pelagia* and the infected strain is known as HSIC-1a pseudolysogen. Growth of the pseudolysogen is characterized by sigmoidal growth curves with high production of phage particles (>10^{10} mL^{-1}) (66-68). Probing of southern transfers of host genomic DNA indicated chromosomal integration of the prophage yet phages were not inducible by Mitomycin C (116). Infected cells were also homoimmune, a hallmark of lysogeny. Genomic sequencing did not yield any recognizable lysogeny genes. In fact, only 9 of 47 genes could be assigned a putative phage function (large and small terminase subunits, β-subunit of DNA polymerase, capsid protein, tail tape-measure protein, lysin, helicase, and resolvasome helicase) (82). In an effort to putatively identify the function of more genes, we initiated expression analysis by macroarray studies.

Salinity is thought to influence viral lysis in other phage-host systems. Most of the studies have focused on dairy phages and only two have extensively examined environmental phages. Additionally, the results of the different experiments disagree with one another. For example, studies with lysogenic strains of *S. thermophilus* showed that when sodium chloride concentrations were increased beyond the cell's normal range, lysis occurred almost immediately. Bacteriophage fragments were observed with electron microscopy indicating that the bacteriophages produced were not stable (37). However, increased concentrations of sodium chloride led to an increase in the phage latent period during induction experiments with *Vibrio* spp. (30).

Induction studies with CTXϕ, a phage that infects *V. cholerae*, showed that when the salinity was at or below 0.1% (w/v), the majority of transducing particles were

inactivated. CTXϕ was most stable at salinities above 0.5%. Additionally, the frequency of spontaneous induction of ϕLC3, an *L. lactis* phage, significantly decreased as the osmolarity of the solution was increased from 0 to 1.0%. This indicates that the stability of the prophage was increasing as salinity increased (27, 56). High induction rates were also observed at high salinities.

Salinity experiments with the ϕHSIC/ *L. pelagia* marine phage-host system have shown that growth and phage production were stimulated at high salinities and depressed at low salinities (114). Since this provided us with a method to experimentally manipulate the lysogenic response in this organism, we reasoned that gene expression studies might help identify genes involved in lysogeny in this phage-host system.

Macroarrays have been successfully used to study a number of different organisms including the bacteriophage Xp10, *S. meliloti* and *L. lactis* as well as microbial gene diversity in environmental samples (3, 5, 39, 89, 92). While they are not as sensitive as microarrays, they are less expensive to produce, require less instrumentation to analyze, and previous studies have shown that gene expression levels can be quantitatively measured (3, 5, 89, 91, 124, 125). To better understand the molecular lysogeny switch in a marine phage and to understand lysogeny in the marine environment, macroarrays were used in this study to map the infection cycle of ϕHSIC during a synchronous infection, and to study ϕHSIC gene expression in normal and low-salinity conditions. We also examined metabolic differences between *L. pelagia* and HSIC-1a.

2.2 Materials and Methods

2.2.1 Cultivation and Growth of *L. pelagia* and the HSIC-1a pseudolysogen

ϕHSIC was isolated from Mamala Bay, Oahu and infects *L. pelagia*, a marine heterotrophic bacterium (43). The uninfected host strain is known as the *L. pelagia* strain and the infected strain is referred to as the HSIC-1a pseudolysogen. The HSIC-1a pseudolysogen is a second generation lysogen as the first generation, HSIC-1e, was unstable and the virus segregated from the host (116). All experiments were conducted at 28° C in a bench-top incubator with shaking at 150 RPM and all plates were incubated at 28° C. To alter the salinity of the media, the amounts of NaCl and $MgSO_4 \bullet 7\ H_20$ used to make ASWJP+PY were either halved (22 ppt) or quartered (11 ppt) (Appendix A). The salinity of the media used for ASWJP+PY plates and overlay tubes was 39 ppt.

2.2.2 Biolog Measurements

Differences in carbon metabolism between *L. pelagia* and HSIC-1a were identified using Biolog's Microlog bacterial identification system™ for gram negative bacteria. A single colony of each culture was streaked onto Biolog's BUG (Biolog Universal Growth) + 5% sheep's blood and incubated overnight at 30°C. Each isolate was suspended in Biolog's inoculating fluid for a final transmittance of 52% as measured by a turbidimeter. The turbidity value was set by Biolog. One hundred and fifty microliters of the suspension was pipetted into each well of a 96 well GN2 Microplate™. The plates were incubated overnight at 30° C and read the next day by a Biolog plate reader using Microlog 3 software to score the plates.

2.2.3 PCR of Open Reading Frames

Forward and reverse primers were designed for all 47 ϕHSIC open reading frames using Primer 3 software (http://frodo.wi.mit.edu/cgi-bin/primer3/primer3_www.cgi). In addition, 16S rDNA primers were used to amplify host DNA for the positive control of RNA expression efficiency. Primer sequences are listed in Appendix C. PCR reactions for all the open reading frames except 7, 20, 30, and 42 had a total volume of 50 µL; 2 µL of HSIC template DNA at a concentration of 4.25 ng/µL, 1 µl (100 µM) each of both the forward and reverse primer, 25 µL of Promega PCR Master Mix 2X (Promega, Madison, WI), and 21 µL of sterile deionized water. The PCR Master Mix was comprised of 3 mM $MgCl_2$, 400 µM each of dATP, dCTP, dGTP, and dTTP, and 1.25 units of *Taq* DNA polymerase in a Promega proprietary reaction buffer.

Open reading frames 7, 20, 30, and 42 did not yield appreciable amplification and were cloned using Topo TA kit (Invitrogen, Carlsbad, CA). DNA was isolated from the cloned cells using the Promega Wizard Plus Miniprep DNA Purification. PCR was done to amplify the clones, the DNA was diluted to 5 ng/µL and 1 µL of the dilution was mixed with 1 µL (100 µM) each of the M13 forward and reverse primers (Invitrogen, Carlsbad, CA), 25 µL of Promega PCR Master Mix 2X, and 22 µL of sterile deionized water.

PCR reactions were heated at 95° C for two minutes to ensure template denaturation, and then 40 cycles of denaturation at 94° C for 45 seconds, annealing at the appropriate temperature for 45 seconds, and extension at 72° C for two minutes were done. There was a final extension at 72° C for ten minutes. Annealing temperatures for each ORF are listed in Appendix C. Reactions were confirmed using gel electrophoresis and purified

using a Zymo Clean & Concentrator™-25 kit (Zymo Research, Orange County, CA). Purified PCR products were quantified using the Hoechst 3328 method (80).

2.2.4 Macroarray Production

PCR products were diluted in RNase-free water. To denature the DNA, 10 mM EDTA and 0.4 M NaOH were added to the DNA and the mixture was then boiled for ten minutes. DNA was neutralized after boiling by the addition of an equal volume of cold 2 M ammonium acetate.

Macroarrays were produced by dotting 100 ng of each ORF in duplicate on charged nylon membrane (0.45 μm, Osmonics, Inc.) using a Bio-Rad 96-well dot blotter. The 16S rDNA positive control was spotted in every corner at a concentration of one nanogram per microliter. Due to space constraints (every ORF was dotted in duplicate and the four 16S rDNA positive control dots and two negative controls were included), not all the ORFs could be dotted on one array. The first 45 ORFs were dotted on one array while ORFs 46 and 47 were dotted in duplicate on a strip along with one 16S rDNA positive control dot and one negative control dot (Appendix C). A low vacuum was then used to pull the samples through the dot-blotter. Once all the liquid was through, 500 μL of 0.4 M NaOH was applied to neutralize the DNA. The filter was removed from the blotter and crosslinked using a UV crosslinker (FB-UVXL-1000, Fisher Scientific).

2.2.5 Control Blots

The purpose of the control blots was to verify that arrays were specific for phage DNA and to assess the precision of the method. To verify specificity, ORFs 7, 8, 9, 12, 18, 31,

33, 35, 37, 41, 44, and the *L. pelagia* 16S rDNA were dotted in triplicate on a 0.45 μm charged nylon membrane. Five mL of overnight culture of uninfected *L. pelagia* was transferred into 50 mL ASWJP+PY and cultures were grown at 28° C with shaking until the optical density of the culture was in mid-log phase between 0.400 and 0.600. The culture was split into two 25 mL samples to avoid overloading RNeasy columns with cellular material, and RNA was extracted. cDNA probes were made with 5 μg of RNA and hybridized to the blots overnight.

ORFs 17 and 42 were dotted twenty times each on a membrane along with four negative control spots and four 16S rDNA spots to test the precision of the method. Twenty mL of an overnight culture was transferred into 200 mL of ASWJP+PY. The culture was grown with shaking until the optical density of the culture was between 0.400 and 0.600, when ϕHSIC lysate was added to the culture for an M.O.I. of one. At 60 minutes post-infection, RNA was extracted from the culture. Five μg of RNA was used to make the cDNA probe and probes were hybridized to the blots overnight.

2.2.6 Synchronous Infection Experiments

Twenty-five mL of an overnight culture of uninfected *L. pelagia* was transferred into 250 mL of ASWJP+PY in a 500 mL flask. The culture was grown at 28° C with shaking. Absorbance was monitored and when the A_{600} was between 0.400 and 0.600, the flask was placed on ice for ten minutes to slow cell growth.

After ten minutes, ϕHSIC phage lysate with a known titer of 10^{10} was added for an M.O.I. of one. The culture was kept on ice for thirty minutes to allow adsorption. The culture was transferred into a Beckman centrifuge bottle and spun at 3020 X *g* for ten

minutes at 4° C to remove unattached phages. The supernatant was drained off and the pellet resuspended in an equal volume of ASWJP+PY.

The resuspended pellet was then transferred to a sterile 500 mL flask. Fifty mL of culture were immediately removed for the 0 minutes post-infection sample and RNA was extracted. The flask was placed back in the shaker at 28° C. Fifty mL samples were taken every twenty minutes for an hour and RNA was extracted.

2.2.7 Twenty-Four Hour Salinity Experiment

Nine 20 mL overnight cultures of HSIC-1a cells were combined into two 90 mL cultures and spun in a Beckman centrifuge at 3020 x *g*. Cultures were combined to ensure that the resulting pellet could be resuspended in a large volume for dilution. The supernatant was poured off, and the pellets were washed twice with sterile ASWJP to remove unattached phages. After the second wash, the pellets were resuspended in ten mL of either 22 ppt ASWJP+PY (1.5% w/v) or 39 ppt ASWJP+PY (3.1% w/v). The resuspended pellets were then diluted even further in the appropriate salinity media so that the initial A_{600} measurement was 0.05 at 600 nm. Both treatments were grown at 28° C with shaking.

Optical density measurements were taken once every hour for 24 hours to measure cell growth. Phage production in the two different treatments was measured by plaque overlays made every two hours starting at T_0. One mL of exponentially growing *L. pelagia* was mixed with a melted agar tube (Appendix A). HSIC-1a cells were serially diluted, and 100 µL from the last four dilutions was put in the melted agar overlay tubes

with the host and then poured onto a bottom agar plate in duplicate (Appendix A). Plates were incubated at 28° C overnight.

2.2.8 Gene Expression Analysis at Varying Salinities

Overnight cultures of HSIC-1a cells were combined into two samples, 90 mL each. Samples were then spun in a Beckman centrifuge at 3020 x *g* and the pellets washed twice with sterile ASWJP to remove unattached phages. After the second wash, the pellets were resuspended in 11 mL of either 39 ppt ASWJP+PY or 11 ppt ASWJP+PY (0.39% w/v). The resuspended pellets were then diluted even further in the appropriate salinity media so that the initial optical density of both cultures was 0.05 at 600 nm. Both flasks were grown at 28° C with shaking.

Optical density measurements were taken once an hour for 10 hours and again at 24 hours. To measure phage production in the different cultures, plaque overlays were made, in duplicate, every two hours starting at T_0. One mL of exponentially growing *L. pelagia* was mixed with a melted agar tube (Appendix A). The HSIC-1a culture was diluted and 100 µL from the last four dilutions was put in the melted agar tube with the host and the tube was then poured onto a bottom agar plate (Appendix A). Plates were incubated at 28° C overnight.

At T_4, T_6, and T_8, samples were removed for RNA extraction. Previous experiments indicated that RNA levels were highest at these time points and decreased as the experiment continued. There was also more cellular matter in the 39 ppt sample than in the 11 ppt sample leading to column overloading and loss of sample during RNA

extraction. To accommodate for that, two samples, two mL each, were withdrawn from the 39 ppt, and two samples, five milliters each, were withdrawn from the 11 ppt sample.

2.2.9 RNA Extraction

For all RNA extractions, the Qiagen RNeasy mini-kit protocol was followed with minor changes. Briefly, after the sample was spun for ten minutes at 10,000 x *g* at 4° C, the supernatant was poured off and the pellet dried. The cell pellet was then resuspended in 750 µl Buffer RLT that had been mixed with 10 µg/µl of β-mercaptoethanol (Sigma Chemicals, St. Louis, MO). If the resuspended pellet was to be used the same day, it was kept on ice until use. Otherwise, samples were stored in a -80° C freezer until the next day.

For the synchronous infection experiments, samples were mixed with muffled glass beads and bead-beaten for one minute, put on ice for one minute, bead-beaten for one minute, and then a final ice chill. In the salinity experiments, an additional bead-beating/ice step was added to ensure that the cell walls were being completely lysed.

After bead-beating was complete, the sample was spun down to pellet out the glass beads and transferred to a fresh 1.5 mL tube. Three hundred and fifty microliters of 100% ethanol was added before the sample was split and applied to two RNeasy columns (Qiagen, Valencia, CA). At that point, RNA was extracted following the Qiagen RNeasy Mini protocol for Isolation of Total RNA from Bacteria. The RNA was concentrated and cleaned-up using the Qiagen RNeasy Mini Protocol for RNA Cleanup and Optional On-Column DNase Digestion with the RNase-free DNase set. Quantification of RNA was

done with Ribogreen (Molecular Probes, Carlsbad, CA) according to the manufacturer's protocol.

2.2.10 cDNA Probe Production and Hybridization

cDNA probes were produced using the SuperArray TrueLabeling RT Kit (SuperArray Bioscience, Fredrick, MD) with one modification. Instead of using the gene-specific primer mix provided by SuperArray, random primers (Promega, Madison, WI) were mixed with the viral RNA sample to make the annealing mixture. The recommended amount of RNA for a probe was between 2.5 and 5 μg. For the synchronous infection experiments, 2.5 μg of RNA was used to make the probes. In the first salinity experiment, 4.5 μg RNA was used to make probes, and 2.5 μg of RNA was used in the second salinity experiment.

The SuperArray protocol using Biotin-16-dUTP (Roche Applied Bioscience, Indianapolis, IN) to label the cDNA was followed after the annealing mixture was made. Labeling efficiency was determined by the dilution method as recommended by SuperArray. If the probe had efficient labeling, it was mixed with SuperArray GEAhyb Hybridization Solution that had sheared salmon sperm at a concentration of 0.1 mg/mL. Sheared salmon sperm DNA (SuperArray Bioscience, Fredrick, MD) was diluted from 10 mg/mL to 0.1 mg/mL, heated at 100° C for five minutes, and mixed with the warmed GEAhyb hybridization solution. The SuperArray protocol for pre-hybridization, hybridization, and washing of the arrays was followed with some modifications. The volume of the reagents was doubled and the amount of hybridization solution was tripled. This was done to account for the size difference between the HSIC macroarrays and the

typical arrays used by SuperArray. All blots were put in hybridization tubes, and hybridization and washing were done at 60° C in a rotisserie style hybridization oven (Fisher Scientific, Pittsburgh, PA). After the probe was removed from the hybridization tubes, the blots were washed in a series of increasing stringency washes (2X SSC, 1% SDS and 0.1X SSC, 0.5% SDS) as recommended by SuperArray.

2.2.11 Chemiluminescent Detection of Arrays

The protocol for chemiluminescent detection was developed from the SuperArray protocol, and was done using their Chemiluminescent Detection Kit (SuperArray Biosciences, Fredrick, MD) using doubled reagent volumes. Briefly, blots were blocked and streptavidin-alkaline phosphatase was applied. Strep-AP was removed, the blots were washed, and CDP-Star was applied. Maximum emission of CDP-Star typically occurs two to four hours after application. As such, the blots were wrapped in Saran Wrap, placed in a drawer for two hours, and then placed on X-Ray film (Fisher Scientific, Pittsburgh, PA).

2.2.12 Array Analysis

Blot images were processed using the AlphaImager™ System (Alpha Innotech, San Leandro, California). X-Ray films were photographed using the AlphaImager camera system and converted to TIFF files. Spot density analysis was done using the AlphaEase FC© system. Blots were split into quadrants and the 16S rDNA and negative control specific to the quadrant were used for normalization in all experiments. For the synchronous infection experiments, the negative control served as the background image

and was manually subtracted from the spot density value. The subtracted value was then divided by the average 16S rDNA spot density to give the normalized value that was used in all further data analysis. For the salinity experiments, either the negative control or a blank spot on the blot served as the background value which was automatically subtracted from the sample spot density, and spot density was then divided by the subtracted 16S rDNA spot density to give a normalized expression value.

2.2.13 Identification of Promoter and Termination Sites

In the ϕHSIC genome, open reading frames located near one another had similar patterns of expression. This prompted us to manually search the genome for -10 and -35 promoter sites using FruitFly software (http://www.fruitfly.org/seq_tools/promoter.html). TransTerm software (http://www.genomics.jhu.edu/TransTerm/transterm.html) was used to examine the genome for putative termination sites.

2.2.14 Real-Time PCR

A Taqman probe was designed for ϕHSIC ORF 11 with a FAM molecule on the 5' end of the probe and a TAMRA~6~FAM molecule on the 3' end (Appendix C). Primers for ORF 11 were originally designed for PCR amplification for macroarray production and the same sequences were used for the real-time PCR (Appendix C). The Oligo Analysis and Plotting tool kit on the Operon web site (http://www.operon.com/oligos/toolkit.php) was used to check that the primers and the probe were not complementary or self-complementary.

Duplicate one mL samples were taken from the 11 and 39 ppt treatment at T_4, T_6, and T_8 during the second salinity experiment. Samples were spun for ten minutes at 10,000 rpm, the supernatant was aspirated off, and the pellet air-dried for five minutes. The dried pellets were then stored at -80° C until the DNA could be extracted. To extract the DNA, the Promega Genomic DNA extraction kit (Promega Madison, WI) protocol for gram negative bacteria was followed, and DNA was quantified using the Hoescht 3328 method (80).

A standard curve was made with diluted ϕHSIC DNA that ranged from 10^5 copies per reaction to 10^1 copies per reaction. DNA from all three time points was was diluted to 1:100 and 1:10,000 and duplicate reactions were done. Each reaction mixture was 0.25 µL (500 nM) of the forward primer, 0.25 µL of the reverse primer (500 nM), 0.05 µL (100 nM) of the probe, 25 µl of the Taqman master mix (Roche Applied Biosystems, Branchsburg, NJ), 5 µL of the template at the appropriate dilution, and 19.45 µL of sterile water for a total reaction volume of 50 µL. The PCR reactions were heated at 95° C for ten minutes to ensure template denaturation and then underwent 40 cycles of denaturation at 95° C for 45 seconds, annealing at 53° C for 1 minute, and extension at 72° C for one minute.

2.2.15 Growth Curves of Bacterial Cell Counts at Varying Salinities

To calibrate growth curves using A_{600} measurements, two overnight cultures of HSIC-1a, 90 mL each, were spun down at 3020 x *g* and washed twice with ASWJP to remove any unattached phages. After the second ASWJP wash was done, pellets were resuspended in 11 mL of ASWJP+PY of the appropriate salinity. The absorbance was

then measured, and the cultures further diluted so that the initial absorbance reading would be 0.05. Absorbance readings were taken once an hour for eight hours and five mL samples were withdrawn from both the 11 ppt and the 39 ppt treatments at T_2, T_4, T_6 and T_8. Samples were fixed with 0.02 μm filtered formalin at a final concentration of 1% and diluted to 1:100 with 0.02 μm filtered sterile ASWJP.

Bacterial abundance was enumerated by filtering 0.5 mL of sample onto 0.02 μm 25 mm Anodisc filters (Whatman Maidstone, England) followed by staining with Sybr Gold nucleic acid stain (1:10,000 final dilution) (70). Filters were stained for twelve minutes in the dark and mounted with an anti-fade solution composed of p-phenyldiamine in 50/50 filter-sterilized glycerol and phosphate-buffered saline.

Cell counts were then averaged and plotted against A_{600} measurements in Microsoft Excel. A first-order linear regression was done for both the 11 ppt and the 39 ppt treatment and the equation of the line was determined. Using absorbance readings from the first two salinity experiments, the bacterial cell counts were calculated for both experiments, and the ratio of plaque forming units to bacterial cells calculated. Additionally, the bacterial cell counts were used with real-time PCR data from the second salinity experiment to calculate the number of viral genomes per cell in the 11 ppt and 39 ppt treatments.

2.2.16 Effects of Salinity on Growth of Uninfected *L. pelagia*

As there were concerns that low salinity might affect host physiology, leading to the observed differences in cell growth between the treatments, growth curves were done using uninfected *L. pelagia* cultures at two different salinities. Five mL of an overnight

culture of uninfected *L. pelagia* was added to either fifty mL of 39 ppt ASWJP+PY (Appendix A) or fifty mL of 11 ppt ASWJP+PY (Appendix A), both in a 250 mL flask. Flasks were put in a bench-top shaker set at 28° C and shaken for 24 hours. Optical density measurements (600 n.m.) were taken every hour from T_0 to T_8 and again at T_{24}.

2.2.17 Statistical Analysis

To classify genes based on time of expression during the synchronous infection experiment, the highest normalized expression value was divided by the lowest normalized expression value for the ORF in question. The $\log_2$ of the ratio was then found to give the *M* value. If the *M* value was above 0.80, then there was a significant change in gene expression between those two time points and the ORF was grouped accordingly. Genes with the highest *M* value at 0 minutes post-infection were classified as early, genes that had the highest *M* values at either 20 or 40 minutes post-infection were classified as middle genes, and genes with the highest *M* values at 60 minutes post-infection were labeled late genes.

The number of plaque forming units for all three salinity experiments were first log-transformed before the statistical significance of the differences between the two treatments were calculated using paired t-tests in Minitab v. 13. Phage production and cell growth were plotted in SigmaPlot v. 8.0. Average normalized gene expression values for both salinity experiments were plotted in SigmaPlot v 8.0 and negative values were set to zero. The ratio of difference between the two salinity treatments was calculated in Excel by dividing the average normalized expression value for the 39 ppt treatment by the average 11 ppt treatment expression value and the $\log_2$ of the ratio was then

determined. If the $\log_2$ was greater than 0.80 or less than -0.80, there was a significant difference in expression between the two treatments (3, 24). All gene expression values that were equal to zero in the salinity experiments were set to 0.1 so that the $\log_2$ of the ratio could be done.

2.3 Results

2.3.1 Biolog Experiments

Phenotypic characterization of exponentially growing cultures of HSIC-1a and *L. pelagia* was performed using the Biolog GN2 MicroPlate™ system. The Biolog system uses colorimetric tests to determine which of the ninety-five carbon sources the organism is able to use for growth, and produces a metabolic fingerprint for the organisms. The percent difference between the scores in the two different plates was calculated by the following formula:

[((HSIC-1a - L. pelagia)/HSIC) * 100]

Uninfected *L. pelagia* was able to utilize 39 of the different carbon sources, while HSIC-1a utilized 38 carbon sources (Table 2). With some exceptions, the two strains were able to use the same carbon sources. Increases in utilization of carbon sources by the HSIC-1a was observed for thymidine, D-psicose, glycogen, L-histidine and γ-amino butyric acid. Conversely, *L. pelagia* was able to better utilize cellobiose, malonic acid, tween-80, L-proline, and mono-methyl succinate than HSIC-1a. Decreases in substrate utilization, detected by differences in pigment intensity between the host and lysogenic strains, were seen in 29 of the wells while increases were seen in 13 wells. In terms of change from utilization level (+ to /, / to -), the uninfected had increased utilization for six

substrates, whereas HSIC-1a only had three substrates of greater utilization. Notable increases in utilization by HSIC-1a occurred with glycogen and D-alanine.

Table 2. Biolog results for *L. pelagia* and HSIC-1a. Only ones that experienced a significant change are listed. * indicates that pigment was darker in the infected plate than in the uninfected plate. / indicates inconclusive results.

Carbon Source	*L. pelagia*	HSIC-1a	Raw Change	% Difference in carbon utilization
Dextrin	+	+	.	.
Glycogen	/	+	36	25.3
Tween 40	/	/	-26	-38.2
Tween 80	+	/	-38	-41.7
N-acetyl-D-glucosamine	+	+	-6	-1.9
L-arabinose	+	+	-34	-15.7
D-arabitol	+	+	-9	-3.9
Cellobiose	/	-	-37	-336.3
D-fructose	+	+	-44	-45.7
Gentiobiose	+	+	-9	-3.02
α-D-glucose	+	+	-1	-.31
Maltose	+	+	3	1.1
D-mannitol	+	+	1	.31
β-methyl-D-glucoside	+	+	-10	-3.1
D-psicose	/	+	7	6.5
L-rhamnose	+	+	-25	-12.0
Sucrose	+	+	-11	-3.6
D-trehalose	+	+	5	1.4

Table 2 Cont.

Carbon Source	*L. pelagia*	HSIC-1a	Raw Change	% Difference in carbon utilization
Mono-methyl Succinate	/	-	-20	-42.5
D-gluconic acid	+	+	-2	-0.64
β-hydroxybutyric acid	+	+*	-61	-40.9
D,L-lactic acid	+	+	-76	-42.4
Malonic acid	/	-	-39	-100
Quinic acid	+	+	-25	-16.8
Succinic acid	+	+	-44	-23.6
Bromo succinic Acid	+	+*	46	26.7
D-alanine	+	+	21	15.9
L-alanine	+	+	-39	-25.3
L-alanyl-glycine	+	+	-78	-55.7
L-asparagine	+	+	-76	-31.4
L-aspartic acid	+	+	-52	-19.1
L-glutamic acid	+	+	-85	-37.7
Glycyl-L-aspartic acid	-	-	-6	-35.2
Glycyl-L-glutamic acid	+	+	-8	-6.5
L-histidine	-	/*	55	98.2
L-proline	+	/	-90	-95.7
L-serine	+	+	8	-3.9
L-threonine	+	+	21	10.1
γ-amino butyric acid	-	-*	27	93.1
Inosine	+	+	11	-3.7
Thymidine	-	/*	52	96.2

Table 2 Cont.

Carbon Source	*L. pelagia*	HSIC-1a	Raw Change	% Difference in carbon utilization
Putrescine	+	+	-17	-14.0
Glycerol	+	+	-41	-17.2

2.3.2 Control Blots

To demonstrate that host cDNA was not hybridizing to the blots, RNA was extracted from uninfected *L. pelagia* and a cDNA probe was made. There was faint hybridization to three of the 11 ORFs dotted (ORFs 33, 35, and 37). We concluded that cross-hybridization was not as issue due to the lack of hybridization to other eight ORFS (Figure 7).

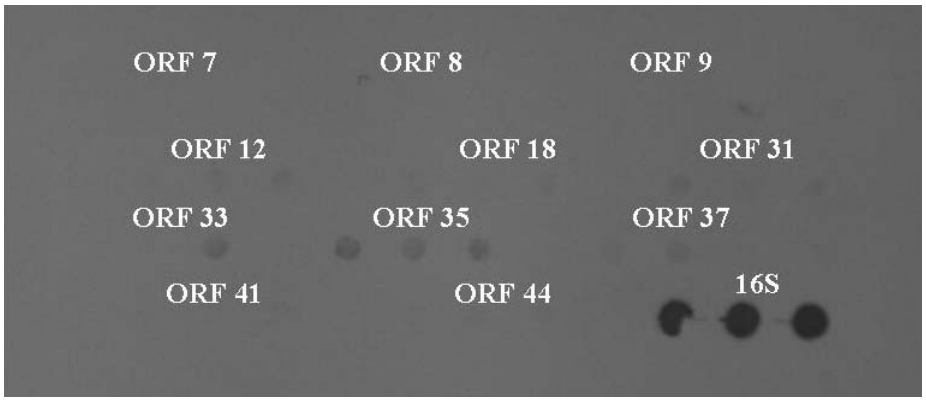

Figure 7. Control macroarray probed with a cDNA probe from *L. pelagia*, the host bacterium. ORFs were dotted in triplicate.

In order to test the precision of our method, ORFs 17 and 42 were dotted twenty times each on a nylon membrane as shown in Figure 8. These two ORFs were chosen because preliminary array studies had indicated that ORF 17 was highly expressed while ORF 42

was expressed at much lower values. In this experiment, ORF 17 was expressed at significantly higher levels than ORF 42 (p=<0.001). The coefficient of variation for ORF 17 was 1.5% and 2.5% for ORF 42. From these results, we concluded that this method was precise enough to measure varying levels of gene expression in hybridization experiments.

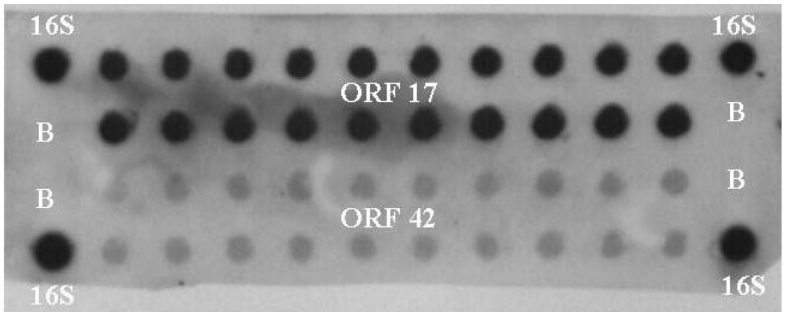

Figure 8. Blot showing the results of the dotting efficiency experiments. The top two rows are ORF 17 and the bottom two rows are ORF 42.

2.3.3 Synchronous Infection of *L. pelagia* with ϕHSIC

The design of synchronous infection experiments was such that all cells in the culture were being infected at the same time and rate. This ensured that secondary infections were not occurring in some cells while other cells were undergoing a primary infection. Background values, as determined by the negative control on each blot, were subtracted from the spot density of each dot. Subtracted dot values were then normalized to the *L. pelagia* 16S ribosomal DNA spot density for that particular quadrant of the blot. In this way, expression of each gene was compared to the 16S ribosomal DNA which was set as the maximum expression value. A typical blot is seen in Figure 9.

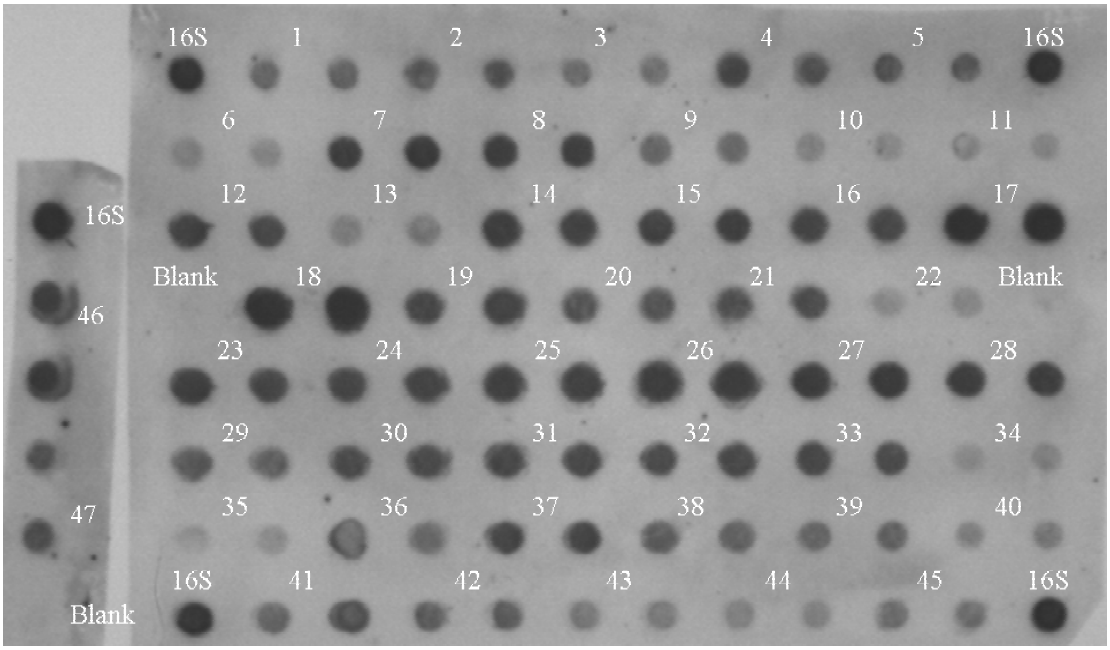

Figure 9. Array probed with cDNA from 60 minutes post-infection. Numbers indicate the ORF number and are located between the duplicate dots.

After obtaining the normalized values, generalized trends in expression were examined. Open reading frames that had high levels of expression throughout the experiment were 7, 15, 17, 23, 27, and 30. ORFs that started out with high levels and then decreased throughout the experiment were ORFs 1 through 6, 9 through 11, 22, 35, 39, and 40 through 48. ORFs 18, 19, 24, 25, and 26 all had the highest level of expression at 60 minutes post-infection.

To classify genes based on time of expression, we found the ratio of expression at the highest time point to the lowest expression value for each of the 47 ORFs. For example, the lowest level of expression for ORF 1 was seen at 60 minutes post-infection, while the highest expression value was seen at 0 minutes p.i. Therefore, the expression values from 0 minutes p.i. were divided by the 60 minutes p.i. value. The $\log_2$ of the ratio was then

calculated to give the *M* value. If the *M* value was ≤ -0.80 or ≥ 0.80, then the levels of expression were considered to be significantly different between the two time points (3, 24). *M* values for each ORF are listed in Table 3.

Admittedly, this method is designed for comparing gene expression levels in two treatments, and not over the course of an infection cycle. While most of the ORFs could have been classified according to the time-point at which expression was highest, several ORFs appeared to have no significant change in expression with time, and so the *M* value was necessary to determine if changes in expression were significant. In fact, twelve ORFs (7, 12, 15, 16, 17, 23, 27, 29, 30, 33, 37, and 46) did not have *M* values above the cut-off value; therefore expression levels for these ORFs did not significantly change over time. These ORFs were designated as continuously expressed. Half of these ORFs are structural phage genes located near putative promoter sites, and it is possible that they are continuously expressed for continuous production of phage.

Almost half of ϕHSIC genes are early genes. Early genes are clustered at the beginning and the end of the genome, while the middle, late, and continuously expressed genes are randomly distributed in the middle of the genome. Plots of the expression values for each ORF are shown in Figure 10.

Table 3. *M* values for the synchronous infection experiment. Bolded values are the highest and were used when classifying ORFs based on time of peak expression. (p.i. - post-infection)

		***M* value**			
ORF	**Predicted Function**	**0 min p.i.**	**20 min p.i.**	**40 min p.i.**	**60 min p.i.**
1	Hypothetical phage protein	**1.693399**	0.889923	1.014047	0

Table 3. Cont.

		M value			
ORF	**Predicted Function**	**0 min p.i.**	**20 min p.i.**	**40 min p.i.**	**60 min p.i.**
2	DNA Polymerase III	**1.222271**	0.33021	0	0.130417
3	Unknown	**1.496018**	0.782858	0.821112	0
4	Unknown	**0.826423**	0.234109	0	0.098754
5	Unknown	**1.378085**	0.93154	0	0.536553
6	Unknown	**2.598762**	0.961006	0.710571	0
7	Terminase, small subunit	0.013271	0.197858	0	0.201228
8	Terminase, large subunit	0	0.893124	0.267357	**1.113956**
9	Unknown	**1.512062**	0.61516	0.780219	0
10	Unknown	**3.029158**	0.17233	2.023883	0
11	Unknown	**3.119356**	2.133856	1.120559	0
12	60 kDa structural phage protein	0	0.601822	0.442132	0.772919
13	Unknown	3.625478	0	**3.765162**	3.541494
14	Hypothetical phage protein	0	**2.204245**	1.500638	1.966399
15	Unknown	0.058463	0.130548	0.045271	0
16	Unknown	0.649243	0.382304	0	0.252353
17	Hypo. phage protein, *Salmonella* phage KS7	0	0.652156	0.239142	0.340075
18	Major capsid protein	0	1.205359	0.838866	**1.396356**
19	Unknown	0	5.151778	5.837213	**6.056471**
20	Unknown	**2.574974**	0	2.121678	1.795134
21	Unknown	1.293518	0	**1.539301**	1.460261
22	Unknown	**3.82985**	2.281954	2.555496	0
23	Hypo. *Y. pestis* phage protein	0	0.533126	0.191571	0.451596
24	Hypo. *Y. pestis* phage protein	0	1.156367	1.145709	**1.606452**

Table 3 Cont.

		M value			
ORF	**Predicted Function**	**0 min p.i.**	**20 min p.i.**	**40 min p.i.**	**60 min p.i.**
25	Hypo. *Y. pestis* phage protein	0	2.662862	3.046623	**3.272072**
26	Unknown	0	2.866717	2.402345	**2.929517**
27	Unknown	0.442164	0.32266	0	0.093307
28	Unknown	0	**4.95819**	3.699412	4.369391
29	Unknown	0	0.566094	0.51759	0.585203
30	Unknown	0.650416	0.383329	0	0.087873
31	Tail tape measure protein	0	**6.155258**	5.765887	5.936723
32	Hypothetical protein	0	3.625709	**5.958284**	5.780828
33	Tail fibers/Streptococcal hemagglutinin protein	0	0.633186	0.690672	0.752682
34	Unknown	0	**2.949827**	2.4411	1.484034
35	Cyanophage P60 protein	**5.860026**	4.442943	4.66374	0
36	Unknown	0.366424	**1.091148**	0	0.899849
37	Baseplate subunit and tail lysozyme	0.298218	0.650575	0	0.359796
38	Unknown	**5.762308**	0	4.127756	4.940294
39	Unknown	**2.902703**	0	0.567041	0.597902
40	Unknown	**2.961526**	0.915722	1.86485	0
41	Hypothetical phage protein	**6.193572**	2.67611	0	5.735004
42	Putative Helicase	**3.794012**	0.631716	0	2.854109
43	Unknown	**4.110407**	1.512741	0	1.991344
44	Unknown	**7.42115**	0.754888	0	3.937752
45	Unknown	**3.199617**	1.571176	0	0.379424
46	Hypothetical phage protein	0.749924	0.226564	0	0.008264
47	Putative Primase/Integrase	**1.0689**	0.896188	0.056088	0

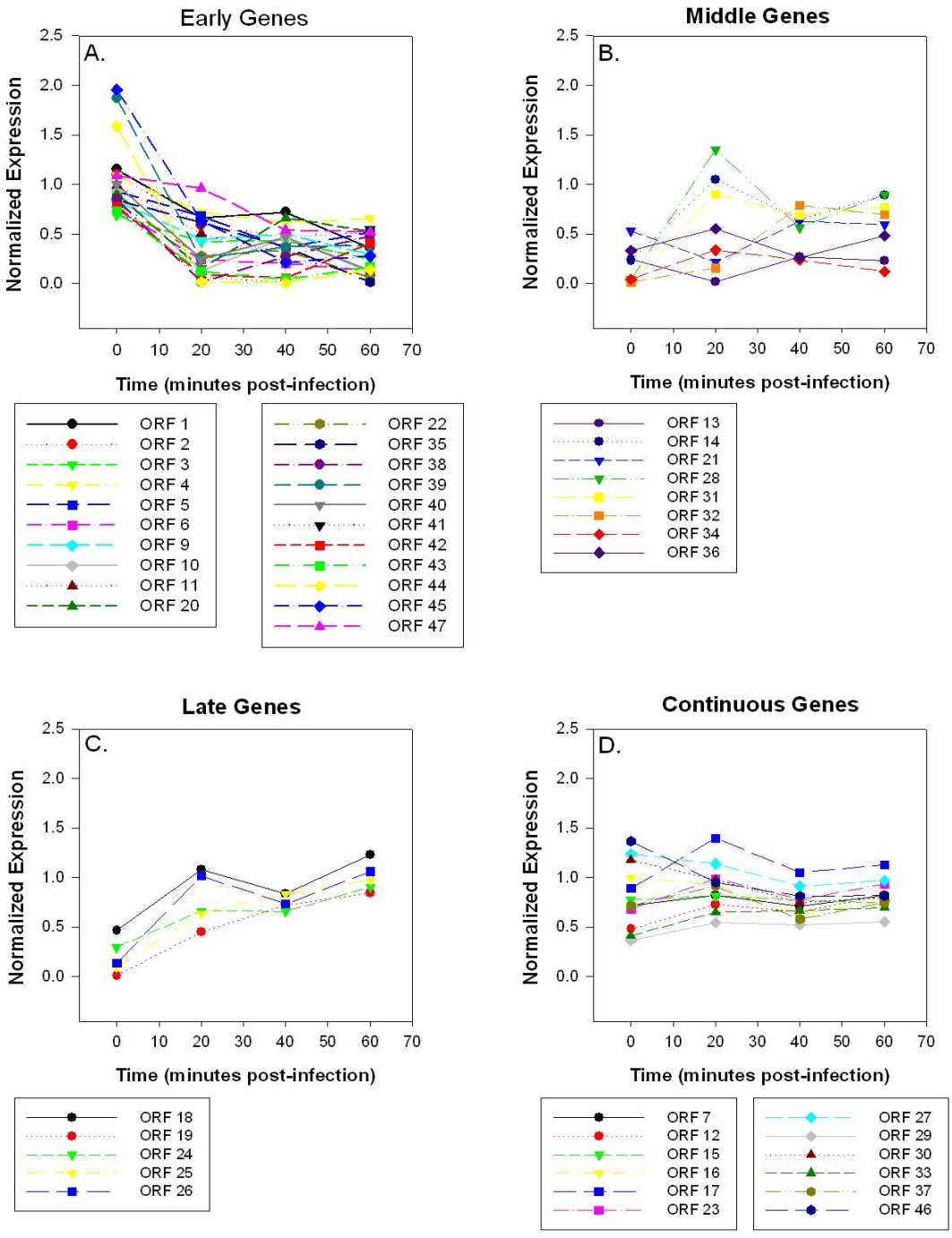

Figure 10. Expression values for all ϕHSIC ORFs. ORFs are grouped by time of peak expression into early (panel A), middle (panel B), and late (panel C) genes during the synchronous infection. Panel D is all genes that had relatively continuous levels of gene expression throughout the infection cycle.

Using computer software, eleven putative promoters including a putative host promoter, and twelve rho-independent terminators were found scattered throughout the genome. In Figure 11, the genome map of ϕHSIC has been arranged with each ORF colored by peak expression, and includes the location of the putative promoters and termination sites. The location of the promoters agrees with the temporal classification of the genes. For example, there is a promoter for ORFs 1 through 6 located after ORF 47, and there is a termination site found between ORFs 6 and 7. ORFs 7 and 8, the small and large terminase subunits, have a separate promoter and termination site than the ORFs surrounding them.

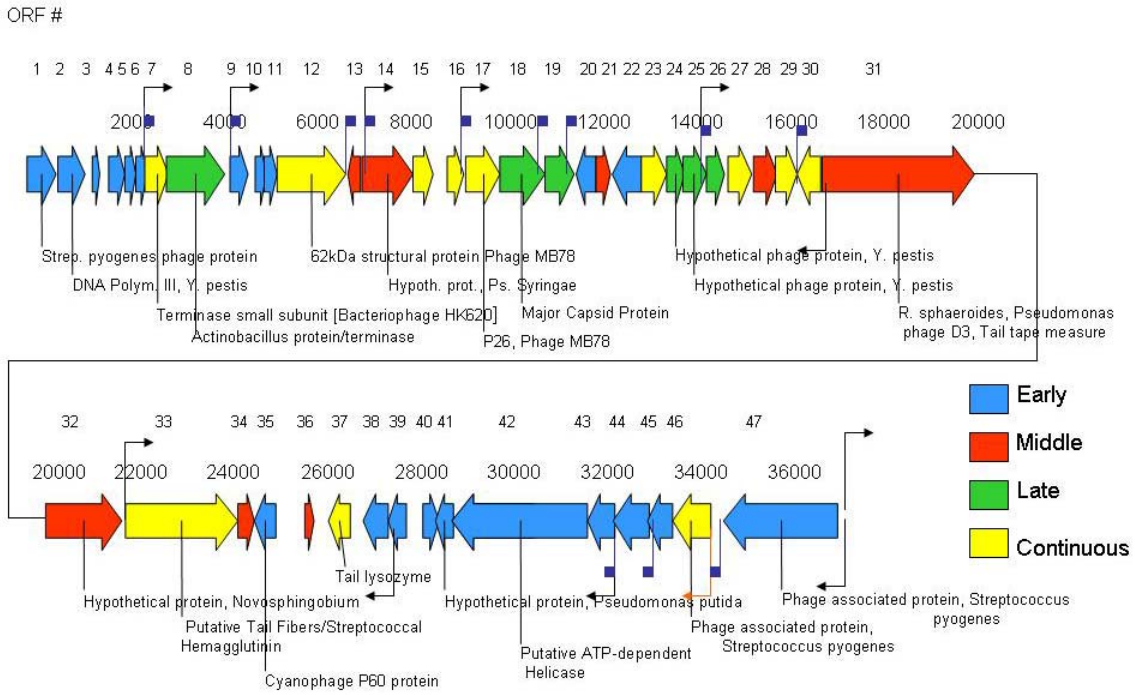

Figure 11. ϕHSIC gene expression map. Black arrows are putative viral promoters, orange arrow is the putative host promoter, and purple boxes are the putative termination sites. Blue arrows are ORFs that have been classified as early genes, red arrows are the middle genes, and green arrows are the late genes. Yellow arrows are ORFs that do not have significant change in expression with time.

2.3.4 Twenty-Four Hour Salinity Experiment

In previous growth experiments with the HSIC-1a, measurements were not taken between 10 hours and 24 hours. To fully understand how salinity affects cell growth and differences in phage production that may have been missed in previous samplings, a twenty-four hour growth curve was done with the HSIC-1a cells growing in either 22 or 39 ppt ASWJP+PY (Appendix A). As seen in Figure 12A, cell growth in the 39 ppt culture had a sigmoidal growth curve typical of pseudolysogenic cultures. At T_9, the O.D. dropped to 0.31 before it rebounded and reached a maximum O.D. of 1.2 at T_{24}. A sigmoidal growth curve was also seen in the 22 ppt culture although it was not as pronounced as that seen in the 39 ppt treatment. At T_{13}, the optical density of the 22 ppt culture decreased to 1.1 but by T_{24}, the optical density of the culture had increased to 1.3 (Figure 12A).

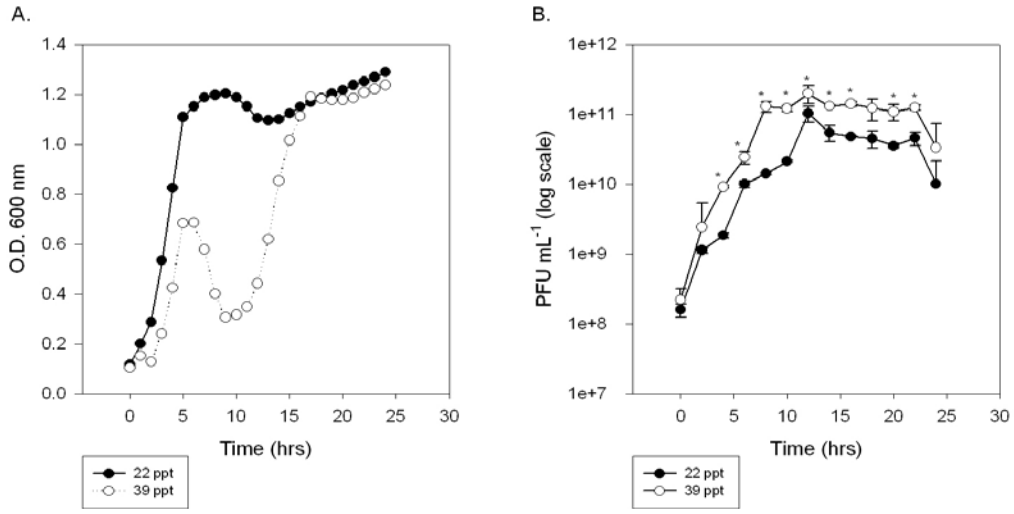

Figure 12. Cell growth and phage production in the twenty-four hour salinity experiment. Cell growth (panel A) and phage production (panel B) of HSIC-1a growing in either 22 ppt ASWJP+PY or 39 ppt ASWJP+PY. * denotes statistical significance and error bars represent duplicate measurements.

Overall, the pattern of phage production between the two treatments was similar, increasing from T_0 until the peak at T_{12} and then decreasing until T_{24}. However, the 39 ppt treatment had a higher concentration of free phages throughout the entire experiment as shown in Figure 12B. The difference in free phage concentration between the two treatments was statistically significant at T_4 ($p=0.002$), T_6 ($p=0.043$), T_8 ($p=0.028$), T_{10} ($p=0.009$), T_{12} ($p=0.037$), T_{14} ($p=0.011$), T_{16} ($p=0.049$), T_{20} ($p=0.007$), and T_{22} ($p=0.006$). It had been previously thought that phage production in HSIC-1a cells growing at normal salinity levels steadily increased from T_{10} to T_{24}, and that the free phage concentration was greatest at T_{24}. This is not the case as phage production peaked at T_{12} in both cultures. At T_{12}, free phage abundance in the 39 ppt culture reached as 1.96×10^{11} PFU mL^{-1} while it was 1.02×10^{11} PFU mL^{-1} in the 22 ppt culture. By T_{24}, the free phage abundance in the 39 ppt treatment had dropped to 3.3×10^{10} PFU mL^{-1} and 1×10^{10} PFU mL^{-1} in the 22 ppt treatment.

2.3.5 Effects of Salinity on Uninfected *L. pelagia*

To determine if salinity was affecting viral gene expression, it was necessary to show that the observed changes in cell growth were not a result of the changes in salinity affecting *L. pelagia* physiology. Uninfected strains of *L. pelagia* were grown at both 11 ppt and 39 ppt as shown in Figure 13. While the optical density of the strain grown at 11 ppt was always slightly less than that of the 39 ppt strain, it was never as drastically different as that observed in the infected strain grown at different salinities. We concluded that lowered salinity did not noticeably affect host cell physiology, and

differences in viral gene expression are most likely the result of the effects of salinity changes on viral gene expression.

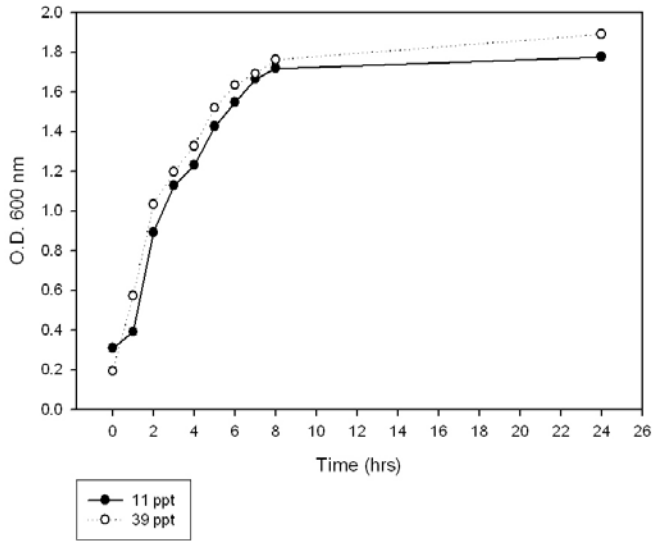

Figure 13. Effects of salinity on *L. pelagia* growth. Optical density measurements of *L. pelagia* cells grown in ASWJP+PY at either 11 ppt or 39 ppt.

2.3.6 Expression Analysis of ϕHSIC Grown at Different Salinities

Previous research had indicated that HSIC-1a had significant changes in both cell growth and phage production when grown at different salinities, and that high salinities favored lytic phage production while low salinities favored lysogeny (114). To understand what occurs at the lysogenic switch on the molecular level during salinity stress, gene expression analysis of HSIC-1a cells growing in both 11 ppt and 39 ppt ASWJP+PY was done in two separate experiments. Phage production and growth were also measured during these experiments. The salinity of the media was adjusted to 11 ppt to accentuate differences in cell growth, phage production, and gene expression.

Cell growth measurements had the same trend in both salinity experiments. Between T_1 and T_2, there was a sharp increase in cell growth in the 39 ppt treatment as compared to the 11 ppt treatment. The growth rate between these two time points in the 39 ppt treatment was 1.1 hr^{-1} in the first salinity experiment and 1.2 hr^{-1} in the second salinity experiment. Conversely, the growth rate for the same period of time in the 11 ppt treatment was 0.67 hr^{-1} in the first experiment and 0.63 hr^{-1} in the second experiment. After T_2, cell growth steadily and rapidly increased in the 39 ppt treatment until T_8, at which point it decreased until the T_{10} reading in both experiments. By T_{24}, the optical density in the 39 ppt treatment had increased again, up to 1.3 in both experiments (Figures 14A and 15A).

For the initial portion of both experiments, cell growth in the 11 ppt treatment was significantly less than that of the 39 treatment. The greatest difference in cell growth occurred at T_4 in both experiments. However, at T_7 in the first experiment and T_8 in the second experiment, the optical density of the 11 ppt culture caught up to that of the 39 ppt treatment. Growth in the 11 ppt culture was greater after that time point for the duration of both experiments. There was no sigmoidal growth curve observed in the low salinity treatment.

Phage production in the 11 ppt treatment was less than that of the 39 ppt treatment throughout both experiments. The differences in phage production for the first experiment can be seen in Figure 14B. While phage production was significantly greater in the 11 ppt treatment at T_0 ($p=0.039$), phage production in the 39 ppt treatment was greater by T_2. Phage production was significantly higher in the 39 ppt treatment as compared to the 11 ppt treatment at T_6 ($p=0.014$), T_8 ($p=0.000$), T_{10} ($p=0.000$) and T_{24}

(p=0.001). At the beginning of the experiment, there were 5.05 X 10^7 PFU mL^{-1} present in the 39 ppt treatment and 1.34 X 10^8 PFU mL^{-1} in the 11 ppt treatment. By the end, phage production had increased in the high salinity treatment to 1.97 X 10^{11} PFU mL^{-1} and 2.18 X 10^{10} PFU mL^{-1} in the low salinity treatment.

Figure 15B illustrates the differences in phage production between the two salinities in the second salinity experiment. At the beginning of the experiment, phage production is significantly greater (p=0.002) in the 11 ppt treatment than in the 39 ppt treatment, 5.43 X 10^7 PFU mL^{-1} as compared to 1.22 X 10^7 PFU mL^{-1}. However, by T_2, the number of PFU mL^{-1} in the 39 ppt treatment increased to 6.80 X 10^9 while there were 7.45 X 10^7 PFU mL^{-1} in the 11 ppt treatment. This trend continued for the rest of the experiment, and the differences in phage production were significant at T_2 (p=0.024), T_4 (p=0.000), T_6 (p=0.002), T_8 (p=0.000) T_{10} (p=0.000), and T_{24} (p=0.000).

After the T_{24} measurement in the second salinity experiment, the cultures were transferred into fresh ASWJP + PY of the appropriate salinity and continued for another 30 hours. At T_{54}, the A_{600} measurement for the 39 ppt treatment was still high, 1.10. The cell density of the 11 ppt culture was high as well, even though it had dropped from an A_{600} of 1.3 at T_{54} from an A_{600} of 1.6 at T_{24}. By T_{54}, the 11 ppt culture had a free phage concentration of 1.70 X 10^{10} PFU mL^{-1}, and the 39 ppt treatment had a concentration of 1.30 X 10^{11} PFU mL^{-1}, which was significantly greater (p=0.000).

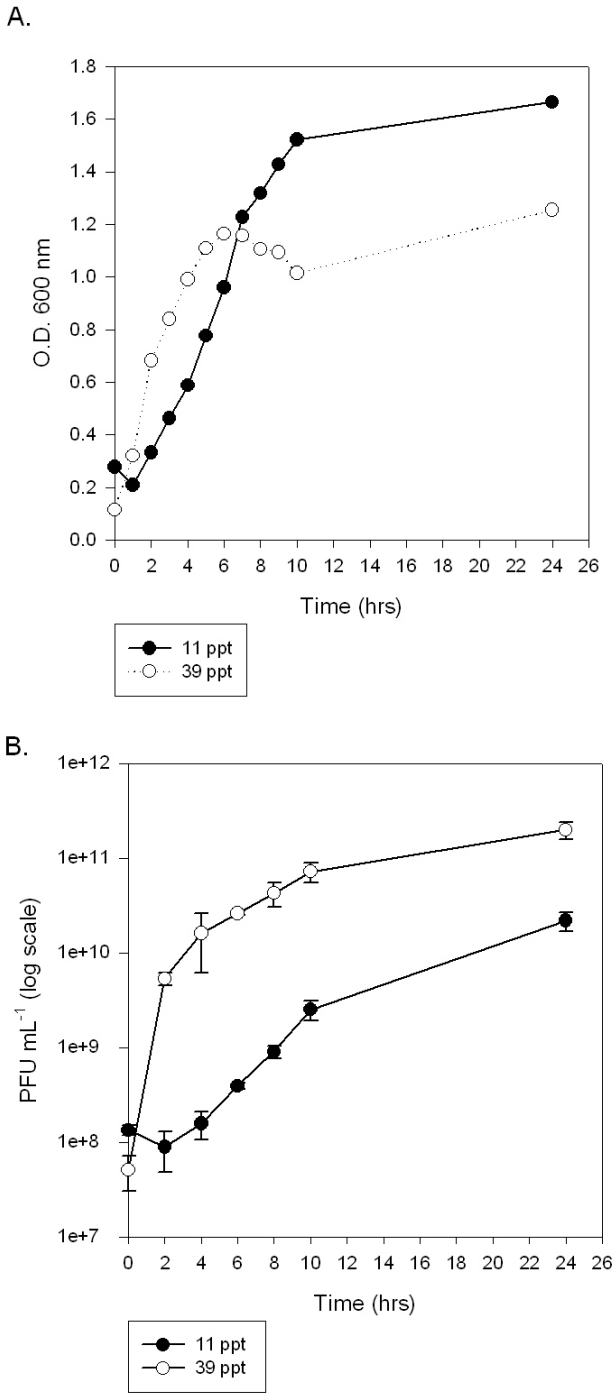

Figure 14. Cell growth and phage production in salinity experiment 1. Cell growth (panel A) and phage production (panel B) by HSIC-1a when grown in ASWJP+PY that was either 11 ppt of 39 ppt. Error bars represent duplicate measurements.

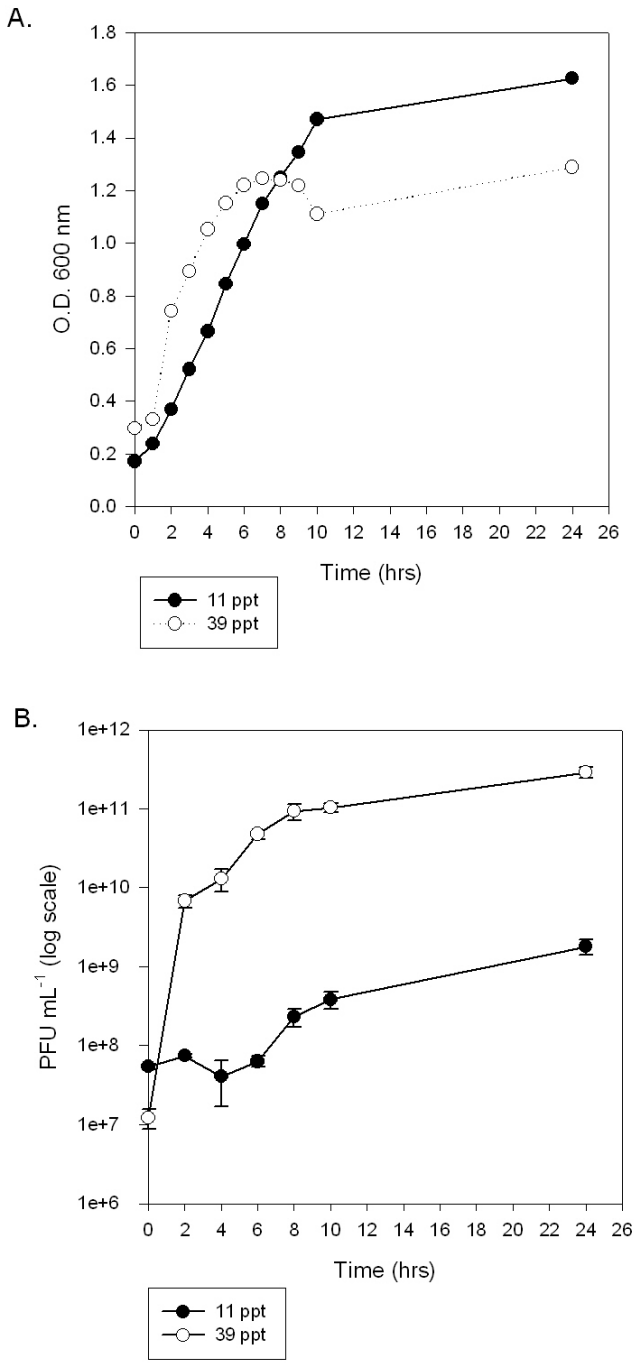

Figure 15. Cell growth and phage production in salinity experiment 2. Cell growth (panel A) and phage production (panel B) by HSIC-1a when grown ASWJP+PY that had a salinity of either 11 ppt of 39 ppt. Error bars represent duplicate measurements.

Normalized gene expression values for the salinity experiments were calculated in a similar way to the synchronous infection experiment. However, in the salinity experiments, the background was automatically subtracted from the spot density value before normalization to the 16S rDNA. ORFs 46 and 47 were normalized to the 16S ribosomal DNA and the negative control on that strip. In both experiments, several ORFs had negative expression values. Negative values do not mean that there was negative gene expression; rather they indicate that the spot density of the ORF was lower than that of the negative control. To account for this, all negative values were set to zero for graphs.

To quantitatively analyze the expression data and isolate any patterns that may have occurred, the ratio of expression in the 39 ppt treatment to expression in the 11 ppt treatment was calculated at both time points. It was at this point that the zero or negative expression values were set to 0.1 so that the ratio could be found and the $\log_2$ value could be determined to give the *M* value. If the *M* value was ≤ -0.80 or ≥ 0.80, then the levels of hybridization were considered to be significantly different (3, 24). One issue with using 0.1 for negative and zero values is that, if the non-negative gene expression value is less than 0.1, there may be a false positive. This would cause the *M* value to appear significant when expression differences are not significantly different. However, this phenomenon was observed for only three ORFs between the two salinity experiments. As a result, we decided that this was the most accurate way to compare gene expression between the 11 and 39 ppt treatments. *M* values for the three ORFs were not considered when analyzing the data.

Negative *M* values signify that expression in the 11 ppt treatment was significantly greater than that of the 39 ppt treatment. In the first experiment, values were only significantly greater in the 11 ppt treatment at T_6. This was not true in the second experiment where values were significantly greater in the 11 ppt treatment at both T_4 and T_6.

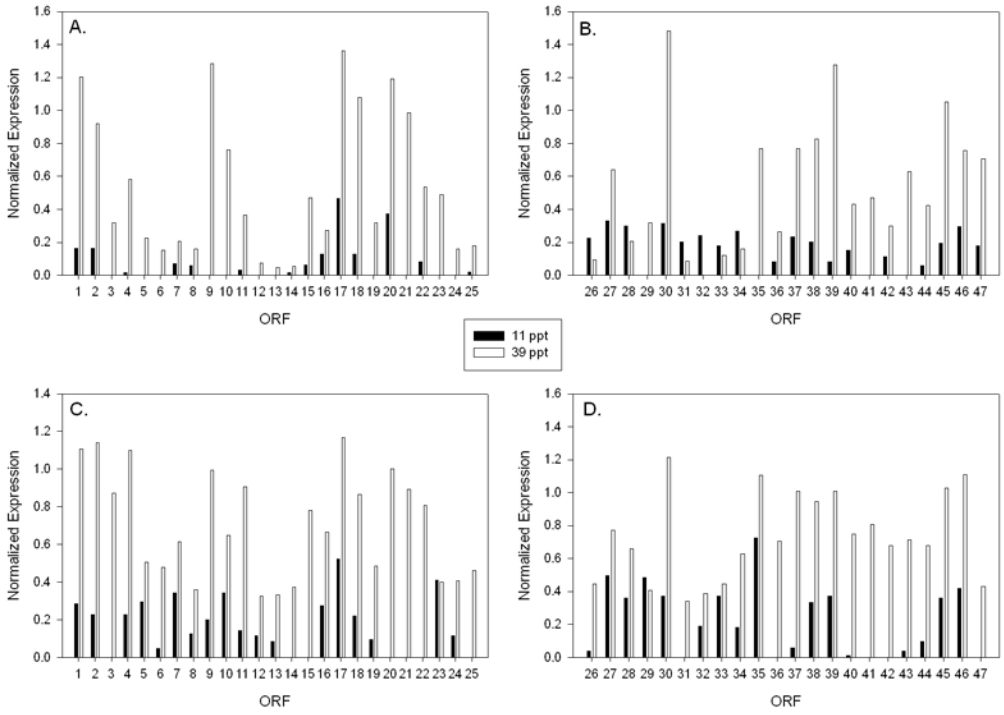

Figure 16. Average normalized expression values for 11 ppt and 39 ppt at T_6 and T_8 from the first salinity experiment. Panels A and B are from T_6, A is ORFs 1-25 and B is ORFs 26-47. Panels C and D are from T_8, panel C is ORFs 1-25 and panel D is ORFs 26-47.

Most phage genes had higher gene expression values in the 39 ppt treatment than in the 11 ppt treatment for both experiments. In the first salinity experiment, gene expression at T_6 and T_8 was analyzed. Figures 16A and 16B show the normalized gene

expression values for each ORF from the T_6 sample. ORFs 26, 28, 31, 32, 33 and 34 all had greater levels of expression in the 11 ppt treatment than the 39 ppt treatment at T_6. All of these ORFs are middle or late genes, and four have cryptic functions while the other two, 31 and 33, are the putative tail tape measure protein and the tail fibers/streptococcal hemagglutinin protein. Quite a few ORFs had no gene expression in the 11 ppt treatment at T_6 while only one ORF, 32, a hypothetical protein, had no gene expression in the 39 ppt treatment.

At T_8, only ORF 29, a middle gene with no known function, had greater gene expression in the 11 ppt treatment than in the 39 ppt treatment. Only one ORF, 23, had comparable expression levels to its counterpart in the 39 ppt treatment at the same time point. ORF 23 is a middle gene with no known function although it has hits to a *Y. pestis* phage protein. Every ORF had positive expression in the 39 ppt treatment at T_8. There were negative and zero gene expression values in the 11 ppt treatment. As all of these genes were expressed at T_6, it can be assumed that transcription of these genes was down-regulated between the two sampling points.

Many ORFs had higher levels of expression at 39 ppt than 11 ppt when gene expression was examined at T_4 and T_6 in the second salinity experiment. The average normalized expression values of each ORF for both the 11 ppt and the 39 ppt treatment at T_4 are plotted in Figures 17A and 17B. Expression values for the 11 ppt treatment are greater than the 39 ppt treatment values at ORFs 1 through 7, 11, 12, 15, and 16. ORFs 10, 23, and 47 have almost equal expression values to their counterparts in the 39 ppt treatment at T_4. Again, ORFs that had negative expression values at T_4 in both the 11 ppt and the 39 ppt treatment were set to zero when graphed.

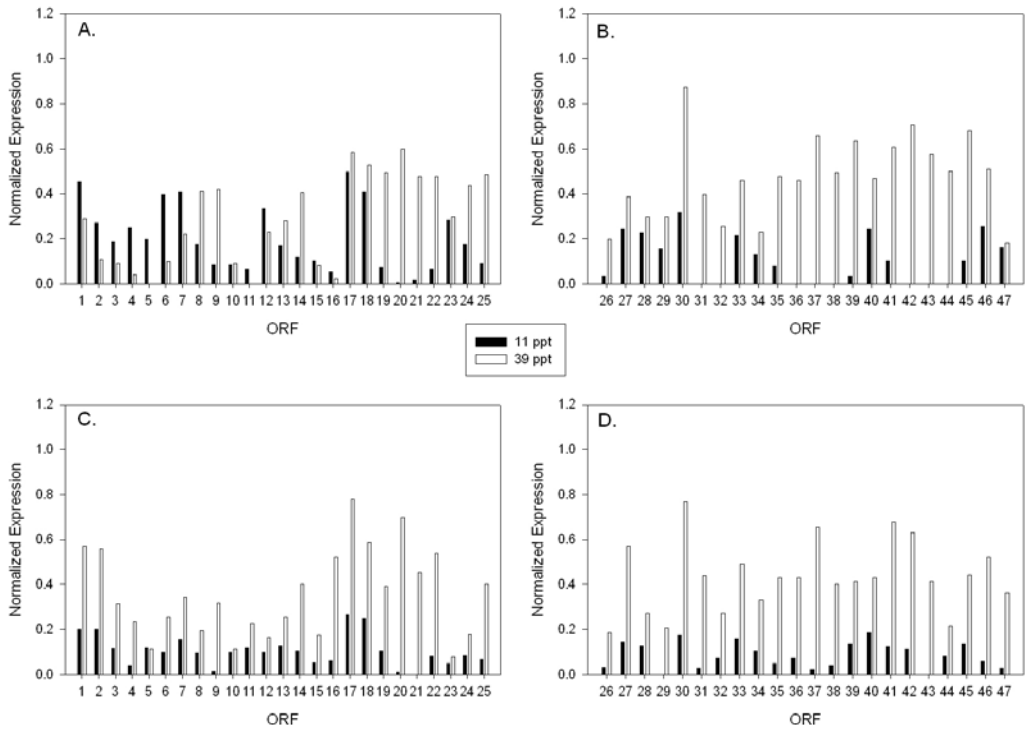

Figure 17. Average normalized expression values for 11 ppt and 39 ppt at T_4 and T_6 from the second salinity experiment. Panels A and B are from T_4, A is ORFs 1-25 and B is ORFs 26-47. Panels C and D are from T_6, panel C is ORFs 1-25 and panel D is ORFs 26-47.

At T_6, ORF 5 was the only ORF that had similar expression values in both the 11 ppt and 39 ppt treatment (Figure 17C). Additionally, many of the genes that were not expressed at T_4 in the 11 ppt treatment, such as the latter half of the genome from ORF 32 onwards, were expressed by T_6. In fact, all ORFs except for 21, 29, and 43 were expressed at T_6 in the 11 ppt treatment. In the 39 ppt treatment, all genes were expressed as well.

Table 4. *M* values for each ORF from salinity experiments 1 and 2. $^{+}$ indicates that the initial expression was either zero or negative and so 0.1 was substituted. * indicates a false positive. *M* values that are greater than the cutoff are bolded.

ORF	Predicted Function based on best BLASTP Hits	Experiment 1		Experiment 2	
		T_6 *M* Value	T_8 *M* Value	T_4 *M* Value	T_6 *M* Value
1	Hypothetical protein, *S. pyogenes*	**2.875344**	**1.953576**	-0.65975	**1.507484**
2	DNA Polymerase III, Beta Subunit	**2.490054**	**2.318317**	**-1.33252**	**1.482393**
3	Unknown	**1.674681**	**3.126532**$^{+}$	**-1.03587**	**1.411385**
4	Unknown	**5.173683**	**2.266787**	**-2.6115**	**2.553658**
5	Unknown	**1.172181**$^{+}$	0.779158	**-0.98262**$^{+}$	-0.07861
6	Unknown	0.587218^{+}	**3.333424**	**-2.00054**	**1.349942**
7	Terminase, small subunit	**1.582703**	**0.839064**	**-0.87368**	**1.141356**
8	Terminase, large subunit	**1.403379**	**1.539875**	**1.244767**	**1.053893**
9	Unknown	**3.685251**$^{+}$	**2.312278**	**2.323962**	**4.576742**
10	Unknown	**2.927068**$^{+}$	**0.915415**	0.110968	0.184425
11	Unknown	**3.504889**	**2.665999**	0.602345^{+}*	**0.92139**
12	60kDa Structural Phage Protein	-0.41278^{+}*	**1.515174**	-0.54111	0.736966
13	Unknown	-1.09085^{+}*	**1.959358**	0.739	**0.996306**
14	Head morphogenesis protein	**1.708234**	**1.900464**$^{+}$	**1.751674**	**1.929052**
15	Unknown	**2.863343**	**2.963474**$^{+}$	-0.30664	**1.707987**
16	Unknown	**1.077468**	**1.271302**	**-1.12607**	-0.20
17	Hypothetical phage protein, *Salmonella* phage KS7	**1.541415**	**1.155278**	0.233599	**1.548997**
18	Capsid protein	**3.061871**	**1.984233**	0.371429	**1.234465**
19	Unknown	**1.674681**$^{+}$	**2.353323**	**2.78082**	**1.893428**

Table 4 Cont.

ORF	Predicted Function based on best BLASTP Hits	Experiment 1		Experiment 2	
		T_6 *M* Value	T_8 *M* Value	T_4 *M* Value	T_6 *M* Value
20	Unknown	**1.674909**	**3.321928**$^{+}$	**6.648716**	**5.974706**
21	Unknown	**3.301464**$^{+}$	**3.159199**$^{+}$	**4.73191**	**3.862496**$^{+}$
22	Unknown	**2.730449**	**3.011973**$^{+}$	**2.857441**	**2.749209**
23	Hypothetical phage protein, *Y. pestis*	**2.287658**$^{+}$	-0.03395	0.074228	0.6746
24	Hypothetical phage protein, *Y. pestis*	0.674681^{+}	**1.831202**	**1.328831**	**1.068879**
25	Hypothetical phage protein, *Y. pestis*	**3.127928**	**2.201634**$^{+}$	**2.434644**	**2.59368**
26	Unknown	**-1.26594**	**3.551516**	**2.458892**	**2.529698**
27	Unknown	**0.949398**	0.642968	0.655929	**1.969827**
28	Unknown	-0.53054	**0.866856**	0.380889	**1.089126**
29	Unknown	**1.674681**$^{+}$	-0.25626	**0.928377**	**3.594181**$^{+}$
30	Unknown	**2.229585**	**1.707819**	**1.458892**	**2.138547**
31	Tail tape measure protein	**-1.272**	**1.765535**$^{+}$	**1.982078**$^{+}$	**3.863634**
32	Hypothetical protein, *Silicibacter*	**-1.27462**	**1.02148**	**1.351312**$^{+}$	**1.919201**
33	Tail fibers/Streptococcal hemagglutinin protein	-0.53951	0.266114	**1.096322**	**1.603699**
34	Unknown	-0.73744	**1.792088**	**0.806815**	**1.65**
35	Cyanophage P60 protein	**2.94477**$^{+}$	0.612539	**2.616433**	**3.160027**
36	Unknown	**1.687355**	**2.82103**$^{+}$	**2.204471**$^{+}$	**2.575064**
37	Baseplate hub subunit and tail lysozyme	**1.71399**	**4.138869**	**2.719044**$^{+}$	**4.762063**
38	Unknown	**2.035062**	**1.505891**	**2.304006**$^{+}$	**3.317395**
39	Unknown	**3.985021**	**1.438429**	**4.140716**	**1.586626**

Table 4 Cont.

ORF	Predicted Function based on best BLASTP Hits	Experiment 1		Experiment 2	
		T_6 *M* Value	T_8 *M* Value	T_4 *M* Value	T_6 *M* Value
40	Unknown	**1.495121**	**6.292782**	**0.93423**	**1.21**
41	Hypothetical phage protein, Bacteriophage JK06	**2.231075**$^{+}$	**3.011973**$^{+}$	**2.580882**	**2.419786**
42	Helicase	**1.420569**	**2.765535**$^{+}$	**2.82338**$^{+}$	**2.462296**
43	Unknown	**2.653308**$^{+}$	**4.226894**	**2.526399**$^{+}$	**3.821892**$^{+}$
44	Unknown	**2.903985**	**2.835924**	**2.327853**$^{+}$	**1.419274**
45	Unknown	**2.441879**	**1.504286**	**2.7437**	**1.686161**
46	Hypothetical phage protein	**1.355848**	**1.40576**	**0.984175**	**3.142958**
47	Primase/Integrase	**1.978946**	**2.106199**$^{+}$	0.1686	**3.624491**

Twenty ORFs were significantly greater in the 39 ppt treatment at every sampling point in both experiments. The majority of these were early genes but there was also three middle genes, three late genes, and three uniformly expressed genes. The large terminase subunit which is a late gene, ORF 8, was significantly expressed in the 39 ppt treatment for both experiments. Some of the genes that were consistently greater in the 39 ppt treatment include the head morphogenesis protein (ORF 14), the helicase protein (ORF 42), the tail lysozyme (ORF 37), and several unknown proteins. Many other ORFs were significantly greater at three of the four time-points in the 39 ppt treatment. Conversely, gene expression was never significantly greater at both time-points studied in the 11 ppt treatment in either salinity experiment.

Overall, the majority of the ORFs were significantly greater in the 39 ppt treatment than in the 11 ppt treatment for all four time points examined. At T_6 in the first salinity experiment, 39 ORFs had greater gene expression in the 39 ppt treatment and of those, 37 were significantly greater. Three of the eight ORFs that were greater in the 11 ppt treatment at the same time point were significantly greater. At the second time point, T_8, 45 ORFs had greater gene expression in the 39 ppt treatment and all were significantly greater in the high salinity treatment. In the second salinity experiment, 28 of the 37 ORFs that were expressed in the 39 ppt treatment were significantly greater at T_4 while seven ORFs had significantly greater levels of gene expression in the 11 ppt treatment. At T_6, 42 of the 45 ORFs were significantly greater in the 39 ppt treatment. There were instances where the *M* value at T_6 in the first experiment was negative while it was positive at T_6 in the second experiment and vice versa. Hybridization levels were lower overall in second experiment as was the amount of RNA used to prepare the probe. This may explain those discrepancies.

2.3.7 Free Phage Concentration versus Intracellular Phage Concentration

To understand the A_{600} measurements in terms of bacterial abundance, another salinity experiment was performed. Instead of making plaque overlays, samples were taken at T_2, T_4, T_6, and T_8 to determine the amount of bacterial cells in the two different treatments using epifluorescence microscopy. Using the A_{600} readings from the first two salinity experiments and cell counts from this experiment, the number of bacterial cells per mL was calculated for both salinity experiments. The estimated number of bacterial cells per mL and plaque forming units per mL for both salinity experiments is shown in Table 5.

Also included in Table 5 is the ratio of plaque forming units to bacterial cells for the two different salinities in both experiments. In both experiments, the ratio of plaques to bacterial cells was significantly higher in the 39 ppt treatment as opposed to the 11 ppt treatment. The greatest difference between the ratios of the two treatments in the first experiment occurred at T_8, where there were 68.9 PFU to 1 bacterial cell at 39 ppt and 2.48 PFU to 1 bacterial cell at 11 ppt. In the second salinity experiment, there were 119.2 PFU for every bacterial cell at 39 ppt, and 0.68 PFU for every bacterial cell in the 11 ppt treatment at T_8.

Table 5. Bacterial growth and free phage concentration from both salinity experiments. The ratio of PFU mL^{-1} to bacterial cells mL^{-1} in both salinity experiments is also listed.

Salinity	Time (hrs)	Experiment 1			Experiment 2		
		Bacterial cells mL^{-1}	**PFU mL^{-1}**	**PFU mL^{-1} : Bacterial cells mL^{-1}**	**Bacterial cells mL^{-1}**	**PFU mL^{-1}**	**PFU mL^{-1} : Bacterial cells mL^{-1}**
11	4	1.165×10^8	1.56×10^8	1.33	1.42×10^8	4.05×10^7	0.28
	6	2.0×10^8	3.9×10^8	1.95	2.1×10^8	6.30×10^7	0.3
	8	3.6×10^8	8.95×10^8	2.48	3.375×10^8	2.30×10^8	0.68
39	4	4.725×10^8	1.60×10^{10}	33.8	5.5×10^8	1.30×10^{10}	23.6
	6	6.8875×10^8	2.6×10^{10}	37.7	7.6×10^8	4.75×10^{10}	62.5
	8	6.1625×10^8	4.25×10^{10}	68.9	7.825×10^8	9.33×10^{10}	119.2

The HSIC-1a lysogen is unstable, and ϕHSIC has previously segregated from *L. pelagia* by multiple platings (116). Due to this instability, it was hypothesized that segregation was occurring in the low salinity treatments, which would explain the low numbers of plaque forming units and low gene expression values. Quantitative real-time PCR was done using host cell DNA extracted from samples taken at T_4, T_6, and T_8 during the second salinity experiment to determine if the viral genome was still in the cell. ORF 11 was chosen for this procedure because, even though it has a cryptic function, it satisfied all the guidelines for the target sequence in order to successfully design a real-time PCR probe. In addition, it was expressed at both salinities during the first salinity experiment.

Using the results of the real-time PCR and bacterial counts, we were able to approximate the number of intracellular phage genes per host cell. Table 6 lists the viral genomes per cell for the two different treatments from the second salinity experiment. The number of viral genomes increased from 1.94 at T_4 to 3.15 at T_6 in the 39 ppt treatment, and from 1.19 to 1.52 in the 11 ppt treatment during the same time period. The number of viral genomes decreased in both treatments from T_6 to T_8 by about one-fold, which is expected in the 39 ppt treatment as that is when the optical density of the culture begins to decrease. However, the decrease in viral genomes at the 11 ppt treatment was unexpected.

Table 6. Number of viral genomes per cell in the 11 and 39 ppt treatments.

Time (hrs)	# of viral genomes per cell at 11 ppt	# of viral genomes per cell at 39 ppt
4	1.19	1.94
6	1.52	3.15
8	0.5	2.3

The ratio of plaque forming units in the 39 ppt treatment to the 11 ppt treatment was calculated. The ratio of bacterial cells in the two different treatments was calculated as well to confirm that there were no real differences in host cells between the two experiments. Both ratios are given in Table 7. The ratio of phages between the two different treatments is, on average, two hundred-fold. Conversely, the ratio of bacterial cells between the two treatments was relatively low throughout the course of both experiments and ranged from 1.7 to 4 cells.

Table 7. Ratio of cells in 39 ppt to 11 ppt treatment.

Ratio of 39 ppt to 11 ppt	Time (hrs)	Experiment 1	Experiment 2
Plaque Forming Units mL^{-1}	4	102	320.9
	6	66.6	753
	8	47.4	405.6
Bacterial Cells mL^{-1}	4	4	3.87
	6	3.44	3.61
	8	1.71	2.31

2.4 Discussion

In this study, it was shown that HSIC-1a cells grown at low salinity produce less phages, and gene expression is significantly less compared to the 39 ppt treatment. Even as cell growth in the low salinity treatment caught up to cell growth in the normal salinity treatment, intracellular and free phage concentrations remained significantly lower. Further experiments showed that lowered salinity did not appear to affect uninfected *L. pelagia* physiology. Synchronous infection experiments led to the classification of ϕHSIC ORFs into time classes corroborated by the identification of putative promoters and termination sites in the ϕHSIC genome. Finally, infection of the host cell by ϕHSIC caused changes in the substrate utilization between the two strains.

To our knowledge, there is only one other experiment that has looked at the changes in carbon utilization between an uninfected host and the lysogen in marine bacteria. In that study, it was found that the phenotype of *Vibrio harveyi* was altered when infected with the VHML phage. VHML infection of *V. harveyi* strains 645 and 45 led to an inability to use gluconate as a carbon source, and more genes appeared to be down-regulated than up-regulated (102). Additionally, *V. harveyi* strain 20 was unable to use γ-glutamyl transpeptidase in the enzyme substrate tests.

Overall, HSIC-1a was unable to utilize five carbon sources that *L. pelagia* could utilize. However, HSIC-1a was able to use several other sources including thymidine, L-histidine and γ-amino butyric acid that *L. pelagia* could not utilize. It appears that infection with ϕHSIC may shut down certain pathways within the host cell while opening up alternative pathways which was also seen in *V. harveyi*. In addition, there was an

overall decrease in the magnitude of substrate utilization in many of the HSIC-1a wells. This indicates that viral infection is somehow suppressing these pathways leading to a lowered ability to use carbon sources such as L-glutamic acid.

Differences in colony morphology between infected and uninfected strains of *L. pelagia* have been noted in other studies (116). Briefly, HSIC-1a colonies are flat and crinkled with irregular edges while *L. pelagia* colonies are rounded with smooth edges. It has been long suspected the outer membrane of the cells, a layer of lipopolysaccharide, is somehow disrupted by ϕHSIC infection leading to the crinkled flat colony. The polysaccharide component of the outer membrane of gram negative bacteria is comprised of six- and seven-carbon sugars linked together while the lipid portion is made of fatty acids that are linked to *N*-acetylglucosamine phosphate by an ester amine bond. The results of the Biolog^{TM} tests, such as a decreased utilization of N-acetyl-D-glucosamine by the pseudolysogen, lend support to our hypothesis that pathway changes may be responsible for changes in the outer membrane of ϕHSIC infected cells.

After it was shown that macroarrays were both quantitative and specific enough to analyze ϕHSIC gene expression, synchronous infection experiments were done. By slightly altering the method used by Kobiler et al (2005), we were able to follow the infection cycle. The differences in gene expression peaks indicated that ϕHSIC is polycistronic, the mRNA product encodes for more than one protein at a time, which was not previously known.

A host promoter site with a -35 start site and a -10 TATA box was located between open reading frames 46 and 47. ORF 46 is a conserved hypothetical bacteriophage

protein with strong hits to phages isolated from *S. thermophilus* and *B. clarkii* while ORF 47 has several hits to different phage-associated primases as well as hits to putative integrases from Vibriophage VP2 and VP5. Primases are responsible for producing the RNA primer that is necessary for the initiation of DNA replication.

Data from the synchronous infection experiment led to the temporal classification of ϕHSIC genes. By plotting the genes according to peak expression, we were able to group genes into early, middle and late genes as well as those that had no significant change in expression with time. Over half of the ORFs had the highest levels of expression at 0 minutes post-infection. Early genes are clustered at the ends of the genome, and include a homolog (ORF 2) to the β-clamp subunit of DNA polymerase III, a multi-subunit enzyme that is responsible for the duplication of the bacterial chromosome in *E. coli*. The β-clamp joins the polymerase to the strand of DNA being replicated (17). Homologs to the DNA polymerase III θ subunit have also been observed in the bacteriophage P1 and it is believed that this homolog can substitute in the DNA polymerase III holoenzyme (17). Most likely, the ϕHSIC homolog is responsible for joining the host replication machinery to the viral DNA, thereby ensuring transcription of viral DNA.

While there has been no lysogeny module identified in the ϕHSIC genome, it is hypothesized that the lysogeny genes are located somewhere in the early gene cluster found from ORFs 38 through 47 and 1 through 6 on the circularly permuted genome. The putative identification of some of the genes in this region as well as the presence of the host promoter supports this hypothesis. The lysogeny module of the temperate phage Sfi21 has been located between the host lysis and replication modules on that phage's

genome (101). A lysozyme gene has not yet been found on the ϕHSIC genome, but a putative primase gene has been located at ORF 47. It is possible that the lysogeny module is located within this region as six of nine early genes in this region have no known function. Granted, helicases, primases, and polymerases are used in the initiation of the lytic cycle but this provides a starting point for finding the lysogeny module.

The small and large terminase subunits, ORFs 7 and 8, had relatively constant levels of expression throughout the course of the infection, although ORF 8 is technically a late gene. In phages that use the sequence-independent headful packaging mechanism such as ϕHSIC, the small terminase subunit is responsible for site-specific assembly and DNA recognition, while the large terminase subunit prepares the DNA for packaging into the prohead and has ATPase activities (38). The two subunits also work together to form a complex that moves the DNA into the empty capsid through the portal. If cells are constantly producing phages as they are in a pseudolysogenic culture, then the terminase activities are necessary at all times.

Late genes that were significantly up-regulated from their initial expression value included the major capsid protein (ORF 18) and the large terminase subunit (ORF 8). Capsid proteins have been identified as late genes in the vibriophage KVP40, and both terminase subunits are known late genes in the lytic cycle (14, 65, 77). In a typical lambda phage, the order of morphogenetic genes on an mRNA strand is 5' – small terminase – large terminase – portal – a homolog to T7 head assembly factor –decoration – coat – 3' (14). While ϕHSIC does not have this particular sequence, largely because the genes surrounding ORFs 7 and 8 are of unknown function, there are six late genes in the

ϕHSIC genome. These genes have been putatively identified as the terminase subunits, the major capsid protein, a structural protein, possible tail fibers, and several unknown phage proteins.

The ϕHSIC/*L. pelagia* marine phage-host system is unique in that there is an uninfected host strain and it is a pseudotemperate phage whose genome sequence is known. Not only does it allow for experiments that study gene expression in a pseudotemperate phage, something that has not been done before, but environmental factors that affect the lysis/lysogeny decision can also be examined. Previous experiments with HSIC-1a had shown that changes in aeration, temperature, and media salinity led to significant differences in both cell growth and phage production. It was hypothesized that these changes in salinity were changing the interactions of the repressor molecules (114). As ionic strength decreases, interactions between charged molecules become more stabilized and bind tighter to one another (4). It is thought that in the ϕHSIC system, the repressor molecule has a greater affinity for the operator sites and as such, HSIC-1a cells enter the lysogenic state when the salinity of ASWJP+PY is lowered.

After analysis of the results of the 24-hour growth experiment, we decided to decrease the low salinity media from 22 ppt to 11 ppt to ensure significant changes in phage production and cell growth would be observed as well as marked differences in gene expression between the two cultures. The effect of low salinity on *L. pelagia* growth was also tested to ensure sure that differences in cell growth were not a result of salinity changes affecting *L. pelagia* physiology, which they were not.

In the 39 ppt treatment in both salinity experiments, there was expression of nearly all ORFs. Gene expression in the 11 ppt treatment was significantly greater in the first

salinity experiment at T_6 for ORFs 26, 31, and 32. In the second salinity experiment, ORFs 2 through 7 and 16 had significantly higher levels of expression in the 11 ppt treatment at T_4. Gene expression was not significantly greater in the 11 ppt treatment at the later time points in both salinity experiments.

Cell growth was depressed in the initial stages of the 11 ppt treatment when compared to cell growth in the 39 ppt treatment. Eventually, the 11 ppt treatment surpassed the 39 ppt growth, most likely due to a lack of phage lysis in the 11 ppt treatment. Phage production in the 11 ppt treatment was depressed in both salinity experiments as well, and it did not catch up to the 39 ppt treatment by T_{24}. When the cultures were transferred to fresh media of corresponding salinity at T_{24} and allowed to grow for another 30 hours, free phage concentration in the 11 ppt increased to 2.33×10^{10} PFU mL^{-1} while the free phage concentration in the 39 ppt treatment had dropped to 1.55×10^{11} PFU mL^{-1} as determined by plaque overlays using overnight cultures of uninfected *L. pelagia* for the host. However, free phage concentrations were still significantly higher in the 39 ppt treatment.

In the first salinity experiment, gene expression in the 11 ppt treatment for ORFs 1 through 25 increased from T_6 to T_8 overall. However, gene expression in the second half of the genome appeared to decrease in the 11 ppt treatment from T_6 to T_8. The opposite is true in the second salinity experiment, which analyzed gene expression at T_4 and T_6. In that experiment, gene expression in the first half of the genome decreased overall from T_4 to T_6 but, in the second half of the genome, gene expression increased overall. However, in the same experiment during the same time period, the number of viral genomes in cells

essentially remained the same, going from 1.2 to 1.5. At T_8, the number of viral genomes in the cell decreased to 0.5 in the 11 ppt treatment.

As both experiments had a T_6 sampling point, we were able to compare gene expression from the two different salinity experiments and see if there were any noticeable trends at that time point. In both the 11 and 39 ppt treatments, ORFs 17 and 30 had some of the highest expression values of all ORFs. Overall, more genes were expressed in the 11 ppt treatment at T_6 in the second salinity experiment than in the first salinity experiment at the same time point. Genes that had high expression values in the 11 ppt treatment at T_6 included ORFs 27, 28, and 33. A similar pattern of gene expression was observed in the 39 ppt treatment. While gene expression levels were higher at T_6 in the first salinity experiment, more genes were expressed at T_6 in the 39 ppt treatment during the second salinity experiment. ORFs 17, 30, and 45 all had high levels of gene expression in both experiments.

While there were some ORFs in the 39 ppt treatment that decreased in expression with time, for the most part, gene expression in the 39 ppt treatment either increased or stayed constant in both experiments. Gene expression in the 39 ppt treatment was significantly greater than that in the 11 ppt treatment for many of the genes, especially the early genes suspected to be involved in the integration of the ϕHSIC genome and initiation of DNA replication as well as the large terminase subunit. Other genes that had high levels of expression in the 39 ppt treatment included ORFs 9, 14, 17, 30, 39. The number of viral genomes per cell in the 39 ppt treatment increased from 2 to 3 from T_4 to T_6 before dropping back down to 2 at T_8. The differences in expression between the two treatments were not a result of the amount of total RNA labeled as similar amounts were used for

both 11 and 39 ppt in the experiments. Additionally, the signal intensity for the 16S rDNA positive control was similar between the 11 ppt and the 39 ppt blots.

Intracellular phage concentrations were compared between the two treatments as well. The most notable difference was seen at T_6 when there were roughly 3 viral genomes for every bacterial cell in the 39 ppt treatment but only 1.5 viral genomes for every bacterial cell in the 11 ppt treatment. The ratio of free phages between the two different treatments agreed with this data. There was typically an order of magnitude difference in free phage concentration between the 11 ppt and the 39 ppt treatment. Additionally, limited host density, which has been suggested as a possible factor in influencing the lysis/lysogeny decision, did not appear to be a factor in these experiments. The number of *L. pelagia* cells in the 11 ppt treatment was on the order of 4.08×10^8 BDC mL^{-1} at T_8. In the 39 ppt treatment, there were, on average, 7.06×10^8 BDC mL^{-1} at the same time point. The differences between host cell abundance in the 11 ppt and the 39 ppt treatments were not significant.

These data, when combined with the cell growth data, shows that pseudotemperate phage production may fluctuate along with gene transcription throughout a growth experiment but new phage production is always occurring. There was a clear increase in phage gene expression in most of the ORFs in the 39 ppt treatment. The implication is that, at low salinity, there was a repression of nearly all phage ORFs, which was most likely a stress response to low salinity possibly by host control. This is consistent with the idea that lytic phages are found under favorable conditions, 39 ppt in this case, while low salinity leads to the lysogenic response and gene expression is shut down. The lysogenic

response was also noted in repression certain pathways in the metabolic substrate utilization experiment.

Data gathered from various salinity experiments indicates that decreased salinity increases the latent period of the phage as well and that this is directly related to molecular changes in the virus. It may be that the repressor protein is not cleaved due to an increased binding affinity for the viral DNA and the transition from lysogenic to lytic is delayed as was previously suggested for the ϕHSIC system (114). Conversely, it is also possible that the host promoter is unable to bind to the viral genome to begin transcription, or transcription machinery is not as efficient at lowered salinities.

These experiments have shown that unfavorable environmental conditions, such as low salinity, may be responsible for the transition of HSIC-1a cultures from the lytic life-cycle to the lysogenic life-cycle. Lower levels of viral gene expression in the 11 ppt treatment support this conclusion, as does the decrease in free and intracellular phage concentrations even as cell growth is increasing. The exact mechanism of this switch is still unknown, as are the mechanisms that lead to changes in substrate utilization upon infection of the host cell by a virus. It is possible that the decreases in salinity are leading to an increase in protein-protein interaction within the cell which would inhibit viral gene transcription. It is also possible that, in 11 ppt media, there are changes in ionic strength of the host cell cytoplasm leading to changes in viral gene expression. Further experiments with this system and others are necessary to pinpoint the exact cause as well as complete our understanding of the lysis/lysogeny decision in marine phages.

Chapter 3

Phage Lysis and Lysogeny in Bacterioplankton Populations in the Gulf of Mexico

Abstract

The occurrence of bacteriophages infecting bacterioplankton in the Gulf of Mexico was studied during a research cruise in July of 2005. Microbial activity was measured via bacterial productivity and primary production, and the frequency of visibly infected cells (FVIC) was also determined. Viral abundance decreased with depth in the nutrient-rich Mississippi River Plume from 3.66×10^7 VLP mL^{-1} at 3 meters to 3.06×10^6 mL^{-1} at 100 meters. At an oligotrophic station, viral abundance decreased significantly from 3 meters to 30 meters but then increased until a secondary peak in viral abundance was seen at 76 meters, above the subsurface chlorophyll maximum. The occurrence of lysogens (by prophage induction with Mitomycin C) and lytic viral production were measured at eleven stations by direct counts with epifluorescence microscopy. The slope of the viral abundance versus time in viral reduced samples was used to determine viral production rates. Significant lytic viral production was seen at three of the eleven stations in both surface and subsurface waters, while significant prophage induction was observed at three of eleven stations in subsurface waters (SCM or 500 meters deep). An estimated burst size of 18.72 was determined from FVIC counts and used to calculate the lysogenic fraction for each station. There is a statistically significant negative correlation between bacterial productivity and the lysogenic fraction ($P=0.0013$).

3.1 Introduction

Viral infection of a bacterial cell can lead to several different outcomes. One possible outcome is lysis which occurs when lytic phages infect a host and use the host cell replication machinery to produce new viral particles, lysing the host cell within a half-hour to two hours after infection and releasing the progeny phage. Pseudolysogeny, a persistent infection where both phage and host cells exist in high abundance simultaneously and the phage DNA does not integrate into the host genome, is another possible outcome (1). While pseudolysogeny has been studied in several marine phage/host systems, natural population studies have not been done (45, 67, 82).

The third and final possible outcome of a viral infection is lysogeny. A temperate phage infects the host but instead of lysing it immediately, the phage genome integrates into the host genome as a prophage or exists as a plasmid in the cytoplasm of the cell. Theoretically, when a prophage is in the latent stage, every time the host genome replicates, the viral genome will be replicated as well.

It has been hypothesized that lysogeny is a survival mechanism for phages. When host cell density is high, virulent phages are more prevalent (93). However, in environments where host cell density is low, such as oligotrophic or deep-water environments, the likelihood of contact between the host and the phage is less. As a result, it is advantageous to be a temperate phage and to remain a prophage until host cell density is again abundant and successful contact will ensue (93).

Previous studies have shown that 40% of isolates from the Atlantic and Pacific Oceans had inducible prophages and 71% of isolates from the Gulf of Trieste had inducible prophages (41, 42, 95). Despite the large abundance of inducible prophages in marine

bacteria, lysogenic viral production only contributes an estimated 0.02% of viral production (41). As such, the lysogenic cycle is not as important as the lytic cycle in the production of phage particles. In fact, phage infection in most systems is only responsible for 1 to 25% of all bacterial mortality in the open ocean. Phage mortality only becomes significant in highly eutrophic environments such as estuaries and coastal regions (35).

Nonetheless, viral-induced mortality is important to the marine trophic system. Marine microbes are regulated by two different top-down controls, grazing and viral-induced mortality. Cellular carbon from the microbe stays in the food-web and is transferred up trophic levels when predation occurs. In contrast, viral lysis of bacterioplankton leads to the release of cellular carbon into the DOM pool which is used by only heterotrophic bacteria. Bacterial carbon released via viral lysis is estimated to be between 8 and 42% in offshore environments and 6 to 25% in nearshore environments (111).

To fully understand how viral production affects and uncouples the marine microbial food web, viral production rates for different trophic systems are necessary. While direct counts give an indication of viral abundance, it is a static measurement that does not take viral turnover into account. Previous methods for measuring viral production include measuring viral decay rates but in order to estimate production from decay, it must be assumed that production is balancing decay which is not necessarily true. Additionally, viral decay measurements are affected by the method used and the system being studied making it hard to interpret and compare results. For example, Suttle and Chen (1992) found decay rates to be as high as 0.17 h^{-1} in coastal areas in the Gulf of Mexico while other studies in the Gulf of Mexico had rates ranging from 0.22 to 0.59 d^{-1} in the oligotrophic zone (97, 113). Finally, studies with two different phages in the Chesapeake

Bay found differing decay rates, 0.11 h^{-1} and 0.06 h^{-1}, between the two phages studied, under full sunlight (122).

Currently, the most direct method to measure viral production is the dilution technique (112). In the dilution technique, a sample is diluted with virus-free seawater thereby reducing the number of viruses. Samples can be taken over time to measure changes in viral concentrations using epifluorescence microscopy. In this way, an estimate of the viruses produced per hour from cells infected before the beginning of the experiment can be obtained. Viral production can also be measured by determining the frequency of visibly infected cells using transmission electron microscopy and using it to analyze the frequency of infected cells (69, 95, 109).

The dilution technique has been used to measure viral production in several different trophic systems. In general, viral production is greatest in eutrophic coastal zones where it can get as high as 1.84 X 10^9 VLP L^{-1} d^{-1} in the Baltic Sea (109). Viral production typically decreases from eutrophic zones to oligotrophic areas, and in a trophic gradient along the North Adriatic Sea, viral production decreased from 48.66 X 10^8 VLP L^{-1} hr^{-1} to 11.54 X 10^8 VLP L^{-1} hr^{-1} (8). Viral production will also decrease as depth increases as found in the Mediterranean Sea where production rates ranged from 0.082 X 10^9 VLP L^{-1} d^{-1} at less than 100 meters to 0.0001 X 10^9 VLP L^{-1} d^{-1} at 800 meters (109). However, these general trends are not always true. High levels of lysogeny have been observed in the heterotrophic bacterial population off the coast of British Columbia in the middle of a *Synechococcus* bloom, a decidedly eutrophic environment (75). This suggests that sweeping generalizations regarding viral production and lysogeny cannot be made and each system must be studied individually.

The Gulf of Mexico is characterized by eutrophic coastal waters and an oligotrophic open ocean. The northern Gulf of Mexico is heavily influenced by freshwater discharge from both the Mississippi and Atchafalaya Rivers. The Mississippi River is the largest river in North America and drains 41% of the United States (53). The large volume of flow from this river is responsible for what is known as the Mississippi River plume (MRP). The plume is a lens of low salinity, high-productivity that forms during spring and summer months due to nutrient loading from the river. Primary productivity rates in the MRP during summer months are higher there than anywhere else in the Gulf (53, 105, 115). However, the strength and distribution of the plume is dependent on the rate and quantity of nutrient loading from the Mississippi.

Samples were taken from both the oligotrophic waters of the Gulf of Mexico and the Mississippi Rive Plume to compare lytic viral production in these dynamic systems to prophage induction. Frequency of infected cells and the lysogenic fraction at varying depths were measured as well.

3.2 Materials and Methods

3.2.1 Sample Collection

Samples were obtained from sites located in the oligotrophic open ocean and in the eutrophic Mississippi River Plume in July of 2005 during a research cruise in the Gulf of Mexico (Figure 18). Surface samples were collected three meters below the surface using a submersible pump. Water samples at depth were collected using Niskin bottles mounted on a conductivity-temperature-depth (CTD) rosette with sensors for temperature, salinity, and fluorescence. All samples were pre-filtered to remove macro-organisms using a 50

μm mesh screen. Depth profiles were performed at station 2 which was located in oligotrophic waters and station 3, located within the MRP. At station 7, a free-floating marker buoy was placed in the water allowing lagrangian sampling of a discrete parcel of the plume every four hours for 24 hours for a total of six samples. Chlorophyll concentrations and primary productivity were measured at all stations and depths excluding stations 1 and 1X.

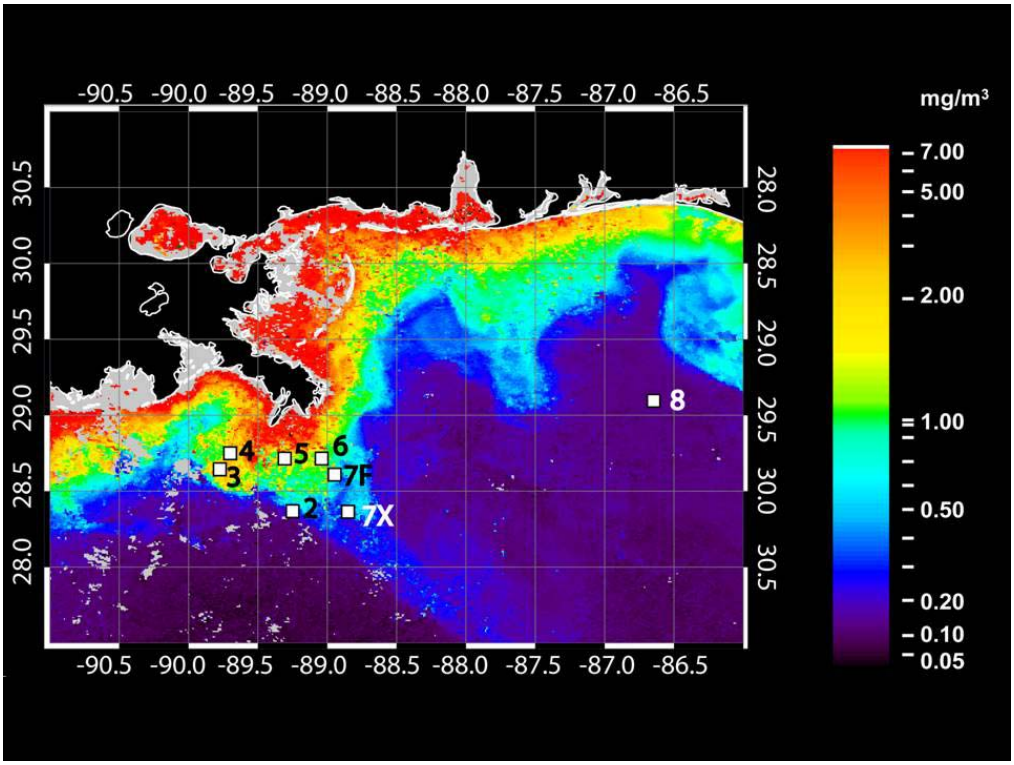

Figure 18. Sea-Viewing field-of-view sensor (SeaWiFS) image showing chlorophyll a concentrations in the Gulf of Mexico during the cruise. All stations are labeled except Station 1 which is off the image.

3.2.2 Enumeration of Bacteria and Viruses

Bacterial and viral populations were enumerated by filtering an appropriate sample volume onto 0.02 μm 25 mm Anodisc filters (Whatman Maidstone, England) followed by

staining with Sybr Gold nucleic acid stain (1:10,000 final dilution) (70). The volume filtered was dependent on the sample location and depth. Filters were stained for twelve minutes in the dark and mounted with an anti-fade solution composed of p-phenyldiamine in 50/50 filter-sterilized glycerol and phosphate-buffered saline.

3.2.3 Viral Production and Prophage Induction

Samples for lytic viral production and prophage induction were pretreated by the viral reduction method to decrease the background level of viruses in the samples (108). Briefly, samples were pre-filtered through a 2.0 μm-pore-size filter to remove grazers, and then filtered through a 0.2 μm pore-size filter to a volume of 5 mL to remove ambient viruses while retaining the majority of the bacterial population on the filter. Virus-free seawater (0.02 μm pore-size filtered) collected from the Gulf was added to the retentate to return it to the original sample volume. This procedure was repeated once, and then the filter was gently but thoroughly washed in the reconstituted sample to dislodge as many of the attached bacteria as possible before being discarded. The sample was then divided into aliquots for experimental manipulation.

Viral production rates were determined by performing a first order linear regression on the average viral counts from T_0, T_4, T_8, and T_{24}. The slope of the line is the rate of viral particles produced per hour. Viral production rates and prophage induction were measured at stations 1A, 1B, 1XS, 1XD, 2A, 2F, 4A, 7F, 7G, 8A, and 8B. Viral-reduced samples were divided into lytic viral production and prophage induction treatments (control and treatment). Prophage inductions were incubated with Mitomycin C at a concentration of 1 μg mL^{-1}. All samples were incubated in polymethylpropylene flasks

and kept under 14:10 light:dark cycle at room temperature. Sub-samples were taken from the treatment and control flasks at T_0, T_4, T_8, and T_{24} and Sybr slides for viral and bacterial enumeration were made in triplicate. The volume used for slides was dependent upon sample location and depth. Slides were foil wrapped and stored at -20 °C until they could be counted.

Environmental factors thought to be possible natural triggers of prophage induction were examined at stations 2A and 4A. Factors tested included ultraviolet (UV) light exposure, arsenite addition, and heat or cold shock. Arsenite was added to samples at a concentration of 1 μg mL^{-1} and samples were incubated as described above. Heat treatment incubations were performed in a waterbath set at 40 °C and cold treatments were performed in a refrigerated cooler set at 9 °C. Both treatments were incubated at the respective temperature for two hours and were then removed and incubated at room temperature as above. UV exposure treatment and control samples were incubated in a deck-top waterbath for 24 hours in sterile shallow glass containers covered with plastic wrap, and a UV shield was placed over the negative UV treatment to block UV rays. Sub-samples were taken at T_{24}, and slides for enumeration of bacteria and viruses were prepared as discussed previously.

3.2.4 Leucine Incorporation

Leucine incorporation was performed using Kirchman's method (46). Briefly, ambient water samples from each station were split in two, a treatment and control. The control flask contained 5% TCA to kill bacteria. 4,5-^{3}H-leucine was added to both flasks to a final concentration of 8 nM. Three 10 mL sub-samples were taken from each flask at T_0

and immediately filtered onto a 0.2 um Millipore GS filter. Each filter was rinsed twice with 5% TCA followed by two rinses with 80% ethanol. Filters were dried in glass scintillation vials with foil lined caps.

Treatment and control flasks were wrapped in aluminum foil and incubated at ambient water temperature in a deck-top incubator. Sub-samples were taken at 60 and 120 minutes after T_0 and were filtered as described above. Once the filters were dry, ethyl acetate was added to each vial to dissolve them. Ecoscint A was then added to each vial and the vials were allowed to sit for 24 hours to ensure maximal dispersal into the counting fluid. Each vial was counted in a scintillation counter with read times of 30 seconds.

The efficiency standard was calculated by making a 1:100 dilution of 4,5-^{3}H-leucine in sterile water. 0.1 μCi was spotted onto duplicate filters which were dissolved with ethyl acetate before Ecoscint A was added. Vials were counted in a scintillation counter. CPM was calculated by subtracting the blank count from the average count of two standards. The efficiency standard was calculated as CPM/DPM. Net rate was calculated as treatment rate- control rate. Leucine incorporation was calculated as follows:

$$\text{Moles Leu} = \frac{[(\text{CPM-blank})/\text{efficiency}]}{\text{DPM Added}} \quad X \quad \text{Moles Added}$$

Production rate as biomass was calculated by multiplying the net rate of leucine incorporation by 1.5 kg carbon mole^{-1}. Leucine uptake measurements were log 10 transformed before being used in statistical analysis.

3.2.5 Frequency of Visibly Infected Cells

In addition to measuring viral production and prophage induction rates by the viral reduction technique, the frequency of visibly infected cells (FVIC) was measured at stations 1A, 1B, 1XS, 1XD, 2A, 2F, 4A, 7F, 7G, 8A, and 8B. At each station, 10 mL of an ambient sample, in duplicate, was fixed with 2% final concentration of 0.2 μm filtered alkaline buffered formalin and stored in the dark at 4 °C until counted.

To prepare the samples for transmission electron microscopy, samples were ultra-centrifuged at 20 000 r.p.m onto a formvar-coated grid for twenty minutes. Grids were negatively stained for 30 seconds with uranyl acetate then rinsed three times with 0.02 μm filtered DI water and air dried. The grids were then examined using a Hitachi 7100 electron microscope utilizing 125 KeV accelerating voltage to allow visualization of viral particles within the intact bacterial cells. Cells containing at least five phages were considered infected and the total number of viral particles per cell were enumerated for an estimation of viral burst size (69). The FVIC was the proportion of total cells examined which contained visible viral particles. The frequency of infected cells (FIC) was estimated by the formula FIC = 9.524 FVIC – 3.256 (110).

The lysogenic fraction of each station where a production experiment was done was calculated by the following equation:

$$\frac{[(V_i - V_c)/B_z]}{Bact_c} \times 100$$

In this equation, V_i is the number of viruses counted in the induced sample, V_c is the number of viruses counted in the control sample, B_z is the calculated burst size, and $Bact_c$ is the number of bacterial cells counted in the control sample (79).

3.2.6 Statistical Analysis

All statistical analysis was done in SigmaStat v. 3.5 and Minitab v. 13. One-way ANOVA using the Holm-Sidak method as the post-hoc test, a pair-wise multiple comparison procedure, was done to determine which stations were significantly different from one another for the ambient viral and bacterial measurements. Viral and bacterial counts from the diel failed a normality test and so the Kruskal-Wallis One-way ANOVA on ranks was done on this data. The post-hoc test used for this data was a Tukey multiple pair-wise comparison test.

Significant increases in viral production from T_0 to T_4, T_8, or T_{24} were determined by using a 2-sample Student's t-test to analyze viral counts from the two time points. Induction was defined as the difference between viral abundance in the Mitomycin C treatment and the control treatment (108). Viral counts from the control and Mitomycin C treatment samples were compared by a 2-sample Student's t-test to determine if prophage induction was significant at a given time point.

One-way ANOVAs were performed using viral counts from the environmental factor experiments, control treatment, and Mitomycin C treatment at T_{24} to determine if any of the treatments were significantly different from one another. The post-hoc test used was the Holm-Sidak method. To test the differences in bacterial abundance, the Kruskal-Wallis one-way ANOVA was done using Dunn's method for the post-hoc test for station 2A and a Tukey test was used for station 4A. All correlations were done using the Pearson Product Moment Correlation in Minitab v. 13. To test the significance of the linear regression for viral production rates and lysogenic fraction versus leucine uptake, an ANOVA was done in SigmaStat using the linear regression option.

3.3 Results

3.3.1 Ambient Bacterial and Viral Populations

Sites sampled during this cruise represented strongly contrasting trophic systems near one another within the Gulf of Mexico. To assess differences in microbial communities between these trophic systems, ambient bacterial and viral populations were measured at each surface station and at varying depths including the subsurface chlorophyll maximum at stations 1B, 2F, 7G, and 8B (Figure 19). One-way ANOVA confirmed that surface viral populations were significantly greater at stations located within the plume (3A, 4A, 5A, 6A, and 7F) than at stations located in oligotrophic waters and on the shelf (1A, 1XS, 2A, and 8A). Bacterial concentrations in the surface plume samples were also significantly greater than those surface samples in oligotrophic waters. Within the plume, there were significant differences in bacterial abundances. Stations 4A and 7F were significantly greater than stations 5A and 6A. Ambient viral and bacterial counts as well as depth, salinity and temperature for each station are listed in Table 8.

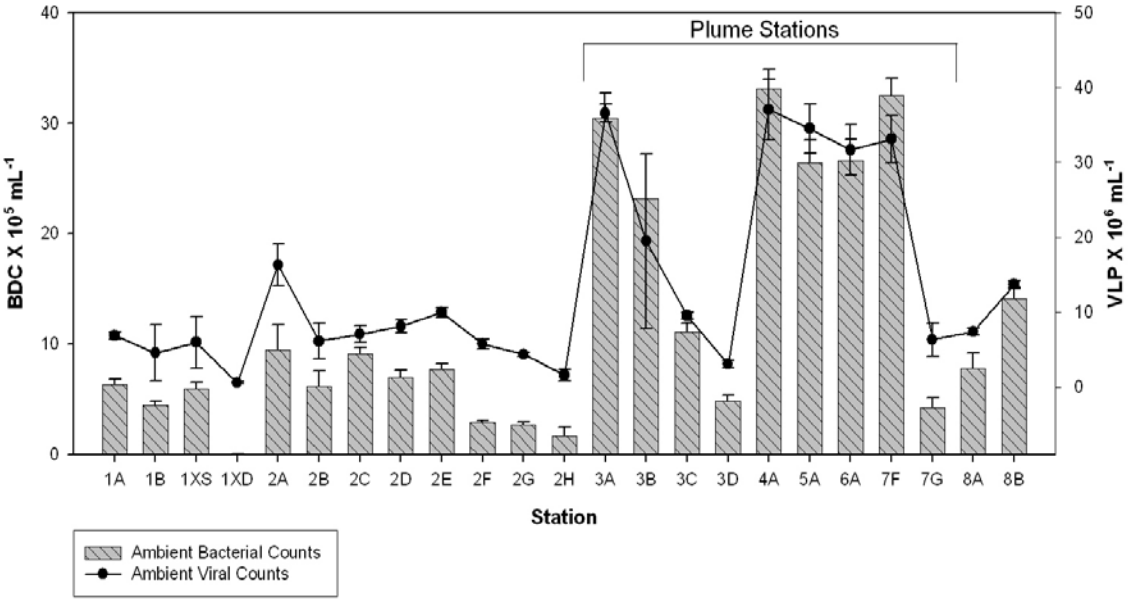

Figure 19. Ambient viral and bacterial counts at all stations. Error bars indicate triplicate slides.

The average ambient VBR (virus-to-bacteria ratio) was calculated for each station and is listed in Table 9. Overall, the total average VBR was 11.12. The largest surface VBR was measured at station 2A where it was 17.55 while the lowest VBR, 6.97, was seen at station 7B. The VBR at station 2A was significantly greater than all other surface stations ($p=<0.001$), but all other differences in VBR at surface stations were not significant. The VBR of samples collected at the SCM (1B, 2F, 7G and 8B) ranged from 9.38 at station 1B to 14.55 at station 7G. Stations 2F and 7G were both significantly greater than stations 1B and 8B which were not significantly different from one another ($p=<0.001$). Additionally, station 2F, a non-plume station, was significantly greater than 7G, a plume station.

Table 8. Ambient viral and bacterial counts from each station. Physical parameters, VBR, leucine uptake, chl *a*, and primary production are included.

Station	Sample	Location	Depth (m)	Temp (°C)	Salinity	VLP X 10^6 mL^{-1} (± S.D.)	BDC X 10^6 mL^{-1} (± S.D.)	VBR (Virus to bacteria ratio)	Leucine Uptake (pM Leucine LH^{-1})	Chl *a*	Primary Prod.
1	A	Shelf	3	27.2	36	6.90 (0.453)	0.636 (0.0491)	10.92	32.4	N/A	N/A
	B		60	22.22	36.36	4.60 (3.75)	0.452 (0.356)	9.38	12.82	N/A	N/A
	XS		3	28.9	36.07	5.99 (0.152)	0.598 (0.0553)	10.06	45.2	N/A	N/A
	XD		500	9	35	5.87 (0.151)	0.0655 (0.009)	9.03	0	N/A	N/A
2	A	Oligotrophic	3	29.5	34.3	16.4 (2.74)	0.946 (0.231)	17.55	83.05	0.266	3.71
	B		30	25.32	35.86	6.15 (2.40)	0.620 (0.139)	9.63	24.74	0.322	3.08
	C		40	25.48	36.4	7.11 (1.13)	0.911 (0.0582)	7.77	30.74	0.471	2.95
	D		50	24.58	36.24	8.11 (0.881)	0.700 (0.0658)	11.61	71.93	0.76	3.36
	E		76	21.2	36.45	10.0 (0.649)	0.769 (0.0513)	13.13	2.23	0.37	0.683
	F		88	20.7	36.5	5.77 (0.639)	0.295 (0.0164)	19.58	0.87	0.26	0.784
	G		100	20.1	36.5	4.41 (0.286)	0.275 (0.0180)	16.05	0.33	0.20	0.453
	H		140	17.6	36.57	1.62 (0.804)	0.172 (0.0786)	9.32	1.48	N/A	N/A
3	A	Plume	3	29.32	30.9	36.6 (1.23)	3.05 (0.228)	12.07	452.00	1.82	2.48
	B		8	28.95	31.4	19.5 (11.7)	2.32 (0.399)	9.07	807.8	1.40	2.28
	C		35	25.41	35.8	9.54 (0.409)	1.11 (0.0843)	8.66	10.97	0.296	1.80
	D		100	19.45	36.4	3.06 (0.476)	0.482 (0.0580)	6.34	3.51	0.213	1.64
4	A	Plume	3	29.39	30.12	37.1 (4.04)	3.31 (0.173)	11.21	661.5	2.103	3.40
5	A	Plume	3	28.5	31.98	34.5 (3.25)	2.64 (0.209)	13.06	517.1	1.64	4.22
6	A	Plume	3	29.07	31.6	31.7 (3.38)	2.66 (0.192)	11.95	295.84	1.86	1.51
7	A	Plume	3	29.1	31.32	35.3 (0.669)	3.23 (0.704)	11.09	540.54	1.73	3.43
	B		3	28.9	31.41	30.2 (1.91)	4.34 (0.345)	6.97	641.78	1.68	1.67
	C		3	28.9	31.47	29.2 (0.792)	2.98 (0.141)	9.83	386.96	1.54	3.20
	D		3	28.85	31.99	28.4 (8.50)	2.57 (0.310)	10.89	425.57	0.971	0.78
	E		3	28.86	31.99	16.1 (1.50)	1.41 (0.131)	11.43	471.04	0.55	10.31
	F		3	29.29	31.81	33.1 (3.15)	3.25 (0.155)	10.19	438.44	0.800	2.97
	G		67	23.2	36.5	6.36 (2.23)	4.25 (0.0849)	14.55	6.83	0.299	0.585
8	A	Oligotrophic	3	28.64	35.67	7.43 (0.533)	0.779 (0.140)	9.67	66.7	0.136	5.14
	B		55	23	36.27	13.7 (0.563)	1.41 (0.104)	9.80	30.97	0.48	0.92

Depth profiles were performed at stations 2 and 3. Salinity, temperature and fluorescence profiles both stations 2 and 3 are shown in Figure 20. The profile at the plume station, station 3, went to 100 meters while the profile at the oligotrophic station, station 2, went to 140 meters. The subsurface chlorophyll maximum at station 2 was at 88 meters (station 2F) while there was no SCM observed at station 3. Salinity at station 2 gradually increased with depth as did salinity at station 3, However, the salinity at Station 3 was extremely low at 3 and 8 meters due to the freshwater influx from the Mississippi. Conversely, fluorescence values were much higher in the surface waters of the MRP than in the oligotrophic surface waters. Fluorescence increased with depth at station 2 finally peaking at the SCM, while fluorescence values at station 3 increased from 3 meters to 8 meters before a sharp decrease signaling the plume boundary.

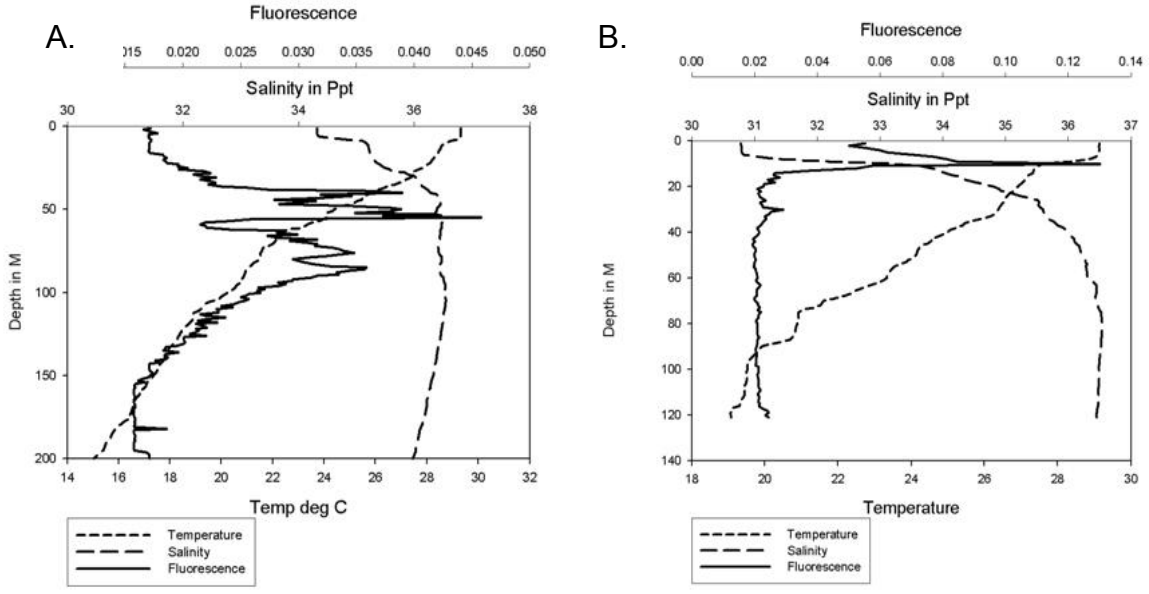

Figure 20. CTD profiles of stations 2 and 3. Temperature, salinity, and fluorescence are plotted versus depth for the profiles done at station 2 (panel A) and station 3 (panel B).

As was indicated by different CTD profiles from stations 2 and 3 and shown in Figure 21, differences in viral and bacterial abundance at these two stations was observed in the surface and upper water column samples. For example, viral abundance at station 2A was 1.64 X 10^7 VLP mL^{-1} whereas viral abundance at station 3A was significantly higher, 3.66 X 10^7 VLP mL^{-1}. Viral abundance at station 2 decreased as depth increased although a peak in abundance was observed at station 2E, the station above the SCM. While viral abundance at station 3 decreased with depth as well, abundance was higher overall at 3 than was seen at station 2. Additionally, there was a sharp decrease in viral and bacterial abundance past 8 meters at station 3 as we moved past the plume boundary. By 100 meters, viral and bacterial populations at the two stations were roughly equal.

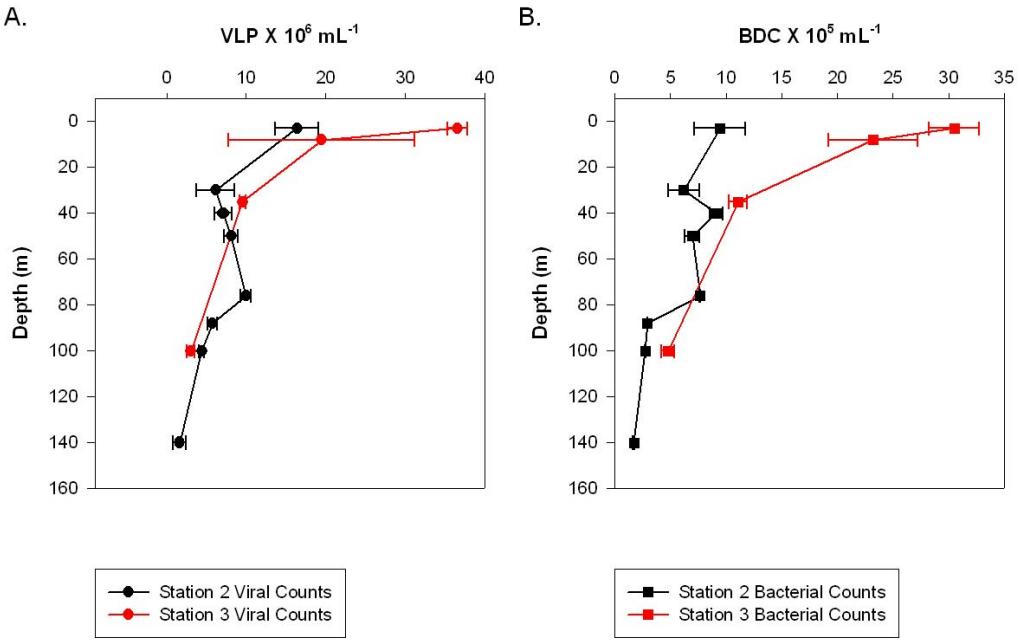

Figure 21. Viral and bacterial profiles at stations 2 and 3. Panel A is the viral profile and Panel B is the bacterial profile from both stations. Error bars represent triplicate slides counts.

3.3.2 Diel Experiment

Bacterial and viral abundance were measured over the course of 24 hours in a discrete parcel of the plume that was followed using a free-floating buoy (Figure 22). The starting time was at 18:41 on 17 July and measurements were taken every four hours until 14:33 on 18 July. Viral measurements ranged from 3.53 X 10^7 VLP mL^{-1} at station 7A to 1.61 X 10^7 VLP mL^{-1} at station 7E. There were no significant differences in viral abundance over the course of the diel. The average bacterial abundance over the course of the diel was 2.96 X 10^6 BDC mL^{-1}. Station 7B had a significantly larger bacterial population than 7E ($p=0.014$) but that was the only significant difference between bacterial abundance at the different stations.

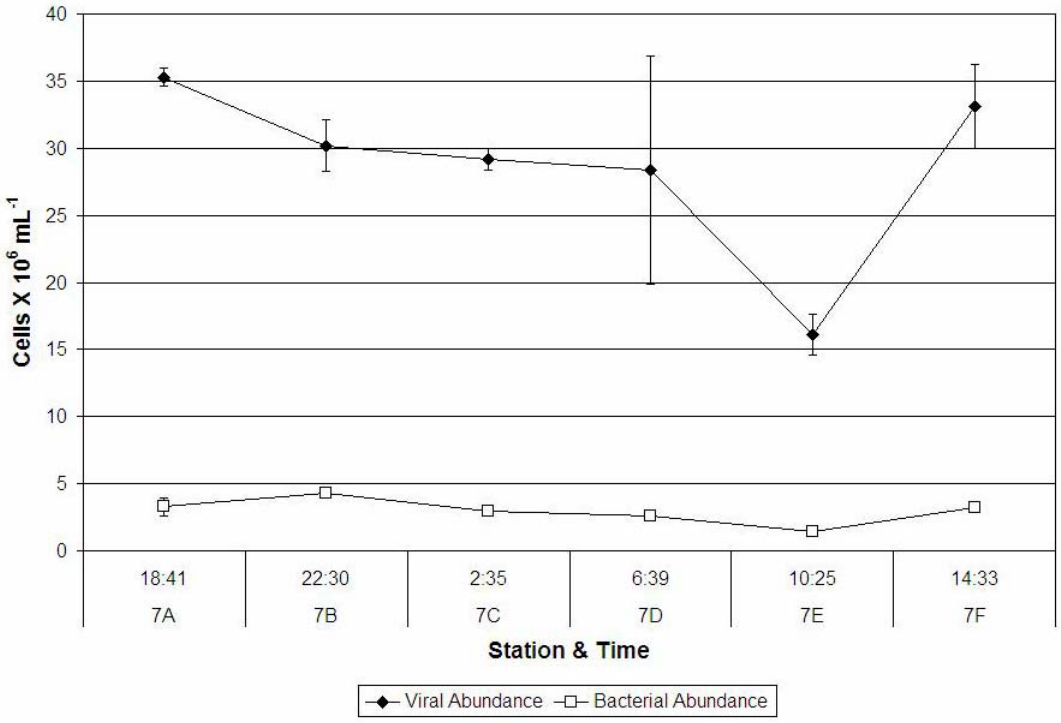

Figure 22. Viral and bacterial abundance during the diel. Error bars represent triplicate slides.

A Pearson Product Moment Correlation was done to see if there was a relationship between viral abundance at all time points and bacterial abundance at all time points. The correlation coefficient was 0.874 ($p=<0.001$) indicating that as bacterial populations increased, so did viral populations over the course of a diel.

3.3.3 Environmental Induction Experiments

Arsenate is in the same periodic group of elements as phosphorus and is an analog to it. Due to their valence similarities, arsenate is able to replace phopsphorus in the oxidative phosphorylation reaction thereby stopping ATP production and effectively killing the cell (74). Arsenite, a derivative of arsenate, works by binding to sulfhydryl groups and inhibiting protein function. It is also able to impair respiration by binding to the thiol groups of pyruvate dehydrogenase and 2-oxogluterate dehydrogenase (74). We decided to test its ability as an inducing agent in natural samples after previous experiments indicated that arsenate was an effective inducing agent in environmental sediment samples (63).

Numerous experiments have shown that ultraviolet light affects viral decay and can cause prophage induction (27, 32, 71, 97, 108, 113, 118, 122). As such, we compared induction between samples exposed to UV light and samples shielded from UV light.

In the lambda model of lysogeny, the lytic pathway is blocked at temperatures around 20°C. As the temperature increases to 37°C, however, the repressor protein is denatured and lambda will enter the lytic cycle (72). Previous experiments in our lab had seen significant induction in environmental samples incubated at either 40° C or 8° C. For that reason, we tested these factors on samples from the MRP and oligotrophic waters.

Viral and bacterial abundances at T_{24} for the environmental induction factors experiments are listed in Table 9. There was no indication of induction at either station although the –UV treatment did have significantly more viruses than the control and Mitomycin C treatments at station 4A. Bacterial abundances in the different treatments were significantly different from one another at station 2A but the post-hoc test did not reveal which were different. At station 4A, bacterial abundance was significantly greater than that in the Mitomycin C treatment. All other differences in bacterial abundances between the treatments were not significant.

Table 9. Viral and bacterial counts from the environmental induction experiments.

Treatment	2A VLP X 10^6 mL^{-1} (± S.D.)	2A BDC X 10^6 mL^{-1} (± S.D.)	4A VLP X 10^6 mL^{-1} (± S.D.)	4A BDC X 10^6 mL^{-1} (± S.D.)
Control	1.55 (0.51)	1.01 (0.079)	9.33 (0.074)	5.51 (0.61)
Mitomycin C	1.19 (0.25)	0.475 (0.091)	9.73 (0.82)	0.857 (0.048)
+UV	1.01 (0.09)	1.37 (0.089)	11.4 (1.07)	4.89 (0.020)
-UV	0.812 (0.095)	1.64 (0.0067)	13.0 (1.60)	6.35 (0.54)
Heat	0.551 (0.17)	2.12 (1.24)	5.76 (0.22)	3.27 (0.56)
Cold	0.704 (0.027)	1.02 (0.037)	5.06 (0.21)	2.74 (0.26)
Arsenite	0.971 (0.058)	0.622 (0.062)	9.74 (1.02)	3.83 (0.15)

3.3.4 Lytic Viral Production and Prophage Induction

Viral production rates were measured at six stations: 1; 1X; 2; 4; 7; and 8. A surface sample and an SCM sample were collected at all stations except for station 4 which was a surface station only and station 1XD which was collected at 500 meters. Sub-samples were taken from the control treatment every four hours and the average viral counts for

each time point were used to determine lytic viral production rates in the different trophic systems by doing a first-order linear regression. Viral production rates for each station at T_4, T_8, and T_{24} are listed in Table 10.

If a station had positive production rates at T_{24}, a Student's t-test was done comparing viral abundances at the T_0 sub-sample and in the T_{24} control. Significant viral production occurred if T_{24} viral abundance was significantly greater than T_0 viral abundance at a 90% confidence interval or greater. At T_{24}, the only stations that had positive, significant changes in viral abundance were the oligotrophic stations 2A (p=0.067), 8A (p=0.005), and 8B (p=0.042). Station 7F had a positive production rate but it was not statistically significant. The linear regression of these stations is plotted in Figure 23.

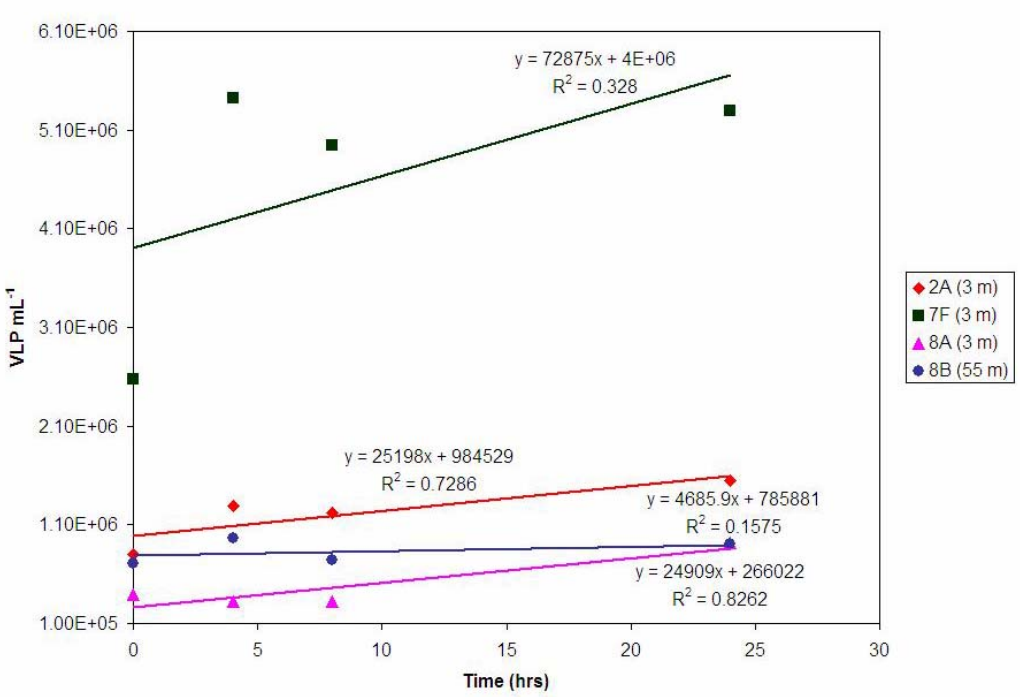

Figure 23. Lytic viral production at T_{24} (VLP per mL per hour). Stations 2A, 8A, and 8B were the only ones with significant changes in viral abundance between the T_0 and T_{24} time-points.

At T_4, positive rates of production were seen at stations 1XS, 1XD, 2A, 2F, 7F, and 8B. Of those, stations 2A, 7F, and 8B were statistically significant. At T_8, positive rates of production were seen at stations 1A, 1XS, 2A, 2F, 7F, and 8B. Only stations 1A and 8B were not significant at this time points. Again, a Student's t-test was done to determine if the differences between the time point in question and T_0 were significantly different. Production rates along with p-values are listed in Table 11. While the production rates do change depending upon the time used, and different stations are significant at different times, we felt that the T_{24} count was the most accurate. Other studies measuring lytic viral production have used the later time points as well (75).

The significance of each regression was determined for all stations that had a positive production rate at T_4, T_8, and T_{24}. The regression was a perfect fit at T_4 meaning that the differences between the two points at stations 1XS, 1XD, 2A, 2F, 7F, and 8B were significant. This was expected, however, because there were only two points in the regression. At T_8 and T_{24}, none of the regressions performed at stations where viral production rates were positive were significant.

To find the significance of the differences in between viral abundance in the control treatment and in the Mitomycin C treatment, a Student's t-test was done on the viral counts from both the treatment and the control at each of the three time points. The differences in viral abundance between the two samples as well as p values from the significance testing are listed in Table 10. Significant prophage induction occurred at station 1B at T_4. At T_8, stations 1A, 1B, and 4A all had significantly more viruses in the Mitomycin C treatment than in the control. Finally, at T_{24}, stations 1XD, 2F, and 8B all saw significant prophage induction as seen in Figure 24.

Table 10. Viral Measurements. Production Rates, induction values, % FIC, % lysogenic fraction, and burst size are listed. Prophage induction is defined as the difference between VLP in the Mitomycin C and control treatments. Italicized numbers were significantly greater at the 90% level and bolded numbers were significantly greater at the 95% level, P values are given in parentheses.

Station	Viral Prod. T_4 (VLP mL^{-1} hr^{-1})	Viral Prod. T_8 (VLP mL^{-1} hr^{-1})	Viral Prod. T_{24} (VLP mL^{-1} hr^{-1})	Induction T_4 (VLP mL^{-1})	Induction T_8 (VLP mL^{-1})	Induction T_{24} (VLP mL^{-1})	Burst Size	Avg. % FIC (± S.D.)	% Lysogenic Fraction
1A	-1.80×10^4	1.68×10^2	-1.60×10^3	6.03×10^3	*5.99×10^4 (0.060)*	-4.69×10^3	N/A	0 (0)	-0.039
1B	-1.62×10^4	-7.95×10^2	-1.75×10^3	*5.80×10^4 (0.082)*	-8.44×10^4	-1.14×10^4	25.6	4.1 (3.0)	-0.134
1XS	1.04×10^4	**7.11×10^3 (0.017)**	-1.99×10^3	-2.19×10^4	1.09×10^4	2.51×10^4	15	4.1 (0.1)	0.225
1XD	7.57×10^3	-1.76×10^3	-2.85×10^3	3.35×10^2	4.58×10^4	*8.13×10^4 (0.056)*	21	0.7 (N/A)	6.64
2A	**1.22×10^5 (0.018)**	**5.28×10^4 (0.004)**	*2.52×10^4 (0.067)*	-2.48×10^5	-2.05×10^5	-3.57×10^5	17.5	2.4 (0.4)	-2.02
2F	3.69×10^4	**2.36×10^4 (0.025)**	-5.15×10^3	1.72×10^4	-5.99×10^4	**3.83×10^5 (0.030)**	10	0.65 (0.9)	6.94
4A	-2.14×10^5	-5.80×10^5	-1.77×10^5	-3.29×10^6	*2.16×10^6 (0.056)*	4.02×10^5	>24.9	7.05 (0.4)	0.649
7F	*7.13×10^5 (0.074)*	*2.95×10^5 (0.079)*	7.29×10^4	-4.16×10^5	-1.53×10^6	1.18×10^6	21.2	3.15 (1.5)	-0.798
7G	-1.07×10^5	-1.58×10^5	-2.84×10^4	9.55×10^4	3.49×10^5	2.72×10^5	19	3.32 (0.3)	1.68
8A	-1.82×10^4	-9.76×10^3	**2.49×10^4 (0.005)**	-4.62×10^4	1.69×10^5	-1.53×10^5	>20	0.69 (1.0)	-1.05
8B	**6.39×10^4 (0.012)**	3.46×10^3	**4.69×10^3 (0.042)**	-1.76×10^5	-1.26×10^5	**6.63×10^5 (<0.001)**	13	0.70 (1.0)	2.52

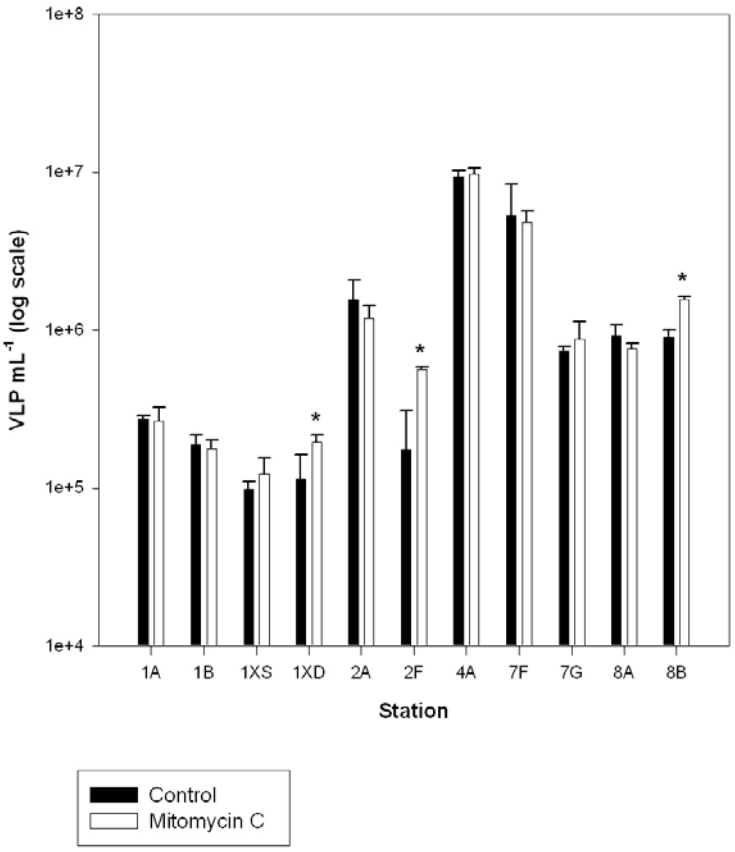

Figure 24. Prophage induction at T_{24}. * denotes stations where viral abundance was significantly greater in the Mitomycin C treatment. Error bars represent triplicate slides.

3.3.5 Frequency of Infected Cells and Lysogenic Fraction

Using the method developed by Weinbauer et al. (2002), we were able to relate FVIC as measured by TEM to the % frequency of infected cells at stations where production and induction experiments were done. As there was no significant difference between the burst sizes obtained from the different stations, the average burst size, 18.72 viruses per cell, was used. The lysogenic fraction (%) was calculated for each station where production and induction experiments were carried out. Burst sizes and lysogenic fractions for those stations are listed in Table 10.

The lysogenic fraction in surface samples was typically negative and ranged from -0.03% to -2.01% as listed in Table 10. Negative lysogenic fraction occurs when viral abundance in the control treatment is greater than viral abundance in the Mitomycin C treatment. Stations 1XS and 4A had positive lysogenic fractions but the values were not greater than 1%. On the other hand, samples collected at 1XD, 2F, 7G, and 8B, all of which were from the subsurface chlorophyll maximum or deeper, had positive lysogenic fraction values. Values at these stations ranged from 1.67% to 6.94%. The only SCM sample that did not have a positive lysogenic fraction was station 1B, a shelf station.

Lysogenic fraction was greatest at the stations 1XD, 2F, and 8B, the only three stations that had significant prophage induction at T_{24}. Additionally, the highest % FIC values were seen at stations that had low or negative lysogenic fraction values such as stations 1B, 1XS, 2A, 4A, 7F, and 7G. None of these stations had significant induction values at T_{24}.

A linear regression between the lysogenic fraction and the log-transformed values of leucine uptake was calculated and is shown in Figure 25. The Pearson Product Moment correlation for lysogenic fraction and leucine uptake was -0.876 ($p=0.0220$) indicating that there is a strong inverse relationship between the two. Bacterial activity was also negatively correlated with depth, and the correlation value is -0.815 ($p=0.002$) indicating that as depth increases, bacterial activity decreases. Therefore, as bacterial activity decreases with depth, the lysogenic fraction increases.

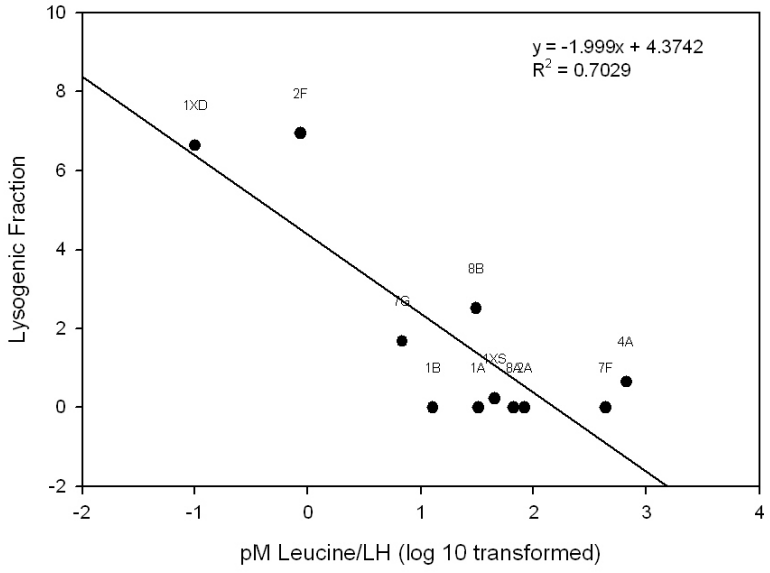

Figure 25. Linear regression of the lysogenic fraction vs. bacterial activity.

3.3.6 Correlations

Pearson Product Moment correlations were done using the physical parameters from the stations where viral production and prophage induction were measured. Table 11 lists the correlation value and the p-value for salinity, depth, temperature, chlorophyll *a*, primary productivity, induction (number of viruses in the treatment minus the number of viruses in the control), leucine uptake, lytic viral production, average % FIC, the % lysogenic fraction, estimated burst size, VBR, and ambient viral and bacterial counts.

Bacterial abundance was positively correlated to viral abundance, leucine uptake, chlorophyll *a*, and induction. Also positively correlated to chlorophyll *a* and leucine uptake was the ambient viral population. Leucine uptake was positively correlated to temperature and chlorophyll *a* was positively correlated to the average % FIC.

Inverse relationships were found as well. Both the ambient viral abundance and the ambient bacterial abundance were negatively correlated with salinity. The % lysogenic fraction was negatively correlated to temperature and leucine uptake while leucine uptake was negatively correlated to depth. Average % FIC and chlorophyll *a* concentrations were negatively correlated to salinity. Finally, depth was negatively correlated to temperature and primary production.

Table 11. Correlation table. The top number is the Pearson Product value and the bottom number is the p-value. Significant relationships are bolded.

Factors	Lytic Prod.	Temp.	Salinity	Depth	Induction	Chl *a*	1° Prod.	Leucine Uptake	Avg. FIC	Lysog. Fraction	Burst Size	VBR	VLP/mL
Temp.	0.293												
	0.382												
Salinity	0.028	-0.273											
	0.935	0.417											
Depth	-0.241	**-0.923**	0.131										
	0.476	**0**	0.701										
Induction	-0.517	0.042	-0.396	-0.074									
	0.103	0.902	0.228	0.829									
Chl. *a*	-0.441	0.293	**-0.86**	-0.382	0.329								
	0.322	0.524	**0.013**	0.398	0.471								
1° Prod.	0.707	0.606	-0.463	**-0.896**	-0.4	0.16							
	0.076	0.149	0.296	**0.006**	0.373	0.732							
Leucine Uptake	0.245	**0.855**	-0.593	**-0.815**	0.231	0.634	0.664						
	0.467	**0.001**	0.055	**0.002**	0.494	0.126	0.104						
Avg. FIC	-0.245	0.414	**-0.605**	-0.305	0.138	**0.888**	0.162	0.521					
	0.468	0.205	**0.048**	0.361	0.686	**0.008**	0.728	0.1					
Lysog. Fraction	-0.098	**-0.849**	0.318	0.696	-0.025	-0.596	-0.527	**-0.876**	-0.766				
	0.854	**0.032**	0.539	0.124	0.962	0.404	0.473	**0.022**	0.076				
Burst Size	-0.055	0.056	-0.51	0.074	-0.07	0.638	0.604	0.294	0.586	-0.33			
	0.88	0.877	0.132	0.838	0.847	0.123	0.151	0.409	0.075	0.523			
VBR	0.199	0.146	0.12	-0.177	-0.142	-0.333	-0.361	-0.173	-0.107	0.398	-0.529		
	0.557	0.669	0.726	0.603	0.676	0.466	0.427	0.611	0.753	0.434	0.116		
VLP/mL	-0.021	0.492	**-0.916**	-0.419	0.57	**0.85**	0.325	**0.77**	0.589	-0.52	0.331	-0.042	
	0.951	0.124	**0**	0.2	0.067	**0.015**	0.477	**0.006**	0.057	0.291	0.351	0.903	
BDC/mL	-0.095	0.455	**-0.891**	-0.395	**0.652**	**0.822**	0.307	**0.77**	0.56	-0.553	0.358	-0.196	**0.982**
	0.781	0.16	**0**	0.229	**0.03**	**0.023**	0.502	**0.006**	0.073	0.255	0.31	0.563	**0**

3.4 Discussion

In this study, we examined the differences in viral production between two strongly contrasting trophic systems, the oligotrophic Gulf of Mexico and the eutrophic Mississippi River Plume. Ambient viral and bacterial populations were significantly greater at surface stations located within the MRP. The MRP is an area of high productivity, and many other studies have shown that viral abundance is greatest in eutrophic zones (8, 41, 42, 75, 108, 109, 112). There was a strong positive correlation between the ambient viral and the ambient bacterial counts at the stations where experiments were done indicating that the viral populations reflect the concentration of the host. In addition to being positively correlated to each other, ambient viral populations and bacterial populations at stations used in the viral production experiments were positively correlated to chlorophyll *a* and leucine uptake, and were negatively correlated to salinity. As the plume is a lens of low-salinity, high productivity and bacterial and viral populations were greatest at stations within the plume where salinity is low and nutrient levels are high, these relationships are not surprising. Similar correlations have been noted in other studies as reviewed in Parada et al (2006).

Excluding station 2, the maximum VBR was at stations within the MRP while the minimum VBR was seen at oligotrophic stations such as station 8. A decline in VBR from eutrophic to oligotrophic environments was also observed in the North Adriatic Sea and between the Baltic and Mediterranean Seas (8, 109). Station 2, an oligotrophic station located near the plume, had high bacterial and viral abundances as compared to the other oligotrophic stations but not as high as the MRP yet VBR was the highest at stations 2A, 2F, and 2G. High VBR means more viral production and greater rates of bacterial lysis

which is true for station 2 (123). Significant lytic viral production was observed at all three times points for station 2A and, at T_8, station 2F had significant lytic viral production. Most importantly, the differences in VBR between the stations suggest that while there may be a sharp change in chlorophyll *a* and other physical parameters between the oligotrophic waters and the eutrophic MRP, there is some flow of nutrients between the two parcels of water leading to large viral populations in the oligotrophic waters surrounding the plume. If this is true, the marine microbial food web and the flow of carbon through the food web in the boundary layers surrounding the MRP would be affected. Models that combine eutrophic and oligotrophic system characteristics would be necessary to predict the effects in this region of the Gulf of Mexico.

Rates of lytic viral production were measured using direct viral counts from four different time points. One of the problems with using first-order linear regressions to determine viral production rates is that the rate will change depending on the length of the experiment and stations used. Most viral production rate experiments only go for eight hours but by carrying the experiments out to 24 hours and sampling at four different time points, we were able to track production and compare the rates at different times (36, 112).

Differences in rates between the different sampling times and the significance of the differences were observed but the overall trend did not change. One of the MRP stations, 7F, had significant lytic viral production at T_4, T_8, and T_{24}. However, station 4A, located in the middle of the MRP, had negative rates of viral production throughout the experiment which may have been a result of the fact that this station was sampled at 15:30. Previous studies have shown that lytic viral production is significantly greater in

eutrophic, non-steady state environments. Rates in the surface waters of the north Adriatic Sea varied from 4.86 X 10^6 VLP mL^{-1} hr^{-1} to 1.154 X 10^6 VLP mL^{-1} hr^{-1} (8). In well-mixed areas of the Strait of Georgia, viral production was anywhere from 2.2 X 10^6 mL^{-1} hr^{-1} to 6.2 X 10^6 mL^{-1} hr^{-1} (112).

Viral production rates in our experiments did not reach levels seen in eutrophic well-mixed environments. Within the MRP, the only positive viral production rates were seen at station 7F and ranged from 7.13 X 10^5 VLP mL^{-1} hr^{-1} at T_4 to 7.29 X 10^4 VLP mL^{-1} hr^{-1} at T_{24}. A similar phenomenon was observed in the Strait of Georgia where low rates of lytic viral production were observed in heterotrophic bacteria. Additionally, inducible lysogens were found in *Synechococcus* populations even though it was the middle of the bloom (75). However, production rates in the oligotrophic Gulf of Mexico were similar to surface rates in the oligotrophic waters of the Mediterranean Sea (109).

Significant lytic viral production occurred at the oligotrophic stations 2A, 8A, and 8B at T_{24}. Yet, when the significance of the linear regression was tested, none of the regressions were significant. Significance testing of linear regression only serves to tell if the independent variable and the dependent variable co-vary. For our purpose, we were looking at the changes in viral abundance with time and were not attempting to predict values. As such, it is fair to assume that stations with high R^2 values such as stations 2A and 8A are accurate estimates of viral production while station 8B is not completely accurate. Viral production at the stations studied had no significant correlations to any of other factors.

In contrast, induction values had a positive relationship to the ambient population of bacteria at the sample sites where induction was measured at T_{24}. The correlation

between bacterial abundance and prophage induction seems to indicate that there were more lysogens within the plume where bacterial abundance was greatest. At T_{24}, this was true as induction occurred at all three plume stations as well as at 1XS, 1XD, 2F, and 8B. Significant prophage induction, however, was only seen at stations from the SCM or deeper.

Lysogeny in the marine environment is believed to be a survival mechanism for phages in periods of low host abundance and our data supports this hypothesis (75, 76, 93, 108, 109, 115). In addition to significant induction at depth, there was a strong negative correlation between the lysogenic fraction and bacterial production as determined by leucine uptake. Leucine uptake also had a strong negative correlation with depth, indicating that as depth increased, bacterial production decreased. Meanwhile, as leucine uptake decreased, the lysogenic fraction increased and was greatest in samples collected at depth. Interestingly, leucine uptake was also at its highest levels at stations located within the MRP where induction events were seen at T_{24}.

Few studies have measured FIC directly while also measuring viral production rates (109). From FIC results, we were able to estimate minimum burst sizes in and out of the MRP rather than using the standard burst size of 50 viruses per cell (35). The mean value of burst sizes for different eutrophic environments is 24.9 as reviewed in Parada et al. (2006). Minimum burst sizes in the Mississippi River Plume were estimated to be 21.7 which is most likely an underestimate as there were bacterioplankton with viral particles that were too numerous to be counted at station 4A. In the oligotrophic waters of the Gulf, the average estimated burst size was 18.92 which is similar to the average burst size of 19.8 for other oligotrophic environments (76). Numerous studies have found that burst

sizes and FIC increased towards eutrophic condition, a finding that was supported by the results of our experiments with one exception (8, 109). Stations 1 and 1X was located on the Florida shelf and is influenced by coastal influx which would explain why the average burst sizes at these stations are comparable to those seen in the MRP.

Burst size was not correlated to any other factors measured during the cruise including bacterial production and average FIC. This is not unexpected as burst size and frequency of infected cells do not correlate with bacterial production in most marine systems (76). FIC, on the other hand, was positively correlated to chlorophyll *a* and negatively correlated to salinity. A positive correlation between chlorophyll *a* and FIC indicates that the more productive a station, such as those located within the MRP, the more viral-infected cells. FIC also had a weak negative correlation to salinity which was most likely a result of the lowered salinity levels seen at stations within the MRP.

The purpose of these experiments was to analyze and compare viral populations in nutrient replete and deplete conditions in the Gulf of Mexico. Lysogeny appears to be the survival mechanism for phages at depth in the Gulf of Mexico where bacterial populations can get as low as 10^4 mL^{-1}. It has been previously suggested that viral production is a hallmark of highly productive, eutrophic ecosystems while prophage induction will be seen in oligotrophic systems. We found that significant lytic viral production was most likely to occur in surface waters, regardless of the trophic system, while significant prophage induction was found in samples obtained in and out of the Mississippi River Plume, an area of high-productivity and high viral abundance. This data indicates that generalizations about viral production and lysogeny and their combined effects on the microbial food web are not necessarily true. To fully understand

the effects of phages on the marine microbial food web and the flow of carbon in the ocean, these parameters must be examined for the system in question.

Chapter 4

Summary and Conclusions

Viruses are the most abundant organism on the planet with the greatest concentration found in the world's oceans (6, 10, 29, 33, 82, 121). Many of these marine viruses are bacteriophages, viruses that infect heterotrophic and autotrophic marine bacteria (81). Viral-induced lysis of marine bacteria leads to the partitioning of carbon and other nutrients that would typically be transferred to higher trophic levels, and may impact global CO_2 levels. Lysogeny is a highly evolved state between viruses and bacteria. Each can influence the other's gene expression and lysogenic infection can alter host phenotype. A survey of marine bacterial isolates as well as characterized bacteria indicated that ~45% of the cultivated bacteria contain inducible prophages (1, 41). As such, it is necessary to study factors that influence the occurrence and control of lysogeny in the marine bacteria. The purpose of this thesis project was to analyze gene expression in the ϕHSIC/*L. pelagia* phage-host system under normal and low-salinity conditions as well as investigate viral production and prophage induction in bacterioplankton populations in the Gulf of Mexico.

By performing a synchronous infection, I was able to follow infection of *L. pelagia* by ϕHSIC over the course of an infection cycle from 0 to 60 minutes post-infection. Not only did these experiments indicate which ORFs were most highly expressed during a typical infection but it also allowed for the classification of ϕHSIC ORFs by peak

expression time. For example, ORFs 38 through 47 excluding ORF 46 had the highest levels of expression at 0 minutes post-infection as did ORFs 1 through 6. Conversely, expression values of ORFs 17, 18, 25, 26, and 28 were greatest at the later time-points in the infection cycle (Figure 10). Additionally, I was able to determine which genes do not have significant changes in expression over the course of the infection cycle. Half of these ORFs are structural phage genes and are located near putative promoters (Figure 11).

In both salinity experiments, cell growth in the 11 ppt treatment was initially low but caught up to the 39 ppt treatment by T_8 and was higher for the rest of the experiment even though the actual growth rate of the 11 ppt culture was only higher than the 39 ppt culture in the second salinity experiment (Figures 14A and 15A). Yet, in both experiments, free phage production was significantly lower in the 11 ppt treatment than in the 39 ppt treatment. When the number of plaque forming units was compared between the two treatments, there were typically 282 free phages in the 39 ppt treatment for every free phage in the 11 ppt treatment. Additionally, there was an average of one phage per bacterial cell in the 11 ppt treatment as compared to the 39 ppt treatment which had an average of 58 phages per bacterial cell. Salinity experiments with the uninfected *L. pelagia* indicated that the low salinity was not affecting host cell physiology in ways that would be detected with growth curve experiments (Figure 13).

Gene expression was consistently higher in the 39 ppt treatment during both salinity experiments (Figures 16 and 17). Some of the ORFs that had higher expression in the normal salinity treatment included ORFs 17, 18 (major capsid protein), 30, 35 (structural phage protein), and 37 (baseplate subunit/tail lysozyme). Very rarely was an ORF

consistently higher expressed in the 11 ppt treatment. To understand what was happening on the cellular level during the salinity experiments, real-time PCR of cellular DNA extracted from HSIC-1a cells at different time points in the second salinity experiment was performed. Results indicated that there were one to two more gene copies per cell in the 39 ppt treatment at all the time points examined.

These findings support my hypothesis that lowered salinity causes the pseudolysogen to enter the lysogenic state and hence, lowered gene expression was measured. To truly prove this hypothesis, salinity experiments in which gene expression and phage concentrations, both free and intracellular, are measured from the start of the experiment to 48 hours or possibly longer are necessary. By doing so, we will know if HSIC-1a cells in the low salinity treatment remain lysogenic with low viral gene expression, or eventually acclimatize to the low salinity and re-enter the pseudolysogenic life-style. This will also tell us if stressful environmental conditions such as low salinity lead to a stable lysogenic state even if there is a high population of host cells, or if the virus is able to adapt and become pseudolysogenic.

In the Gulf of Mexico, viral production was seen at oligotrophic stations as opposed to plume stations where viral production was expected, and was not correlated to any other factors. Prophage induction was seen primarily at depth. The lysogenic fraction had a strong negative correlation to bacterial activity which decreased with depth. As has been previously predicted, lysogeny is more prevalent at depth where host cell density is low (93).

For a better understanding of the ϕHSIC and factors that influence the lysis/lysogeny decision, the function of the unknown ϕHSIC ORFs must be determined. However, this is

limited by our current lack of sequence information for marine phages. Knock-out mutants of ϕHSIC could be designed and viability of mutant phages analyzed to gain some insight into ORF function. However, at this time there is no way to transfect the host using purified viral DNA. It would also be helpful to have the complete genome sequence of *L. pelagia*. By sequencing the host, we would be able to look for the integration site and genes that surround the prophage. In addition, this would provide a better understanding of metabolic pathway changes that occur when ϕHSIC infects *L. pelagia* as was seen in the Biolog results.

While both pseudolysogeny and lysogeny have been extensively studied in laboratory systems and natural populations, neither is completely understood. Gene expression analysis of ϕHSIC has led to a greater understanding of the pseudolysogenic life-style, and factors that influence the switch from pseudolysogeny to lysogeny such as the change in environmental conditions. The Gulf of Mexico experiments show that high levels of bacterial activity do not necessarily mean that there will be high levels of viral production. In conclusion, I have determined that unfavorable environmental conditions such as salinity stress and low host cell density can be used to predict the occurrence of lysogeny in both marine bacteria and the ϕHSIC/*L. pelagia* phage-host system.

List of References

1. **Ackermann, H. W. and M. S. Dubow.** 1987. Viruses of Prokaryotes, Volume I. CRC Press, Boca Raton, FL.

2. **Azam, F., T. Fenchel, J. G. Field, J. S. Gray, L. A. Meyer-Reil, and F. Thingstad.** 1983. The ecological role of water-column microbes in the sea. Marine Ecology Progress Series **10:**257-263.

3. **Becker, A., H. Berges, E. Krol, C. Bruand, S. Rueberg, D. Capela, E. Lauber, E. Meilhoc, F. Ampe, and F. J. de Bruijn.** 2004. Global Changes in Gene Expression in *Sinorhizobium meliloti* 1021 under Microoxic and Symbiotic Conditions. Mol. Plant-Microbe Interact. **17:**292-303.

4. **Bell, A. C. and G. B. Koudelka.** 1993. Operator sequence context influences amino acid-base-pair interactions in 434 repressor-operator complexes. J. Mol. Biol. **234:**542-553.

5. **Bergès, H., E. Lauber, C. Liebe, J. Batut, D. Kahn, F. J. de Bruijn, and F. Ampe.** 2003. Development of *Sinorhizobium meliloti* pilot macroarrays for transcriptome analysis. Appl. Environ. Microbiol. **3:**1214-1219.

6. **Bergh, O., K. Y. Borsheim, G. Bratbak, and M. Heldal.** 1989. High abundance of viruses found in aquatic environments. Nature **340:**467-468.

7. **Bibb, L. A. and G. F. Hatfull.** 2002. Integration and excision of the *Mycobacterium tuberculosis* prophage-like element, phiRv1. Mol. Microbiol. **45:**1515-1526.

8. **Bongiorni, L., M. Magagnini, M. Armeni, R. Noble, and R. Danovaro.** 2005. Viral production, decay rates, and life strategies along a trophic gradient in the North Adriatic Sea. Appl. Environ. Microbiol. **71:**6644-6650.

9. **Breitbart, M., P. Salamon, B. Andresen, J. M. Mahaffy, A. M. Segall, D. Mead, F. Azam, and F. Rohwer.** 2002. Genomic analysis of uncultured marine viral communities. Proceedings of the National Academy of Sciences of the United States of America **99:**14250-14255.

10. **Breitbart, M. D., B. D. Felts, S. D. Kelley, J. M. D. Mahaffy, J. D. Nulton, P. D. Salamon, and F. D. Rohwer.** 2004. Diversity and population structure of a near-shore marine-sediment viral community. Proceedings: Biological Sciences **271:**565-574.

11. **Brussow, H. and F. Desiere.** 2001. Comparative phage genomics and the evolution of *Siphoviridae*: Insights from dairy phages. Mol. Microbiol. **39:**213-222.

12. **Canchaya, C., G. Fournous, S. Chibani-Chennoufi, M. L. Dillmann, and H. Brussow.** 2003. Phage as agents of lateral gene transfer. Curr. Opin. Microbiol. **6:**417-424.

13. **Capone, D. G.** 2001. Marine nitrogen fixation: What's the fuss? Curr. Opin. Microbiol. **4:**341-348.

14. **Casjens, S. R., E. B. Gilcrease, D. A. Winn-Stapley, P. Schicklmaier, H. Schmieger, M. L. Pedulla, M. E. Ford, J. M. Houtz, G. F. Hatfull, and R. W. Hendrix.** 2005. The generalized transducing *Salmonella* bacteriophage ES18: Complete genome sequence and DNA packaging strategy. J. Bacteriol. **187:**1091-1104.

15. **Chen, F. and J. Lu.** 2002. Genomic sequence and evolution of marine cyanophage P60: a new insight on lytic and lysogenic phages. Appl. Environ. Microbiol. **68:**2589-2594.

16. **Chen, Y., I. Golding, S. Sawai, L. Guo, and E. C. Cox.** 2005. Population fitness and the regulation of *Escherichia coli* genes by bacterial viruses. PLoS Biology **3:**1276-1282.

17. **Chikova, A. K. and R. M. Schaaper.** 2005. The bacteriophage P1 hot gene product can substitute for the *Escherichia coli* DNA Polymerase III theta subunit. J. Bacteriol. **187:**5528-5536.

18. **Cochran, P. K. and J. H. Paul.** 1998. Seasonal abundance of lysogenic bacteria in a subtropical estuary. Appl. Environ. Microbiol. **64:**2308-2312.

19. **Cochran, P. K., C. A. Kellogg, and J. H. Paul.** 1998. Prophage induction of indigenous marine lysogenic bacteria by environmental pollutants. Mar. Ecol. Prog. Ser. **164:**125-133.

20. **Datta, A. B., S. Roy, and P. Parrack.** 2005. Role of C-terminal residues in oligomerization and stability of lambda CII: Implications for lysis-lysogeny decision of the phage. J. Mol. Biol. **345:**315-324.

21. **Datta, A. B., S. Panjikar, M. S. Weiss, P. Chakrabarti, and P. Parrack.** 2005. Structure of lambda CII: Implications for recognition of direct-repeat DNA by an unusual tetrameric organization. Proc. Natl. Acad. Sci. U. S. A. **102:**11242-11247.

22. **Dodd, I. B., A. J. Perkins, D. Tsemitsidis, and J. B. Egan.** 2001. Octamerization of lambda CI repressor is needed for effective repression of P_{RM} and efficient switching from lysogeny. Genes Dev. **15:**3013-3022.

23. **Dodd, I. B., K. E. Shearwin, A. J. Perkins, T. Burr, A. Hochschild, and J. B. Egan.** 2004. Cooperativity in long-range gene regulation by the lambda CI repressor. Genes Dev. **18:**344-354.

24. **Dudoit, S., Y. H. Yang, M. J. Callow, and T. P. Speed.** 2002. Statistical methods for identifying differentially expressed genes in replicated cDNA microarray experiments. Statistica Sinica **12:**111-139.

25. **Duplessis, M., W. M. Russell, D. A. Romero, and S. Moineau.** 2005. Global gene expression analysis of two *Streptococcus thermophilus* bacteriophages using a DNA microarray. Virology **340:**192-208.

26. **Farto, R., M. J. Perez, A. Fernandez-Briera, and T. P. Nieto.** 2002. Purification and partial characterisation of a fish lethal extracellular protease from *Vibrio pelagius*. Vet. Microbiol. **89:**181-194.

27. **Faruque, S. M., Asadulghani, M. M. Rahman, M. K. Waldor, and D. A. Sack.** 2000. Sunlight-induced propagation of the lysogenic phage encoding cholera toxin. Infect. Immun. **68:**4795-4801.

28. **Frye, J. G., S. Porwollik, F. Blackmer, P. Cheng, and M. Mcclelland.** 2005. Host gene expression changes and DNA amplification during temperate phage induction. J. Bacteriol. **187:**1485-1492.

29. **Fuhrman, J. A.** 1999. Marine viruses and their biogeochemical and ecological effects. Nature **399:**541-548.

30. **Gnezda-Meijer, K., I. Mahne, M. Poljsak-Prijatelj, and D. Stopar.** 2006. Host physiological status determines phage-like particle distribution in the lysate. FEMS Microbiol. Ecol. **55:**136-145.

31. **Gobler, C. J., D. A. Hutchins, N. S. Fisher, E. M. Cosper, and S. A. Sanudo-Wilhelmy.** 1997. Release and bioavailability of C, N, P, Se, and Fe following viral lysis of a marine Chrysophyte. Limnol. Oceanogr. **42:**1492-1504.

32. **Heldal, M. and G. Bratbak.** 1991. Production and decay of viruses in aquatic environments. Marine Ecology Progress Series **72:**205-212.

33. **Hendrix, R. W.** 2003. Bacteriophage genomics. Curr. Opin. Microbiol. **6:**506-511.

34. **Hendrix, R. W., M. C. M. Smith, R. N. Burns, M. E. Ford, and G. F. Hatfull.** 1999. Evolutionary relationships among diverse bacteriophages and prophages: All the world's a phage. Proceedings of the National Academy of Sciences **96:**2192-2197.

35. **Hennes, K. P. and M. Simon.** 1995. Significance of bacteriophages for controlling bacterioplankton growth in a mesotrophic lake. Appl. Environ. Microbiol. **61:**333-340.

36. **Hewson, I., S. R. Govil, D. G. Capone, E. J. Carpenter, and J. A. Fuhrman.** 2004. Evidence of *Trichodesmium* viral lysis and potential significance for biogeochemical cycling in the oligotrophic ocean. Aquat. Microb. Ecol. **36:**1-8.

37. **Husson-Kao, C., J. Mengaud, J. C. Gripon, L. Benbadis, and M. P. Chapot-Chartier.** 2000. Characterization of *Streptococcus thermophilus* strains that undergo lysis under unfavourable environmental conditions. Int. J. Food Microbiol. **55:**209-213.

38. **Isidro, A., A. O. Henriques, and P. Tavares.** 2004. The portal protein plays essential roles at different steps of the SPP1 DNA packaging process. Virology **322:**253-263.

39. **Jenkins, B. D., G. F. Steward, S. M. Short, B. B. Ward, and J. P. Zehr.** 2004. Fingerprinting diazotroph communities in the Chesapeake Bay by using a DNA macroarray. Appl. Environ. Microbiol. **70:**1767-1776.

40. **Jiang, S. C. and J. H. Paul.** 1998. Gene transfer by transduction in the marine environment. Appl. Environ. Microbiol. **64:**2780-2787.

41. **Jiang, S. C. and J. H. Paul.** 1998. Significance of lysogeny in the marine environment: Studies with isolates and a model of lysogenic phage production. Microb. Ecol. **35:**235-243.

42. **Jiang, S. C. and J. H. Paul.** 1994. Seasonal and diel abundance of viruses and occurrence of lysogeny/bacteriocinogeny in the marine environment. Marine Ecology Progress Series **104:**163-172.

43. **Jiang, S. C., C. A. Kellogg, and J. H. Paul.** 1998. Characterization of marine temperate phage-host systems isolated from Mamala Bay, Oahu, Hawaii. Appl. Environ. Microbiol. **64:**535-542.

44. **Karlsson, F., A. C. Malmborg-Hager, A. S. Albrekt, and C. A. Borrebaeck.** 2005. Genome-wide comparison of phage M13-infected vs. uninfected *Escherichia coli*. Can. J. Microbiol. **51:**29-35.

45. **Khemayan, K., T. Pasharawipas, O. Puiprom, S. Sriurairatana, O. Suthienkul, and T. W. Flegel.** 2006. Unstable lysogeny and pseudolysogeny in *Vibrio harveyi* Siphovirus-Like Phage 1. Appl. Environ. Microbiol. **72:**1355-1363.

46. **Kirchman, D.** 2001. Measuring bacterial biomass prodution and growth rates from leucine incorporation in natural aquatic environments, p. 227-237. In J. H. Paul (ed.), Methods in microbiology: Marine microbiology. Academic Press, London.

47. **Lang, A. S. and J. T. Beatty.** 2000. Genetic analysis of a bacterial genetic exchange element: The gene transfer agent of *Rhodobacter capsulatus*. Proceedings of the National Academy of Sciences **97:**859-864.

48. **Lindell, D., J. D. Jaffe, Z. I. Johnson, G. M. Church, and S. W. Chisholm.** 2005. Photosynthesis genes in marine viruses yield proteins during host infection. Nature **438:**86-89.

49. **Lindell, D., M. B. Sullivan, Z. I. Johnson, A. C. Tolonen, F. Rohwer, and S. W. Chisholm.** 2004. Transfer of photosynthesis genes to and from *Prochlorococcus* viruses. Proceedings of the National Academy of Sciences of the United States of America **101:**11013-11018.

50. **Little, J. W.** 2005. Lysogeny, prophage induction, and lysogenic conversion, p. 37-54. In M. K. Waldor, D. I. Friedman and S. L. Adhya (ed.), Phages: Their Role in Bacterial Pathogenesis and Biotechnology. ASM Press, Washington, D.C.

51. **Lockhart, D. J. and E. A. Winzeler.** 2000. Genomics, gene expression and DNA arrays. Nature **405:**827-836.

52. **Lohr, J. E., F. Chen, and R. T. Hill.** 2005. Genomic analysis of bacteriophage phiJL001: Insights into its interaction with a sponge-associated Alpha-Proteobacterium. Appl. Environ. Microbiol. **71:**1598-1609.

53. **Lohrenz, S. E., D. A. Wiesenburg, R. A. Arnone, and X. Chen.** 1999. What controls primary production in the Gulf of Mexico?, p. 151-170. In H. Kumpf, K. Steidinger and K. Sherman (ed.), The Gulf of Mexico Large Marine Ecosystem: Assessment, Sustainability, and Management. Blackwell Science, Inc., Malden, Massachusetts.

54. **Lua, D. T., M. Yasuike, I. Hirono, and T. Aoki.** 2005. Transcription program of red sea bream iridovirus as revealed by DNA microarrays. J. Virol. **79:**15151-15164.

55. **Lucchini, S., F. Desiere, and H. Brussow.** 1999. Comparative genomics of *Streptococcus thermophilus* phage species supports a modular evolution theory. J. Virol. **73:**8647-8656.

56. **Lunde, M., A. H. Aastveit, J. M. Blatny, and I. F. Nes.** 2005. Effects of diverse environmental conditions on phiLC3 prophage stability in *Lactococcus lactis*. Appl. Environ. Microbiol. **71:**721-727.

57. **MacDonell, M. T. and R. R. Colwell.** 1985. Phylogeny of the Vibrionaceae, and recommendation for two new genera, Listonella and Shewanella. Syst. Appl. Microbiol. **6:**171-182.

58. **Mann, N. H., A. Cook, A. Millard, S. Bailey, and M. Clokie.** 2003. Marine ecosystems: Bacterial photosynthesis genes in a virus. Nature **424:**741.

59. **Maranger, R. and D. F. Bird.** 1995. Viral abundance in aquatic systems: A comparison between marine and fresh waters. Marine Ecology Progress Series **121:**217-226.

60. **Marrs, B.** 1974. Genetic recombination in *Rhodopseudomonas capsulata*. Proc. Natl. Acad. Sci. U. S. A. **71:**971-973.

61. **Matson, E. G., M. G. Thompson, S. B. Humphrey, R. L. Zuerner, and T. B. Stanton.** 2005. Identification of genes of VSH-1, a prophage-like gene transfer agent of *Brachyspira hyodysenteriae*. J. Bacteriol. **187:**5885-5892.

62. **McDaniel, L., L. A. Houchin, S. J. Williamson, and J. H. Paul.** 2002. Lysogeny in marine *Synechococcus*. Nature **415:**496.

63. **McDaniel, L. D., V. McGee, and J. H. Paul.** 2005. Use of the marine prophage induction assay (MPIA) to detect environmental mutagens. Estuaries **28:**634-642.

64. **Middelboe, M. and P. G. Lyck.** 2002. Regeneration of dissolved organic matter by viral lysis in marine microbial communities. Aquat. Microb. Ecol. **27:**187-194.

65. **Miller, E. S., J. F. Heidelberg, J. A. Eisen, W. C. Nelson, A. S. Durkin, A. Ciecko, T. V. Feldblyum, O. White, I. T. Paulsen, and W. C. Nierman.** 2003. Complete genome sequence of the broad-host-range Vibriophage KVP40: Comparative genomics of a T4-related bacteriophage. J. Bacteriol. **185:**5220-5233.

66. **Moebus, K.** 1997. Investigations of the marine lysogenic bacterium H24: I. General description of the phage-host system. Marine Ecology Progress Series **148:**217-228.

67. **Moebus, K.** 1997. Investigations of the marine lysogenic bacterium H24: II. Development of pseudolysogeny in nutrient-rich broth culture. Mar Ecol Prog Ser **148:**229-240.

68. **Moebus, K.** 1997. Investigations of the marine lysogenic bacterium H24: III. Growth of bacteria and production of phage under nutrient-limited conditions. Mar Ecol Prog Ser **148:**241-250.

69. **Noble, R. T. and G. F. Steward.** 2001. Estimating viral proliferation in aquatic systems, p. 66-84. In J. H. Paul (ed.), Methods in microbiology: Marine microbiology. Academic Press, London.

70. **Noble, R. T. and J. A. Fuhrman.** 1998. Use of SYBR Green I for rapid epifluorescence counts of marine viruses and bacteria. Aquat. Microb. Ecol. **14:**113-118.

71. **Noble, R. T. and J. A. Fuhrman.** 1997. Virus decay and its causes in coastal waters. Appl. Environ. Microbiol. **63:**77-83.

72. **Obuchowski, M., Y. Shotland, S. Koby, H. Giladi, M. Gabig, G. Wegrzyn, and A. B. Oppenheim.** 1997. Stability of CII is a key element in the cold stress response of bacteriophage lambda infection. J. Bacteriol. **179:**5987-5991.

73. **Ohki, K.** 1999. A possible role of temperate phage in the regulation of *Trichodesmium* biomass. Bulletin de l'Institut oceanographique, Monaco **19:**287-291.

74. **Oremland, R. S. and J. F. Stolz.** 2003. The ecology of arsenic. Science **300:**939-944.

75. **Ortmann, A. C., J. E. Lawrence, and C. A. Suttle.** 2002. Lysogeny and lytic viral production during a bloom of the cyanobacterium *Synechococcus* spp. Microb. Ecol. **43:**225-231.

76. **Parada, V., G. J. Herndl, and M. G. Weinbauer.** 2006. Viral burst size of heterotrophic prokaryotes in aquatic systems. Journal of the Marine Biological Association of the UK **86:**613-621.

77. **Parreira, R., R. Valyasevi, A. L. Lerayer, S. D. Ehrlich, and M. C. Chopin.** 1996. Gene organization and transcription of a late-expressed region of a *Lactococcus lactis* phage. J. Bacteriol. **178:**6158-6165.

78. **Paul, J. H. and M. B. Sullivan.** 2005. Marine phage genomics: What have we learned? Curr. Opin. Biotechnol. **16:**299-307.

79. **Paul, J. H. and S. C. Jiang.** 2001. Lysogeny and transduction, p. 105-125. In J. H. Paul (ed.), Methods in microbiology: Marine microbiology. Academic Press, London.

80. **Paul, J. H. and B. Meyers.** 1982. Fluorometric determination of DNA in aquatic microorganisms by use of Hoechst 33258. Applied and Environmental Microbiology **43:**1393-1399.

81. **Paul, J. H., M. B. Sullivan, A. M. Segall, and F. Rohwer.** 2002. Marine phage genomics. Comp. Biochem. Physiol. B. Biochem. Mol. Biol. **133:**463-476.

82. **Paul, J. H., S. J. Williamson, A. Long, R. N. Authement, D. John, A. M. Segall, F. L. Rohwer, M. Androlewicz, and S. Patterson.** 2005. Complete genome sequence of phiHSIC, a pseudotemperate marine phage of *Listonella pelagia*. Appl. Environ. Microbiol. **71:**3311-3320.

83. **Proctor, L. M. and J. A. Fuhrman.** 1990. Viral mortality of marine bacteria and cyanobacteria. Nature **343:**60-62.

84. **Ptashne, M.** 2004. A Genetic Switch: Phage lambda Revisited. Cold Spring Harbor Laboratory Press, Cold Spring Harbor, N.Y.

85. **Ripp, S. and R. V. Miller.** 1997. The role of pseudolysogeny in bacteriophage-host interactions in a natural freshwater environment. Microbiology **143:**2065-2070.

86. **Romig, W. R. and A. M. Brodetsky.** 1961. Isolation and preliminary characterization of bacteriophages for *Bacillus subtilis*. J. Bacteriol. **82:**135-141.

87. **Roszak, D. B. and R. R. Colwell.** 1987. Survival strategies of bacteria in the natural environment. Microbiology and Molecular Biology Reviews **51:**365-379.

88. **Sanger, F., A. R. Coulson, T. Friedmann, G. M. Air, B. G. Barrell, N. L. Brown, J. C. Fiddes, C. A. Hutchison 3rd, P. M. Slocombe, and M. Smith.** 1978. The nucleotide sequence of bacteriophage phiX174. J. Mol. Biol. **125:**225-246.

89. **Semenova, E., M. Djordjevic, B. Shraiman, and K. Severinov.** 2005. The tale of two RNA polymerases: Transcription profiling and gene expression strategy of bacteriophage Xp10. Mol. Microbiol. **55:**764-777.

90. **Simidu, U., K. Kita-Tsukamoto, T. Yasumoto, and M. Yotsu.** 1990. Taxonomy of four marine bacterial strains that produce tetrodotoxin. Int. J. Syst. Bacteriol. **40:**331-336.

91. **Steil, L., T. Hoffmann, I. Budde, U. Völker, and E. Bremer.** 2003. Genome-wide transcriptional profiling analysis of adaptation of *Bacillus subtilis* to high salinity. J. Bacteriol. **185:**6358-6370.

92. **Steward, G. F., B. D. Jenkins, B. B. Ward, and J. P. Zehr.** 2004. Development and Testing of a DNA Macroarray To Assess Nitrogenase (*nifH*) Gene Diversity. Appl. Environ. Microbiol. **70:**1455-1465.

93. **Stewart, F. M. and B. R. Levin.** 1984. The population biology of bacterial viruses: Why be temperate? Theor. Popul. Biol. **26:**93-117.

94. **Stolt, P. and W. Zillig.** 1994. Transcription of the halophage phi H repressor gene is abolished by transcription from an inversely oriented lytic promoter. FEBS Lett. **344:**125-128.

95. **Stopar, D., A. Cerne, M. Zigman, M. Poljsak-Prijatelj, and V. Turk.** 2004. Viral abundance and a high proportion of lysogens suggest that viruses are important members of the microbial community in the Gulf of Trieste. Microb. Ecol. **47:**1-8.

96. **Sumby, P. and M. K. Waldor.** 2003. Transcription of the toxin genes present within the Staphylococcal phage phiSa3ms is intimately linked with the phage's life cycle. J. Bacteriol. **185:**6841-6851.

97. **Suttle, C. A. and F. Chen.** 1992. Mechanisms and rates of decay of marine viruses in seawater. Appl. Environ. Microbiol. **58:**3721-3729.

98. **Twort, F. W.** 1915. An investigation on the nature of ultramicroscopic viruses. Lancet **2:**1241-1243.

99. **Venter, J. C., K. Remington, J. F. Heidelberg, A. L. Halpern, D. Rusch, J. A. Eisen, D. Wu, I. Paulsen, K. E. Nelson, and W. Nelson.** 2004. Environmental genome shotgun sequencing of the Sargasso Sea. Science **304:**66-74.

100. **Ventura, M. and H. Brussow.** 2004. Temporal transcription map of the virulent *Streptococcus thermophilus* bacteriophage Sfi19. Appl. Environ. Microbiol. **70:**5041-5046.

101. **Ventura, M., S. Foley, A. Bruttin, S. C. Chennoufi, C. Canchaya, and H. Brussow.** 2002. Transcription mapping as a tool in phage genomics: the case of the temperate *Streptococcus thermophilus* phage Sfi21. Virology **296:**62-76.

102. **Vidgen, M., J. Carson, M. Higgins, and L. Owens.** 2006. Changes to the phenotypic profile of *Vibrio harveyi* when infected with the *Vibrio harveyi* myovirus-like (VHML) bacteriophage. J. Appl. Microbiol. **100:**481-487.

103. **Villamil, L., A. Figueras, A. E. Toranzo, M. Planas, and B. Novoa.** 2003. Isolation of a highly pathogenic *Vibrio pelagius* strain associated with mass mortalities of turbot, *Scophthalmus maximus* (L.), larvae. J. Fish Dis. **26:**293-303.

104. **Waldor, M. K. and J. J. Mekalanos.** 1996. Lysogenic conversion by a filamentous phage encoding cholera toxin. Science **272:**1910-1914.

105. **Wawrik, B.** 2003. Dissertation/Thesis. University of South Florida,

106. **Weinbauer, M. G.** 2004. Ecology of prokaryotic viruses. FEMS Microbiol. Rev. **28:**127-181.

107. **Weinbauer, M. G. and F. Rassoulzadegan.** 2004. Are viruses driving microbial diversification and diversity? Environ. Microbiol. **6:**1-11.

108. **Weinbauer, M. G. and C. A. Suttle.** 1996. Potential significance of lysogeny to bacteriophage production and bacterial mortality in coastal waters of the Gulf of Mexico. Appl. Environ. Microbiol. **62:**4374-4380.

109. **Weinbauer, M. G., I. Brettar, and M. G. Hoefle.** 2003. Lysogeny and virus-induced mortality of bacterioplankton in surface, deep, and anoxic marine waters. Limnol. Oceanogr. **48:**1457-1465.

110. **Weinbauer, M. G., C. Winter, and M. G. Hoefle.** 2002. Reconsidering transmission electron microscopy based estimates of viral infection of bacterioplankton using conversion factors derived from natural communities. Aquat. Microb. Ecol. **27:**103-110.

111. **Wilhelm, S. W. and C. A. Suttle.** 1999. Viruses and nutrient cycles in the sea. Bioscience **49:**781-788.

112. **Wilhelm, S. W., S. M. Brigden, and C. A. Suttle.** 2002. A dilution technique for the direct measurement of viral production: A comparison in stratified and tidally mixed coastal waters. Microb. Ecol. **43:**168-173.

113. **Wilhelm, S. W., M. G. Weinbauer, C. A. Suttle, and W. H. Jeffrey.** 1998. The role of sunlight in the removal and repair of viruses in the sea. Limnol. Oceanogr. **43:**586-592.

114. **Williamson, S. J. and J. H. Paul.** 2006. Environmental factors that influences the transition from lysogenic to lytic existence in the phiHSIC/*Listonella pelagia* marine phage-host system. Microbial Ecology **In press:**

115. **Williamson, S. J. and J. H. Paul.** 2004. Nutrient stimulation of lytic phage production in bacterial populations of the Gulf of Mexico. Aquat. Microb. Ecol. **36:**9-17.

116. **Williamson, S. J., M. R. McLaughlin, and J. H. Paul.** 2001. Interaction of the phiHSIC virus with its host: Lysogeny or pseudolysogeny? Appl. Environ. Microbiol. **67:**1682-1688.

117. **Williamson, S. J., L. A. Houchin, L. McDaniel, and J. H. Paul.** 2002. Seasonal variation in lysogeny as depicted by prophage induction in Tampa Bay, Florida. Appl. Environ. Microbiol. **68:**4307-4314.

118. **Wilson, W. H. and N. H. Mann.** 1997. Lysogenic and lytic viral production in marine microbial communities. Aquat Microb Ecol **13:**95-100.

119. **Wilson, W. H., N. G. Carr, and N. H. Mann.** 1996. The effect of phosphate status on the kinetics of cyanophage infection in the oceanic cyanobacterium *Synechococcus* spp. WH7803. J. Phycol. **32:**506-516.

120. **Wilson, W. H., D. C. Schroeder, M. J. Allen, M. T. Holden, J. Parkhill, B. G. Barrell, C. Churcher, N. Hamlin, K. Mungall, H. Norbertczak, M. A. Quail, C. Price, E. Rabbinowitsch, D. Walker, M. Craigon, D. Roy, and P. Ghazal.** 2005. Complete genome sequence and lytic phase transcription profile of a *Coccolithovirus*. Science **309:**1090-1092.

121. **Wommack, K. E. and R. R. Colwell.** 2000. Virioplankton: Viruses in aquatic ecosystems. Microbiol. Mol. Biol. Rev. **64:**69-114.

122. **Wommack, K. E., R. T. Hill, T. A. Muller, and R. R. Colwell.** 1996. Effects of sunlight on bacteriophage viability and structure. Appl. Environ. Microbiol. **62:**1336-1341.

123. **Wommack, K. E., R. T. Hill, M. Kessel, E. Russek-Cohen, and R. R. Colwell.** 1992. Distribution of viruses in the Chesapeake Bay. Appl. Environ. Microbiol. **58:**2965-2970.

124. **Xie, Y., L. S. Chou, A. Cutler, and B. Weimer.** 2004. DNA Macroarray profiling of *Lactococcus lactis* subsp. lactis IL1403 gene expression during environmental stresses. Appl. Environ. Microbiol. **70:**6738-6747.

125. **Zheng, J., J. Zhao, Y. Tao, J. Wang, Y. Liu, J. Fu, Y. Jin, P. Gao, J. Zhang, Y. Bai, and G. Wang.** 2004. Isolation and analysis of water stress induced genes in maize seedlings by subtractive PCR and cDNA macroarray. Plant Mol. Biol. **55:**807-823.

126. **ZoBell, C. E.** 1946. Marine microbiology: A monograph on hydrobacteriology. Chronica Botanica,

Appendices

Appendix A: Liquid and Solid Culture Media

Recipe for 1.0 L of ASWJP:

Stock	Chemical	g / 100 ml
#1	KCl	5.5 g
	$NaHCO_3$	1.6 g
#2	KBr	0.8 g
	$SrCl_2$	0.34 g
#3	$Na_2SiO_3 \bullet 9H_2O$	0.4 g
#4	NaF	0.24 g
#5	NH_4NO_3	0.16 g
#6	Na_2HPO_4	0.8 g
#7	$CaCl_2 \bullet 2H_2O$	23.8g

Stock solution #44

Chemical	g / volume	ml / L for final stock
Na_2EDTA	12 g / 200 ml	50 ml / 1000 ml
$FeCl_3 \bullet 6H_2O$	3.84 mg / 20 ml	2 ml / 1000 ml
$MgCl_2 \bullet 6H_2O$	4.32 g / 20 ml	2 ml / 1000 ml
$CoCl_2 \bullet 6H_2O$	0.2 g / 20 ml	2 ml / 1000 ml
$ZnCl_2$	0.315 g / 20 ml	2 ml / 1000 ml
$CuCl_2$	4.8 mg / 34.4 ml	2 ml / 1000 ml
H_3BO_3	3.42 g / 100ml	10 ml / 1000 ml

Appendix A (Continued)

Preparation of ASWJP:

Add 22.05 g NaCl and 9.8 g $MgSO_4 \cdot 7\ H_2O$ (4.79 g anhydrous) to 900 ml ultrapure deionized water and dissolve.

Add the following amounts of stock solutions:

Stock #1	10.0 ml
Stock #2	10.0 ml
Stock #3	1.0 ml
Stock #4	1.0 ml
Stock #5	1.0 ml
Stock #6	1.0 ml
Stock #7	10.0 ml
Stock #44	10.0 ml

Bring volume up to 1.0 L with ultrapure deionized water. Sterilize by autoclaving.

Recipe for 1.0 L of ASWJP+PY (liquid):

Follow recipe for ASWJP (1.0 L). Add 5.0 g BactoPeptone and 1.0 g BactoYeast extract prior to bringing volume to 1.0 L. Bring up to volume and sterilize by autoclaving.

Recipe for 1.0 L ASWJP+PY (solid):

Preparation of bottom agar and slants:

Follow recipe for ASWJP+PY. Add 15.0 g (1.5% final concentration) BactoAgar prior to bringing volume to 1.0 L. Dissolve agar by heating on a hot plate. Sterilize by autoclaving.

Preparation of top agar:

Follow recipe for ASWJP+PY. Add 10.0 g (1.0% final concentration) BactoAgar prior to bringing volume to 1.0 L. Dissolve agar by heating on a hot plate. Sterilize by autoclaving.

Recipe for 0.5X ASWJP+PY 1 L:

Add 11.025 g of NaCL and 4.9 g $MgSO_4$•7 H_2O to 900 mL of deionized water. Add the stock solutions, 5 g of peptone, and 1 g of yeast extract. Bring volume up to 1 L and let stir until solids are dissolved. Sterilize by autoclaving.

Recipe for 0.125X ASWJP+PY 1 L:

Add 2.75 g of NaCl and 1.22 g of $MgSO_4$•7 H_2O to 900 mL of deionized water. Add the stock solutions, 5 g of peptone, and 1 g of yeast extract. Bring volume up to 1 L. Sterilize by autoclaving.

Appendix B: Buffers and Solutions

0.5 M EDTA

Add 186.1 disodium ethylenediaminetetraacetate • 2 H_2O (Na_2EDTA) to 800 mL of deionized water. Stir vigorously using a magnetic stirbar on a stirplate. Adjust pH to 8.0 using NaOH pellets, EDTA will not dissolve until pH of 8.0 is reached. Sterilize by autoclaving.

Ethidium Bromide

Add 1 g of ethidium bromide to 100 mL of deionized water. Stir for an hour to ensure complete dissolution. Wrap container in aluminum foil and store at room temperature.

10% SDS

Dissolve 100 g of electorphoresis grade sodium dodecyl sulfate in 900 mL of deionized water. Heat to 68 C and adjust pH to 7.2 using concentrated hydrochloric acid. Bring volume up to 1 L.

20X SSC

Dissolve 175.3 gram sodium chloride and 88.2 g sodium citrate in 800 mL deionized water. Adjust pH to 8.0 using 5 N NaOH. Bring volume up to 1 L and sterilize by autoclaving.

50X TAE

Dissolve 242 g Tris base in 600 mL of deionized water. Add 57.1 mL of glacial acetic acid and 100 mL 0.5 M EDTA pH 8.0. Bring up to 1 L and sterilize by autoclaving.

Wash Solution 1 (2X SSC, 1% SDS)

Mix 10 mL of 20X SSC with 10 mL 10% SDS. Bring up to 100 mL with deionized water which will give it a final concentration of 2X SSC and 1% SDS.

Wash Solution 2 (0.1X SSC, 0.5% SDS)

Mix 0.5 mL of 20X SSC with 5 mL of 10% SDS. Bring up to 100 mL with deionized water so that it's final concentration will be 0.1X SSC and 0.5% SDS.

Appendix C: Primer Sequences and Array Design

Table 12. List of primers used to generate amplicons for the macroarrays.

ORF	Nucleotide Position	Primer Sequence	Annealing Temp. (° C)	Amplicon Size
1/+	2-625	TTCATTGGCGATGGAATGTA ACCCCGAGAAGCTCCACTAT	53	336
2/+	670-1254	GTGATTAACAATTTAGTTC GTTGAATGACTCGCTTAAC	53	331
3/+	1393-1542	ACATCGGCTGGCTGTATGA TTACTCATGAAATGGCGCATA	50	157
4/+	1757-2101	ATGAGATCAACCCTGGCATC CCGCATTGCCTAACAATAAAA	50	260
5/+	2095-2328	AAAGAGGCGCTTGACATCTG TGCCAATTGCGATGAAGTTA	50	101
6/+	2374-2568	AGAAACCCTTGATGCAATCG AATCTGCTTTTTGCCGTGAT	53	126
7/+	2610-3029	GTAAAACGACGGCCAG CAGGAAACAGCTATGCA	53	200
8/+	3010-4236	TATCAAAGAGTCGTTTCACG GTCTGAAGCGCTTGTCAACT	50	319
9/+	4354-4719	TCAACAAAGCACGAGCAATC ATTCATTAAGGCCGGCTACA	53	256
10/+	4874-5107	CTACCAAAAATCGCCGAATC TCATTCTGTCGACGCTCATT	50	99
11/+	5104-5325	CGTTTCCAGGGGAGATAAAA CGTGTAGATGCAAGCCATGT	53	162
12/+	5372-6799	GTTAAACCTTGCTAAAATGC CATTGTGTCGAACTCGGGTT	53	340
13/-	6829-7110	TGGGGGATTAGTTATGAAGATGA TAGTAGTGATTCGGCGTTGC	53	261
14/+	7182-8252	CAAACAAAGAAGCGTCGTGA TGTCAGCCGAGTTAGCATTG	50	275
15/+	8348-8662	ATGGACCAACCTCACAGCA AATTGACACCGTCATCGACA	53	343

Appendix C (Continued)

Table 12 Cont.

ORF	Nucleotide Position	Primer Sequence	Annealing Temp. (° C)	Amplicon Size
16/+	8984-9313	AGTTAGTGATTGGGCGGTGT CCATTTTGACAAAGAAGCTTGA	53	292
17/+	9418-10086	AGCCAAGACGCTGACTTGAT GCCTGACCATGCTCTTGAAT	53	286
18/+	10098-11045	TCTGAGCTAATCGAAGGCG CACATTCATGCCAGCGTTAG	50	317
19/+	11106-11669	TTGTGTTGCAGCTTCAAAGG ACACCGCCACCAGTAAAAAC	53	330
20/-	11702-12130	GTAAAACGACGGCCAG CAGGAAACAGCTATGCA	50	200
21/+	12205-12445	TTTGCTCTGCTGTGCATTTC GGGTAAAACTCAATTGCATCG	50	253
22/-	12474-13058	TTGGAGTATGGGTTCCATCG TTTCTCAGGTCGGACTCGTT	53	293
23/+	13153-13650	AACTGCCGAAGCTGATAGCA GATTTGGTCGGATGGGTATT	53	231
24/+	13654-14052	ACGCGAGACGCTTAAAGAAG GTTGCGCAGTTGGTTGTAGA	53	252
25/+	14057-14485	CGTGGAGCAAAAGCCTAAAA TGGCGTAAGGTAGCGGATTA	53	320
26+	14485-14868	CGCAGTAAAGGCTTTTGAGG TGGATTGGTTAGCTTGCAGA	53	304
27/+	14985-15461	CTGTTGGCACTATCGCAGAA ACTGGCGTGGTTTTATTTGC	53	297
28/+	15530-16012	CAACATGAAACACCGTGAGG CAAGTCTTCGGACTGCATGA	53	285
29/+	16210-16428	CAGGCAAAAAGGAAGAGACG AGTGTGCGGAAATCGTAACC	53	315
30/-	16452-16928	GTAAAACGACGGCCAG CAGGAAACAGCTATGCA	53	200

Appendix C (Continued)

Table 12 Cont.

ORF	Nucleotide Position	Primer Sequence	Annealing Temp. (° C)	Amplicon Size
31/+	17022-20231	ATTGTTCAAATTGGCTTTTC TTTAACCACTCACCGACACG	50	367
32/+	20231-21817	AACGTTGGAACTTTGGTTGC AGGCATCGAGAATGGTATCG	53	279
33/+	21870-24275	GATGACGTAAGAAGCGGAGC CCGTAGGGTATGGAGCGTAA	50	200
34/+	24368-24643	GCAAAGCCCCATAATGACAA CCCACTTTGCAATCTGCTTT	50	252
35/+	24648-25079	CAATTCCAGAGCCAACGATT AAGGATGTCGAAACCCATCA	53	265
36/+	25084-25317	TTTCACTATGGCCTCCTTGG CGCATGAAGAATTGCAACG	50	165
37/-	26214-26672	GGTCAAATAATGAGCTTTAC TAGAATGTCCTGAACGTCTT	50	260
38/-	26940-27488	TATGTGTCTGGTGGCCATGT GAATCCGCACAATGAAAGGT	53	272
39/-	27485-27829	AAACCTATCCACAGCGTCCA TCATTGGTAGCTTTCCGTCA	53	270
40/+	28235-28564	CGGTCACGGTTTCAAAAACT TTACGCCGCAACAATGAATA	50	122
41/-	28476-28859	AAACACAAGCCTCACCTTGG TCCCACCCATAGCACACATA	53	253
42/-	28856-31717	GTAAAACGACGGCCAG CAGGAAACAGCTATGCA	50	200
43/-	31723-32265	CGCAAACACCTAAACGGAAT AAACCGCCCTCCTCTTACAAT	50	292
44/-	32262-32981	TCAGAAGCCGTTGATGACTG AAGAATTGCGCTTTGCATTT	50	309
45/-	33017-33550	ACACTATCAGACGGCCAAGC CCAGCATACGCAATGCTTTA	50	236

Appendix C (Continued)

Table 12 Cont.

ORF	Nucleotide Position	Primer Sequence	Annealing Temp. (° C)	Amplicon Size
46/-	33557-34315	CGGTGACGCAGTTAGAGACA TTTGCAGTTTGACCAATCCA	53	279
47/-	34641-37088	CGGACTGGATAAACCGAAGA AACTTGACTGCGCAAAAGGT	53	270
16S	N/A	CCGAATTCGTCGACAACAGAGTTTGATCCTG GCTCAG CCCGGGATCCAAGCTTACGGCTACCTTGTTA CGACTT	53	1538

Table 13. Probe and primer sequences for real-time PCR

Name	Sequence
HSIC Probe	CCCCATCCCAACGCGCAAAAGAG
11 (Forward)	CGTTTCCAGGGGAGATAAAA
11 (Reverse)	CGTGTAGATGCAAGCCATGT

16S	1	1	2	2	3	3	4	4	5	5	16S	16S
6	6	7	7	8	8	9	9	10	10	11	11	46
12	12	13	13	14	14	15	15	16	16	17	17	46
B	18	18	19	19	20	20	21	21	22	22	B	47
23	23	24	24	25	25	26	26	27	27	28	28	47
29	29	30	30	31	31	32	32	33	33	34	34	B
35	35	36	36	37	37	38	38	39	39	40	40	
16S	41	41	42	42	43	43	44	44	45	45	16S	

Figure 26. Macroarray schematic. The location of each open reading frame as well as the positive and negative controls are shown.